Modeling and simulation of fluid flows

Samuel Kokh

Université Paris-Saclay

École doctorale de mathématiques Hadamard (ED 574)

Mémoire présenté pour l'obtention du

Diplôme d'habilitation à diriger les recherches

Discipline : Mathématiques

par

Samuel KOKH

Modélisation et simulation d'écoulements de fluides
Modeling and simulation of fluid flows

Rapporteurs :	Sergey GAVRILYUK
	Shi JIN
	Bertrand MAURY

Date de soutenance : 25 novembre 2021

Composition du jury :	Sergey GAVRILYUK	(Rapporteur)
	Raphaèle HERBIN	(Examinatrice)
	Shi JIN	(Rapporteur)
	Pierre-Henri MAIRE	(Président)
	Bertrand MAURY	(Rapporteur)
	Christian ROHDE	(Examinateur)

Ce mémoire est dédié à la mémoire de Rosa,
Monsieur Đan et Madame Quy.

Table des matières

Notations and conventions

— $\mathbf{x} = (x_1, \dots, x_d) \in \mathbb{R}^d$, the spatial coordinates

— if $\mathbf{x} \mapsto \mathbf{M} = (\mathbf{M}_{ij})$ is a $m \times d$ matrix, we note $\mathbf{div}(\mathbf{M})$ the column vector whose coordinates are $\mathbf{div}(\mathbf{M})_i = \sum_j (\partial \mathbf{M}_{ij} \big/ \partial x_j)$

— if $\mathbf{x} \mapsto a$ is a scalar field, we note

  — $\partial_x a \in \mathbb{R}$ the line vector whose coordinates are $(\partial_x a)_i = \partial a \big/ \partial x_i$

  — $\boldsymbol{\nabla} a = (\partial_x a)^T$

— if $\mathbf{x} \mapsto \mathbf{A} \in \mathbb{R}^m$ is a (column) vector field, we note

  — $\partial_x \mathbf{A}$ the matrix whose components are $(\partial_x \mathbf{A})_{ij} = \partial \mathbf{A}_i \big/ \partial x_j$

  — $\boldsymbol{\nabla} \mathbf{A} = (\partial_x \mathbf{A})^T$

— if $\mathbf{u} = (u_1, \dots, u_d)^T$ is a material velocity (column) vector, we will note $\mathrm{D}_t f = \partial_t f + (\partial_x f)\mathbf{u}$ the material derivative

Foreword

The present thesis is an overview of my work since 2001. The full list of my publications is presented on p. 6. This list also contains works I achieved during my PhD [26, 28, 29, 27, 30] that will not be discussed here.

My research works have been dedicated to modeling fluid flows, proposing approximation strategies for these models and implementing the resulting discretization strategies in scientific computing codes.

This thesis is divided in four chapters that are briefly summed up hereafter.

Complex flow modeling
This chapter presents several works concerning the modeling of compressible flows that may involve multiple components and put at play phenomena at different scales. I will first present a general routine that relies on two main ingredients : the Stationary Action Hamilton Principle and the design of dissipative structure compatible with an entropy budget equation. This method was polished over the years using elements of the literature and applied to modeling different complex flow problems. I will also discuss equilibrium phenomena that can take place within the composition of a multi-component mixture in order to optimize the entropy associated with the model.

Numerical methods for compressible flows
This chapter is dedicated to my work in the field of numerical methods design. I will introduce interface capture methods that rely on the classic Lagrange-Remap approach. I will then show how these methods can be equipped with an anti-diffusive numerical scheme for an efficient tracking of the interfaces between multiple components in a compressible flow. In a second part, I will present a generic approach modeled after the Lagrange-Remap method that enables a decoupling between the acoustic and the transport effects in the numerical scheme on a fixed Eulerian mesh. I will show how this method was adapted to tackle various issues in different compressible flow models such as preserving the accuracy in the low Mach regime, enabling large time step discretization. The method can also be adapted to bifluid models involving several material velocities. I will also present how this approach can be used to derive well-balanced methods and asymptotic preserving solvers that account for source terms.

Scientific computing practice
In this short chapter I will try to propose an overview of my practice of scientific computing in my research work. I will first briefly present a personal guideline that informally I built over the years through my personal experience. Scientific computing also played an important role in my work for connecting with different communities, sharing knowledge and research topics but also motivate theoretical development in physics. Scientific computing is also a natural end of my work in modeling and numerical scheme design. I will present some outcomes in terms of code implementation and numerical simulations.

Perspectives
In this chapter I will propose possible sequels to the work that was presented in this thesis.

> *In the following, some part of text will be enclosed within gray boxes (like this one). These boxes will be used either at the beginning of the sections for highlighting my academic contributions to the topic either within the section for inserting personal comments.*

In this thesis, my publications will be referred to using numeric tags like [18] while references to other articles will be mentioned using alphanumeric tags like [GS06] that appears in the general bibliography (see p. 63).

List of publications by the author

[1] F. Drui, A. Larat, S. Kokh et M. Massot. *Small-scale kinematics of two-phase flows : identifying relaxation processes in separated- and disperse-phase flow models*. *Journal of Fluid Mechanics* 876, p. 326-355, 2019.

[2] T. Padioleau, P. Tremblin, E. Audit, P. Kestener et S. Kokh. *A High-performance and Portable All-Mach Regime Flow Solver Code with Well-balanced Gravity. Application to Compressible Convection*. *The Astrophysical Journal* 875, p. 128, 2019.

[3] P. Tremblin, T. Padioleau, M. W. Phillips, G. Chabrier, I. Baraffe, S. Fromang, E. Audit, H. Bloch, A. J. Burgasser, B. Drummond, M. González, P. Kestener, S. Kokh, P.-O. Lagage et M. Stauffert. *Thermo-compositional Diabatic Convection in the Atmospheres of Brown Dwarfs and in Earth's Atmosphere and Oceans*. *The Astrophysical Journal* 876, p. 144, 2019.

[4] C. Grenier, H. Anbergen, V. Bense, Q. Chanzy, E. Coon, N. Collier, F. Costard, M. Ferry, A. Frampton, J. Frederick, J. Gonçalvès, J. Holmén, A. Jost, S. Kokh, B. Kurylyk, J. McKenzie, J. Molson, E. Mouche, L. Orgogozo, R. Pannetier, A. Rivière, N. Roux, W. Rühaak, J. Scheidegger, J.-O. Selroos, R. Therrien, P. Vidstrand et C. Voss. *Groundwater flow and heat transport for systems undergoing freeze-thaw : Intercomparison of numerical simulators for 2D test cases*. *Advances in Water Resources* 114, p. 196-218, 2018.

[5] C. Chalons, M. Girardin et S. Kokh. *An all-regime Lagrange-Projection like scheme for 2D homogeneous models for two-phase flows on unstructured meshes*. *Journal of Computational Physics* 335, pp. 885–904, 2017.

[6] C. Chalons, P. Kestener, S. Kokh et M. Stauffert. *A large time-step and well-balanced Lagrange-projection type scheme for the shallow water equations*. *Comm. in Math. Sciences* 15, pp. 765-788, 2017.

[7] C. Chalons, M. Girardin et S. Kokh. *An all-regime Lagrange-Projection like scheme for the gas dynamics equations on unstructured meshes*. *Comm. in Comp. Phys.* 20, pp. 188-233, 2016.

[8] B. Després, S. Kokh et F. Lagoutière. *Chapter 4 - Sharpening Methods for Finite Volume Schemes*. In : *Handbook of Numerical Methods for Hyperbolic ProblemsBasic and Fundamental Issues*. Sous la dir. de R. Abgrall et C.-W. Shu. T. 17. Handbook of Numerical Analysis. Elsevier, 2016, pp. 77-102.

[9] F. Drui, A. Fikl, P. Kestener, S. Kokh, A. Larat, V. Le Chenadec et M. Massot. *Experimenting with the p4est library for AMR simulations of two-phase flows*. In : t. 53. http://dx.doi.org/10.1051/proc/201653014. 2016, pp. 232-247.

[10] M. Billaud-Friess et S. Kokh. *Simulation of sharp interface multi-material flows involving an arbitrary number of components through an extended five-equation model*. *Journal of Computational Physics* 273, p. 488-519, 2014.

[11] C. Chalons, M. Girardin et S. Kokh. *Large time step and asymptotic preserving numerical schemes for the gas dynamics equations with source terms.* English. *SIAM J. Sci. Comput.* 35, pp. a2874-a2902, 2013.

[12] V. Faucher et S. Kokh. *Extended Vofire algorithm for fast transient fluid-structure dynamics with liquid-gas flows and interfaces*. *Journal of Fluids and Structures* 39, pp. 102-125, 2013.

[13] M. Billaud-Friess et S. Kokh. *An anti-diffusive Lagrange-Remap scheme for multi-material compressible flows with an arbitrary number of components*. In : *ESAIM : PROCEEDINGS Congrés SMAI*. T. 35. 2012, pp. 203-209.

[14] G. Faccanoni, S. Kokh et G. Allaire. *Modelling and simulation of liquid-vapor phase transition in compressible flows based on thermodynamical equilibrium*. *M2AN* 46, pp. 1029-1054, 2012.

[15] M. Billaud-Friess, B. Boutin, G. Faccanoni, F. Caetano, S. Kokh, F. Lagoutière et L. Navoret. *A Second Order Anti-Diffusive Lagrange-Remap Scheme for Two-Component Flows*. In : *ESAIM : Proc.* CEMRACS'10. 2011, pp. 149-162.

[16] C. Chalons, S. Kokh et N. Spillane. *Large time-step numerical scheme for the seven-equation model of compressible two-phase flows*. In : *Proceedings in Mathematics, FVCA 6*. Sous la dir. de Springer. T. 4. 1. 2011, pp. 225-233.

[17] G. Faccanoni, S. Kokh et G. Allaire. *Approximation of Liquid-Vapor Phase Transition for Compressible Fluids with Tabulated EOS*. *C. R. Acad. Sci. Paris, Série I* t. 348, pp. 473-478, 2010.

[18] S. Kokh et F. Lagoutière. *An Anti-Diffusive Numerical Scheme for the Simulation of Interfaces between Compressible Fluids by Means of a Five-Equation Model*. *J. Comp. Phys.* 229, pp. 2773-2809, 2010.

[19] G. Faccanoni, S. Kokh et G. Allaire. *Numerical simulation with finite volume of a dynamic liquid-vapour phase transition*. In : *Finite volumes for complex applications V, Problems and perspectives*. Sous la dir. de R. Eymard et al. 2008, pp. 391-398.

[20] S. Kokh et F. Lagoutière. *An Anti-Diffusive Method for Simulating Compressible Two-Phase Flows with Interfaces*. In : *Finite volumes for complex applications V, Problems and perspectives*. Sous la dir. de R. Eymard et al. 2008, p. 519-526.

[21] G. Faccanoni, S. Kokh et G. Allaire. *A strictly hyperbolic equilibrium phase transition model*. *C. R. Acad. Sci. Paris, Série I* t. 344, pp. 135-140, 2007.

[22] F. Caro, F. Coquel, D. Jamet et S. Kokh. *A simple finite-volume method for compressible isothermal two-phase flows simulation*. *Int. J. Finite Volumes* 3, 2006.

[23] F. Caro, F. Coquel, D. Jamet et S. Kokh. *DINMOD : a Diffuse Interface Model for Two-Phase Flows Modelling*. In : *Numerical method for hyperbolic and kinetic problems : CEMRACS 2003*. Sous la dir. de S. Cordier et al. IRMA Series in mathematiques and theoretical physics, 7. 2005.

[24] F. Caro, F. Coquel, D. Jamet et S. Kokh. *Phase change simulation for isothermal compressible two-phase flows*. In : *AIAA Comp. Fluid Dynamics*. AIAA-2005-4697. 2005.

[25] S. Kokh et G. Allaire. *Test-case n°19 : shock-bubble interaction (pn). Multiphase Science and Technology* 16, p. 117-120, 2004.

[26] G. Allaire, S. Clerc et S. Kokh. *A five-equation model for the simulation of interfaces between compressible fluids*. *J. Comp. Phys.* 181, pp. 577-616, 2002.

[27] G. Allaire, S. Clerc et S. Kokh. *A Five-Equation Model for the Numerical Simulation of Interfaces in Two-Phase Flows*. *C. R. Acad. Sci.* t. 331, pp. 1017-1022, 2000.

[28] G. Allaire et S. Kokh. *Numerical Simulation of 2D Two-Phase Flows with Interface*. In : *Godunov Methods Theory and Applications*. Sous la dir. de K. Academic/Plenum. 2000.

[29] G. Allaire et S. Kokh. *Simulating Interfaces in Two-Phase Flows*. In : *Proc. AMIF-ESF Workshop Computing Methods for Two-Phase Flow*. 2000.

[30] G. Allaire, S. Clerc et S. Kokh. *Towards Boiling Crisis Simulation : the Level Set Method*. In : *Nureth-9 Proceedings, San Francisco*. 1999.

Introduction (en français)

Cette thèse propose une synthèse de mes travaux depuis 2001. La liste complète de mes publications se trouve en page 6. Elle contient également les publications portant sur mes travaux de Doctorat qui ne seront pas présentés dans ce document.

L'ensemble de mes recherches porte sur la simulation d'écoulements de fluides, depuis la modélisation, l'élaboration de méthodes d'approximation numérique et également l'implémentation de ces méthodes dans des codes de calcul. Tous ces travaux ont été menés dans le cadre de mes fonctions d'ingénieur-chercheur au CEA Saclay à la Direction des Énergies (DES, ex-Direction de l'Énergie Nucléaire) et à la Maison de la Simulation de 2013 à 2016.

Ce mémoire est structuré en 4 chapitres dont je donne un résumé succinct ci-après.

Chapitre 1 : Modélisation d'écoulements complexes

Je présente dans ce chapitre des travaux liés à la modélisation d'écoulements que je qualifie de «complexes». Sous cette terminologie assez vague, je considère des écoulements qui peuvent comprendre plusieurs matériaux mais aussi des écoulements qui mettent en jeu des phénomènes sur plusieurs échelles.

La nature de mon travail requiert de travailler avec des modèles pour lesquels il est nécessaire de bien cerner les hypothèses sur lesquelles ceux-ci s'appuient ainsi que les limites de ces modèles. Ceci est particulièrement important dans un contexte industriel où la culture des ingénieurs fournit beaucoup de fermetures heuristiques et tolère également l'import brutal d'éléments d'un modèle vers un autre en s'appuyant sur des données expérimentales pour quantifier les erreurs commises.

Une routine de modélisation
À défaut de la véritable intuition d'un physicien, j'ai essayé au fil des ans de me constituer une sorte de «trousse à outils» pour analyser et proposer des modèles d'écoulements. Les deux éléments clefs de cette boite à outils sont le Principe de Hamilton qui permet de décrire les structures conservatives du système et un bilan d'entropie qui permet de décrire des structures dissipatives. Mais ces deux éléments n'opèrent pas seuls. Ils sont articulés dans un environnement d'hypothèses qui est au moins aussi important. En notant $\mathscr{V}(t) \subset \mathbb{R}^d$ le volume occupé par une portion de fluide à l'instant $t \in [t_0, t_1]$ et $\Omega = \{(\mathbf{x}, t) \in \mathbb{R}^d \times [t_0, t_1] \mid \mathbf{x} \in \mathscr{V}(t), t_0 \leq t \leq t_1\}$, je propose de décrire cette boite à outils sous la forme d'une séquence en trois étapes.

1. **Caractérisation du système**.
   (a) Choisir une collection de champs eulériens $(\mathbf{x}, t) \mapsto \mathcal{T} = (\mathcal{T}_1, \dots, \mathcal{T}_m) \in \mathbb{R}^m$ qui vont permettre de décrire l'état du système. Par exemple : une ou plusieurs densités, une ou plusieurs vitesses.
   (b) Munir le système d'une cinématique en définissant les vitesses qui transportent le ou les matériaux.
   (c) Postuler des contraintes constitutives pour le système qui peuvent être :
      — de nature algébrique, par exemple : une loi d'état ;
      — de nature différentielle, par exemple : la conservation de la masse.

2. Modélisation de la **structure conservative du système**.
   (a) Définir une énergie cinétique $\mathcal{T} \mapsto E_{\text{kin}}$ associée au système.
   (b) Définir une énergie potentielle $\mathcal{T} \mapsto E_{\text{pot}}$ associée au système.
   (c) Définir une énergie lagrangienne (ou Lagrangien) $\mathcal{T} \mapsto \mathscr{L} = E_{\text{kin}} - E_{\text{pot}}$ et une action hamiltonienne $\mathcal{T} \mapsto \mathscr{A} = \int_\Omega \mathscr{L}(\mathcal{T}(\mathbf{x}, t))\, \mathrm{d}\mathbf{x}\mathrm{d}t$.
   (d) On applique le principe de Hamilton : si $\overline{\mathcal{T}}$ est une transformation physique du système, on va chercher un jeu d'Équations aux Dérivées Partielles (EDPs) dont elle est solution au sens où elle va vérifier le principe de Hamilton. Pour ce faire, on considère une famille $(\mathbf{x}, t, \zeta) \mapsto \hat{\mathcal{T}}$ de perturbation de $\overline{\mathcal{T}}$ paramétrée par $\zeta \in [-1, 1]$, telle que :
      — $\hat{\mathcal{T}}(\mathbf{x}, t, \zeta = 0) = \overline{\mathcal{T}}(\mathbf{x}, t)$;
      — $\hat{\mathcal{T}}$ vérifie les contraintes constitutives proposées au point 1 pour $\zeta \in [-1, 1]$;
      — $\hat{\mathcal{T}}(\mathbf{x}, t, \cdot) = \overline{\mathcal{T}}(\mathbf{x}, t)$ pour $(\mathbf{x}, t, \zeta) \in \partial\Omega \times [-1, 1]$.
      On exige que $\overline{\mathcal{T}}$ soit un point stationnaire de $\zeta \mapsto \mathscr{A}(\hat{\mathcal{T}})$, à savoir $\frac{\mathrm{d}}{\mathrm{d}\zeta}\left(\mathscr{A}(\hat{\mathcal{T}})\right)\Big|_{\zeta=0} = 0$. C'est cette condition de stationnarité qui va nous fournir les EDPs qui gouvernent le mouvement en l'absence de processus dissipatifs.

3. Modélisation de la **structure dissipative du système**.
   (a) On propose une entropie mathématique η et un flux d'entropie associé $\mathbf{g}$ tels que le système au point 2. en l'absence de dissipation vérifie la loi de conservation supplémentaire $\partial_t \eta + \mathrm{div}(\mathbf{g}) = 0$.
   (b) On ajoute au système conservatif obtenu au point 2 des termes sources voués à piloter la dissipation. Plusieurs expressions différentes pour ces termes sources pourront être testées.
   (c) On réévalue l'expression de $\partial_t \eta + \mathrm{div}(\mathbf{g})$ afin de tenir compte des termes source ajoutés et on obtient une expression de la forme $\partial_t \eta + \mathrm{div}(\mathbf{g}) = \mathcal{Q}$, où $\mathcal{Q}$ est la production d'entropie dans le système.
   (d) On teste des expressions candidates pour les termes source de sorte à assurer que $\mathcal{Q} \leq 0$.

Je dois préciser que cette séquence de 3 étapes n'est pas un programme de travail rigide mais simplement une présentation synthétique d'un ensemble d'éléments qui peuvent intervenir dans un travail de modélisation. Il est important de formuler un certain nombre de remarques concernant cette méthodologie de modélisation.

Tout d'abord, cette méthode n'est absolument pas originale et peut-être considérée comme une compilation d'éléments de la littérature (voir par exemple [Her55, Ser59, Gou78, Sal83, Bed85, Geu86, CG89, Gou90, Sal88, GG99, GG00, Rom98, Tru91, GGP97, Gou07, Ber09, GR09, Pes+18]).

Le principe de Hamilton est un outil puissant qui peut parfoit sembler déroutant. Néanmoins, dans le cadre de mon travail son rôle se résume à proposer une ou plusieurs relations de type bilan d'impulsion qui vont être associées à chaque énergie cinétique mise en jeu dans le système. De plus, il garantit une relation de conservation de l'énergie associée à ces bilans que l'on peut retrouver soit par calcul direct ou en utilisant le théorème de Noether.

Cette présentation synthétique est également une célébration de l'expression «le diable est dans les détails». En effet, comme évoqué précédemment, la méthode s'appuie sur le principe de Hamilton et la proposition d'un bilan d'entropie. Ces deux outils ont besoin d'un cadre d'hypothèses que j'ai présenté. La construction de ce cadre est un élément absolument crucial dans la méthode. Par exemple : dans le cadre d'un mélange de constituants, la définition d'une loi d'état est un problème complexe. Selon l'échelle spatiale ou temporelle à laquelle le modèle est destiné, on peut retenir ou négliger certains phénomènes comme la capillarité. Il est également important de souligner que disposer d'une loi de conservation d'entropie (en l'absence de dissipation) n'est absolument pas trivial.

En aucun cas cette routine en trois étapes ne peut être considérée comme une méthode de modélisation infaillible. Il est possible d'aboutir par exemple à un système mal posé. Ainsi l'intérêt de cette méthode n'est pas de proposer des systèmes dotés de propriétés remarquables par construction, mais plutôt de fournir une sorte de «matériau brut» qui devra être ensuite analysé et comparé à d'autres modèles ou à des résultats expérimentaux.

L'exemple classique d'un écoulement compressible à un constituant
A titre d'exemple, je propose dans ce chapitre de retrouver les modèles classiques d'écoulements compressibles barotropes et non-barotropes donnés par les équations d'Euler. Pour le cas non-barotrope, l'état du milieu est caractérisé par une densité ρ, une vitesse $\mathbf{u}$, une énergie interne e et une entropie (physique) s. Les contraintes constitutives que l'on utilise pour décrire une évolution non-dissipative sont la conservation de la masse, la conservation de l'entropie et une loi d'état $(\rho, s) \mapsto e$ qui est fourni par la théorie thermodynamique.

Un modèle simple d'écoulement diphasique : le modèle hors équilibre (HRM)
Cette section se rapporte aux travaux publiés dans [23, 24, 22, 21, 19, 17, 14].

Je présente ensuite la dérivation d'un modèle diphasique appelé *Homogeneous Relaxed Model* (HRM) qui est structurellement très proche du système des équations d'Euler. On décrit de nouveau le milieu grâce à une densité ρ, une vitesse $\mathbf{u}$, une énergie interne e et une entropie (physique) s auxquelles on ajoute des paramètres qui caractérisent la composition du milieu : la fraction de masse Y, de volume α et d'énergie ψ du fluide 1 (l'autre phase étant le fluide 2). Les contraintes constitutives pour un écoulement non-dissipatif sont : la donnée d'une loi d'état sous la forme d'une fonction $(\tau = 1/\rho, e, Y, \alpha, \psi) \mapsto s$, la conservation de la masse de chaque constituant, de l'entropie et également des quantités $\rho\alpha$ et $\rho\psi$. Bien qu'apparemment similaire aux cas des équations d'Euler, ce modèle s'appuie sur des hypothèses très structurantes qui ne sont pas indiscutables. D'autres choix peuvent être considérés pour les paramètres qui caractérisent la composition, pour la loi d'état du mélange diphasique ainsi que pour les équations vérifiées par α et ψ.

Il est alors possible d'injecter dans le modèle des termes sources supplémentaires dans les équations d'évolution de Y, α et ψ qui gouvernent la composition du mélange. Ces termes sources permettent d'obtenir une inéquation d'évolution pour s. On voit alors que les effets dissipatifs associés tendent à amener le fluide vers un état d'équilibre qui optimise s (pour une énergie e et une densité de mélange ρ fixées).

Équation d'état pour un mélange diphasique
Cette section se rapporte aux travaux publiés dans [23, 24, 22, 21, 19, 14].

J'aborde la question de la définition du mélange et plus particulièrement de l'entropie $(\tau = 1/\rho, e, Y, \alpha, \psi) \mapsto s$. On suppose que les deux fluides qui composent le mélange sont chacun muni de leur propre loi d'état sous la forme d'une fonction strictement concave $(\tau_k = 1/\rho_k, e_k) \mapsto s_k$, $k = 1, 2$. De manière classique la température T_k, la pression P_k et le potentiel chimique g_k du fluide k sont respectivement définis par $1/T_k = (\partial s_k/\partial e_k)$, $P = T_k(\partial s_k/\partial \tau_k)$, $g_k = e_k - T_k s_k + P_k \tau_k$. Nous utilisons pour l'entropie du mélange s une définition classique [Cal85, Del03, Hel05, 21, Fac08, 19, 17, 14] :

$$s(\tau, e, Y, \alpha, \psi) = Y s_1\left(\frac{\alpha\tau}{Y}, \frac{\psi e}{Y}\right) + (1-Y)s_2\left(\frac{(1-\alpha)\tau}{1-Y}, \frac{(1-\psi)e}{1-Y}\right). \tag{i}$$

Cette définition permet de déterminer complètement les termes sources dissipatifs associés au système. Si on se restreint au cas $0 < Y < 1$, l'optimum de l'entropie de mélange est réalisé lorsque les dérivées de s par rapport à α, Y et ψ s'annulent

pour une valeur de (τ, e) fixée. Ceci est équivalent à exiger le triple équilibre classique $T_1 = T_2$, $P_1 = P_2$ et $g_1 = g_2$. On note $Y = Y^{\text{eq}}(\tau, e)$, $\alpha = \alpha^{\text{eq}}(\tau, e)$ et $\psi = \psi^{\text{eq}}(\tau, e)$ les valeurs qui réalisent cet optimum.

Ces relations d'équilibre suggèrent la définition d'une deuxième loi d'état pour le mélange diphasique en supposant que l'équilibre $b = b^{\text{eq}}(\tau = 1/\rho, e)$, $b \in \{Y, \alpha, \psi\}$ est instantané. Dans ce cas, la composition du milieu est définie non plus par des équations d'évolution mais par des fermetures algébriques. La loi d'état du mélange, appelée loi d'état à l'équilibre, prend la forme $(\tau, e) \mapsto s^{\text{eq}}(\tau, e) = s(\tau, e, Y^{\text{eq}}(\tau, e), \alpha^{\text{eq}}(\tau, e), \psi^{\text{eq}}(\tau, e))$. On peut alors voir que deux autres définitions équivalentes de s^{eq} pour $0 < Y < 1$ sont disponibles. La première consiste à écrire s^{eq} comme le résultat d'une sup-convolution entre les fonctions $(m, v, e) \mapsto m s_k(v/m, e/m)$, $k = 1, 2$ (voir [BH05, Hel05, HS06]). La deuxième définition équivalente s'appuie sur un argument géométrique [Car04, 23, 22, 21, Fac08, 14] : si on note $\text{Hypo}(\mathscr{E}) = \{(\tau, e', s') \in (0, +\infty)^2 \times \mathbb{R}) \mid s' \leq \mathscr{E}(\tau', e')\}$ l'hypographe d'une fonction $(\tau, e) \in (0, +\infty)^2 \mapsto \mathscr{E}(\tau, e) \in \mathbb{R}$ dans l'espace τ-e-s alors $\text{Hypo}(s^{\text{eq}})$ est l'enveloppe concave de $\text{Hypo}(s_1) \cup \text{Hypo}(s_2)$.

Ainsi, on peut conclure que la loi d'état à l'équilibre $(\tau, e) \mapsto s^{\text{eq}}$ est obtenue via un processus de «concavification» de l'entropie de mélange s. Il est important de noter que s^{eq} est concave mais pas strictement concave. De plus, ces deux définitions équivalentes fournissent une définition de l'équilibre pour les états de mélange qui correspondent à des phases pures, lorsque $Y = 0$ ou $Y = 1$. Cette loi d'état coïncide avec la construction des équilibres de Maxwell pour les lois d'état non convexes comme la loi de Van der Waals [Van, Kle74].

Un modèle simple d'écoulement diphasique : le modèle à l'équilibre (HEM)
Cette section se rapporte aux travaux publiés dans [23, 24, 22, 21, 19, 14].

Si on considère le système des équation d'Euler complété par l'équation d'état $(\tau, e) \mapsto s^{\text{eq}}(\tau, e)$ on obtient un modèle appelé *Homogeneous Equilibrium Model* (HEM). L'étude des propriétés de ce modèle réserve des surprises. En effet, si on considère tout d'abord le cas barotrope lorsque l'équation d'état s'écrit $\rho \mapsto f^{\text{eq}}(\tau = 1/\rho)$, on voit qu'il existe une zone $\tau_1^* < \tau < \tau_2^*$ dans laquelle f^{eq} est linéaire. Ainsi pour $\tau \in (\tau_1^*, \tau_2^*)$, la pression est constante et la vitesse du son du milieu est nulle. Le système se comporte alors comme un gaz sans pression pour $\tau \in (\tau_1^*, \tau_2^*)$. On perd l'hyperbolicité et on perd l'unicité des solutions entropiques. Néanmoins, il a été démontré que l'unicité des solutions entropiques au sens de Liu [Liu76] pour le problème de Riemann associé au système HEM barotrope est garantie[GS06].

Le cas du modèle HEM non-barotrope est moins pathologique. En effet, bien que l'entropie associée ne soit pas convexe, on peut montrer que la vitesse du son est toujours strictement positive et donc que le système est strictement hyperbolique.

Structure dissipative pour un modèle bifluide
Cette section se rapporte à des travaux réalisés par V. Guillemaud pendant sa thèse de Doctorat [Gui07a] qui a été dirigée par J.-M. HÉRARD et que j'ai encadrée au CEA. Ces travaux ont été publiés dans [Gui07b].

Je m'intéresse ici à un système plus complexe d'écoulements diphasiques dans lequel chaque fluide est muni de sa propre vitesse de transport de la matière u_k (de tels modèles sont parfois appelés *modèles bifluides*). Ces modèles sont structurellement beaucoup plus complexes et bien souvent plus pathologiques que les modèles où la cinématique s'appuie sur une seule vitesse matière [BN86, GSS96, GSS99, GS02, Coq+02, SGR03, Gui07a, Cro+15, Loc16, Loc+16, Che19, CM20, Cor20]. Par exemple, l'hyperbolicité n'est pas toujours garantie de même que la définition des solutions faibles. Un autre point délicat concerne l'établissement d'un bilan d'entropie [Coq+02, Gui07a, Gui07b].

Le système que je considère dans cette partie est un système mettant en jeu une pression P_k pour chaque fluide $k = 1, 2$ ainsi qu'une vitesse u_I et un terme P_I homogène à une pression appelés respectivement vitesse interfaciale et pression interfaciale. La définition de u_I et P_I est un élément clef de cette catégorie de modèles qui a fait l'objet de propositions différentes dans la littérature. En effet, u_I et P_I interviennent via des termes non-conservatifs dans les équations qui rendent très délicate la définition de solutions faibles.

Je ne considère dans cette partie que la question du bilan d'entropie pour ce modèle bifluide, ce qui correspond au point 3 de la routine de modélisation présentée. La question ici n'est pas de trouver une entropie et un flux associé pour un système donné, en s'assurant que la production d'entropie soit correctement signée. Il s'agit de déterminer des contraintes sur u_I et P_I qui permettent d'obtenir un bilan d'entropie pour une entropie η et un flux associé $\mathbf{g}$ déjà choisis. On peut voir que si la définition de u_I ne fait pas intervenir de termes différentiels, alors pour une définition de u_I donnée, le choix de P_I est imposé par la relation

$$\frac{(P_1 - P_I)(u_1 - u_I)}{T_1} = \frac{(P_2 - P_I)(u_2 - u_I)}{T_2}. \tag{ii}$$

La contrainte de positivité pour la production d'entropie permet de suggérer l'expression de termes sources dissipatifs pour les équations d'impulsions, d'énergies, de masses partielles et de fraction de volume. Ces termes sont cohérents respectivement avec une relaxation entre vitesses matières u_k, températures T_k, potentiels chimiques g_k et pressions partielles P_k, $k = 1, 2$.

Un premier pas vers la modélisation multi-échelle
Cette section se rapporte aux travaux publiés dans [1].

Je présente un modèle que je considère comme un premier pas dans mes travaux vers des modèles qui décrivent un écoulement diphasique sur plusieurs échelles. Ce modèle est obtenu en suivant précisément la méthode en 3 points introduite au début du chapitre I.

On suppose connus deux fluides, chacun muni d'une loi d'état barotrope. En utilisant les mêmes notations que pour le modèle HRM, on suppose que l'état du milieu peut être caractérisé par une densité de mélange ρ, une vitesse commune aux deux fluides $\mathbf{u}$, la fraction de masse Y et la fraction de volume α du fluide 1.

Dans ce travail, on se focalise sur un effet multi-échelle particulier qui consiste à tenir compte de mouvements à petite échelle des interfaces entre fluides. Il est important tout d'abord de préciser ce que l'on entend par «sous-échelle». On suppose tout d'abord que les interfaces sont transportées à grande échelle par une vitesse matière $\mathbf{u}$ commune aux deux fluides. On suppose de plus que dans le référentiel associé à $\mathbf{u}$, ces interfaces sont également sujettes à de petits déplacements. On renonce à décrire ces petits déplacements par une cinématique complète au sens où on considère qu'il n'est pas possible d'associer une variation de la position à grande échelle liée à cette vitesse de petite échelle.

La première question est donc de proposer un moyen d'injecter les hypothèses relatives au comportement sous-échelle dans le modèle. Pour ce faire, nous utilisons l'énergie cinétique du système E_{kin}. On suppose que E_{kin} est la somme d'une contribution classique $E_{\text{kin}}^{\text{large}} = \rho|\mathbf{u}|^2/2$ liée au mouvement à grande échelle et d'une énergie cinétique $E_{\text{kin}}^{\text{small}}$ liée aux mouvements des interfaces à petite échelle. Si on note $\mathrm{D}_t(\cdot) = \partial_t(\cdot) + \mathbf{u}^T\nabla(\cdot)$ la dérivée matérielle, on propose de définir $E_{\text{kin}}^{\text{small}} = \nu(\alpha)(\mathrm{D}_t\,\alpha)^2/2$, où $\nu(\alpha)$ est une quantité positive. On associe au système une énergie potentielle définie par un potentiel barotrope de mélange de la forme $E_{\text{pot}}(\rho, Y, \alpha) = f(\rho, Y, \alpha)$ comme celui défini pour le modèle barotrope HRM. On peut alors définir un lagrangien $\mathscr{L}$ pour le système en posant

$$\mathscr{L}(\rho, \mathbf{u}, Y, \alpha, \mathrm{D}_t\,\alpha) = \frac{1}{2}\rho|\mathbf{u}|^2 + \frac{1}{2}\nu(\alpha)(\mathrm{D}_t\,\alpha)^2 - f(\rho, Y, \alpha). \tag{iii}$$

Le principe de Hamilton nous fournit ensuite deux équations d'évolution : une première équation classique de bilan d'impulsion grande échelle $\rho\mathbf{u}$ ainsi qu'une deuxième équation d'ordre deux en temps sur α. En introduisant une nouvelle variable $\omega = (\mathrm{D}_t\,\alpha)/(\rho Y)$, l'équation d'ordre 2 sur α s'écrit comme un système de deux équations d'ordre 1 en temps portant sur les variables α et ω. On voit alors que ω joue un rôle analogue à celui d'une impulsion de petite échelle. Ainsi, le principe de Hamilton nous permet d'écrire un système muni d'un double bilan d'impulsion : un bilan pour les grandes échelles via $\rho\mathbf{u}$ et un bilan pour les petites échelles via ω. Le système conservatif obtenu est ensuite complété par une structure dissipative en établissant un bilan d'entropie. Ce bilan d'entropie suggère l'ajout d'un terme source $-\epsilon\rho Y\omega/\nu$ à l'équation d'évolution de ω. Les coefficients ϵ et ν sont appelés coefficients de micro-inertie et micro-viscosité.

Le modèle ainsi obtenu peut être relié à des systèmes de la littérature utilisés pour la simulation d'écoulements à interface en étudiant des régimes asymptotiques. En effet, en supposant que $\epsilon \to 0$ et $\nu = O(\epsilon^0)$, on retrouve un système à 4 équations [CVV02b, CVV02a, Car04] dans lequel α est gouverné par l'équation $\mathrm{D}_t\,\alpha = (P_1 - P_2)/\epsilon$. Le régime asymptotique $\epsilon \to 0$ et $\nu \to 0$ aboutit à un système à 3 équations dans lequel α est solution de $P_1(\rho Y/\alpha) = P_2(\rho(1-Y)/(1-\alpha))$ pour ρ et Y fixés [CVV02b, CVV02a, Car04].

Il est également possible d'établir des liens avec une autre catégorie de modèles d'écoulements diphasiques, les écoulements à phase dispersée, pour lesquels la description à grande échelle de l'interface entre fluides n'est pas envisageable. En effet, si on injecte dans le modèle l'hypothèse que la présence du fluide 1 correspond à une population d'inclusions sphériques de taille homogène $R(\mathbf{x}, t)$ réparties selon une densité de nombre $n(\mathbf{x}, t)$ alors on peut simplement estimer la fraction de volume par $\alpha(\mathbf{x}, t) = 4n(\mathbf{x}, t)\pi R(\mathbf{x}, t)^2/3$. En négligeant les variations de densité du fluide 2 et en supposant la conservation du nombre d'inclusions, *i.e.* $\partial_t n + \mathrm{div}(n\mathbf{u}) = 0$, on peut en déduire une équation d'évolution sur le rayon des inclusions R. L'équation vérifiée par R est une équation d'ordre 2 en temps qui est similaire à l'équation de Rayleigh-Plesset [Ray17, PP77] utilisée pour décrire le mouvement d'une bulle de gaz au sein d'un liquide. Cette comparaison est non seulement un gage de cohérence avec un modèle connu mais surtout un moyen d'obtenir l'estimation suivante pour les coefficients ν et ϵ

$$\nu = \rho_2(3\alpha)^{-1/3}(4\pi n)^{-2/3}, \qquad \epsilon = 4\mu_2/(3\alpha), \tag{iv}$$

où μ_2 est la viscosité dynamique du fluide 2. En considérant $R = \bar{R}(1 + rz)$ et en supposant $0 < r \ll 1$ on peut mener une analyse similaire dans un régime linéaire de petites perturbations de R autour d'une valeur constante $\bar{R}$. Le calcul aboutit à une équation différentielle ordinaire d'ordre 2 en la variable z que l'on peut alors rapprocher de modèles de la littérature [Pro77, CDL83]. Cette comparaison permet alors d'identifier ν et ϵ comme suit :

$$\nu = \rho_2\bar{R}^2/\bar{\alpha}, \qquad \epsilon = 4\mu_2/(3\bar{\alpha}) + 2\rho_2\bar{R}^2(\gamma_{\text{th}} + \gamma_{\text{ac}})/(3\bar{\alpha}), \tag{v}$$

où les coefficients γ_{th} et γ_{ac} caractérisent une dissipation dans le système due à des effets thermiques et acoustiques [Pro77, CDL83]. Des analyses similaires on été également proposées dans [GS02, Gav14].

Nous avons de plus confronté ce modèle d'écoulement à deux échelles de vitesse à des résultats expérimentaux dans le régime acoustique. Pour ce faire, nous considérons le système linéarisé pour lequel nous cherchons une solution sous le forme d'une onde plane progressive monochromatique. On peut obtenir une relation de dispersion explicite qui relie le nombre d'onde et la pulsation de l'onde plane. L'influence des petites échelles sur le comportement de la solution est très substantielle. Il est ainsi possible de reproduire des effets de résonance qui sont totalement absents dans le cas $\nu = 0$. Des comparaisons avec un modèle bifluide proposé par [CDL85] ainsi que des résultats expérimentaux [Sil57, Ler+08] montrent un bon accord avec les estimations du modèle à deux échelles de vitesse.

Un modèle d'écoulement à N composants séparés par des interfaces minces
Cette section se rapporte aux travaux publiés dans [20, 18, 10, 15, 13, 15, 8].

Plusieurs de mes travaux sont dédiés à la simulation d'écoulements compressibles mettant en jeu $N \geq 2$ fluides séparés par des interfaces. Les méthodes de simulation utilisées dans ces travaux sont parfois appelées *méthodes de capture d'interface*. Pour ces écoulements, on suppose que chaque fluide $k = 0, \dots N-1$ est muni d'une équation d'état EOS_k sous la forme d'une loi de pression $P_k^{\text{EOS}} : (\rho_k, e_k) \mapsto P_k$ ou de manière équivalente $e_k^{\text{EOS}} : (\rho_k, P_k) \mapsto e_k$, si P_k, ρ_k et e_k représente respectivement la pression, la densité et l'énergie interne spécifique du fluide k.

Le problème consiste à modéliser un écoulement dans un domaine $\mathscr{V} \subset \mathbb{R}^d$ où chaque fluide k occupe un sous-domaine $\mathscr{V}_k(t) \subset \mathscr{V}$ à l'instant t, tel que $\mathscr{V}_k(t) \cap \mathscr{V}_{k'}(t) = \emptyset$ quand $k \neq k'$. On fait l'hypothèse que le vide ne peut pas se produire dans $\mathscr{V}$ de sorte que $\overline{\cup_{k=0,\dots,N-1} \mathscr{V}_k(t)} = \overline{\mathscr{V}}$. Dans chaque sous-domaine $\mathscr{V}_k(t)$, on suppose que l'écoulement est régi par les équations d'Euler complétées par la loi d'état EOS_k. L'interface entre le fluide k et le fluide k' est définie par $\overline{\mathscr{V}_k}(t) \cap \overline{\mathscr{V}_{k'}}(t)$ que l'on suppose être une hypersurface de $\mathbb{R}^d$. Lorsque l'on traverse l'interface $\overline{\mathscr{V}_k}(t) \cap \overline{\mathscr{V}_{k'}}(t)$ les propriétés du milieu subissent une discontinuité qui s'exprime par le changement de loi d'état. Sur ces interfaces, on fait des hypothèses liées à la dynamique : on suppose qu'il y a continuité de la vitesse matière et de la pression.

Le modèle ainsi défini s'apparente à un problème de couplage à travers plusieurs frontières libres qui sont transportées à la vitesse du milieu. Dans le cadre de méthodes de capture d'interface, on remplace ce problème de couplage par un problème portant sur un fluide équivalent occupant tout le domaine $\mathscr{V}$. On note $(\mathbf{x}, t) \mapsto Z_k$ la fonction indicatrice de $\mathscr{V}_k(t)$, souvent appelée dans ce contexte «fonction couleur» associée au fluide k. Comme seul un fluide peut occuper la position $\mathbf{x} \in \mathscr{V}$ à l'instant t, les fonctions couleurs doivent vérifier la contrainte $Z_0(\mathbf{x}, t) + \dots + Z_{N-1}(\mathbf{x}, t) = 1$.

Etant donnée la continuité de la vitesse aux interfaces, les fonctions couleurs Z_k évoluent selon

$$\partial_t Z_k + \mathbf{u}^T \boldsymbol{\nabla} Z_k = 0, \quad k = 0, \dots N-1, \tag{vi}$$

où le produit non-conservatif $\mathbf{u}^T \boldsymbol{\nabla} Z_k$ est bien défini du fait que Z_k et $\mathbf{u}$ ne peuvent simultanément être discontinues [1]. On voit alors qu'il est possible de substituer au problème de couplage initial un problème de capture de solutions faibles vérifiant des relations de saut qui reproduisent les conditions de couplage.

Pour capturer la position des interfaces il est alors naturel de chercher à résoudre les équations de transport sur Z_k en utilisant une condition initiale telle que $Z_k \in \{0, 1\}$ et une méthode de discrétisation standard comme les Volumes Finis. Dans ce cas, la discontinuité initiale en Z_k sera diffusée numériquement en une zone pour laquelle $0 < Z_k < 1$, de la même manière que les chocs sont étalés sur quelques cellules du maillage par les schémas numériques de capture de choc. On s'attend cependant à ce que ces solutions convergent vers la discontinuité attendue lorsque le pas de discrétisation spatial tend vers 0. Malheureusement, la situation est plus critique que pour le cas des chocs : dans les région où $0 < Z_k < 1$ il n'y a pas *a priori* d'équation d'état valable. Ainsi, la définition du modèle est trop lacunaire pour capturer la position des interfaces avec de telles techniques numériques.

La solution proposée consiste à utiliser un modèle de mélange à N composants, où les fonctions couleurs Z_k ont un rôle très similaire à celui des fractions volumiques et où on suppose un équilibre de pression entre tous les fluides. Ce modèle est une extension directe d'un modèle proposé dans un travail effectué pendant ma thèse de Doctorat [27, 26]. Il est très important de noter que ce modèle de mélange n'a *a priori* pas vocation à représenter un véritable mélange physique. En effet, il est important de garder à l'esprit que les zones $0 < Z_k < 1$ où apparait ce mélange n'ont ici pour seule vocation que de converger vers les discontinuités qui représentent la position des interfaces matérielles.

Ce modèle à N composants met en jeu les fonctions couleurs Z_k ainsi que des variables de fraction de masse Y_k pour chaque fluide k. De prime abord, pour une condition initiale où $Z_k \in \{0, 1\}$, ces variables sont redondantes dans le système d'équations. Cependant, pour le système discrétisé, lorsque sont présentes des régions où $0 < Z_k < 1$, elles jouent un rôle différent et ne feront pas l'objet du même traitement numérique. Les fractions de masse Y_k sont utilisés pour assurer la conservation des masses partielles, alors que les fonctions couleurs Z_k servent à traquer la position des interfaces. Pour conclure, ce système à N composants est hyperbolique sous des conditions simples portant sur la thermodynamique des fluides mis en jeu.

Chapitre 2 : Méthodes numériques pour les écoulements compressibles

Dans ce chapitre, je présente une série de travaux sur les schémas numériques pour l'approximation des écoulements compressibles.

Un système modèle
Je propose tout d'abord un système modèle qui permet de mettre en exergue les mécanismes sur lesquels vont s'appuyer les schémas numériques présentés. Ce système met en jeu une seule vitesse matière $\mathbf{u}$, une partie convective portant sur la densité ρ, des champs regroupés dans une variable notée $\mathbf{W}$, des termes sources et des champs transportés $\boldsymbol{\Psi}$ à vitesse $\mathbf{u}$. L'état du milieu est représenté par $(\rho, \mathbf{W}, \boldsymbol{\Psi})$ et ce système modèle s'écrit

$$\partial_t \rho + \text{div}(\rho \mathbf{u}) = 0, \qquad \partial_t(\rho \mathbf{W}) + \text{div}(\rho \mathbf{W} \mathbf{u}^T + \mathbf{T}) = \mathbf{R}_{\mathbf{W}}, \qquad \partial_t \boldsymbol{\Psi} + (\partial_x \boldsymbol{\Psi}) \mathbf{u}^T = \mathbf{R}_{\boldsymbol{\Psi}}. \tag{vii}$$

1. En fait, grâce à la conservation de la masse, on peut considérer de manière équivalente l'équation de conservation $\partial_t(\rho Z_k) + \text{div}(\rho Z_k \mathbf{u}) = 0$.

Approche classique Lagrange-Remap pour les écoulements mono-dimensionnels
Je rappelle ici dans un cadre mono-dimensionnel une méthode classique de la littérature : la méthode Lagrange-Remap [GR96, Des17] (aussi appelée Lagrange-Projection). Si $(x_{i+1/2})_{i\in\mathbb{Z}} \subset \mathbb{R}$ est une suite strictement croissante, on considère un maillage de l'espace (dit maillage eulérien) formé des cellules $K_i = (x_{1-1/2}, x_{1+1/2})$, $i \in \mathbb{Z}$ et la donnée $(\rho_i^n, \mathbf{W}_i^n, \mathbf{\Psi}_i^n)$ de l'état fluide à l'instant t^n dans K_i. On peut résumer la méthode Lagrange-Remap en 4 étapes :

— définition des coordonnées lagrangiennes à l'instant t^n : on considère une collection de «particules lagrangiennes» dont la position à l'instant t^n dans le référentiel eulérien est $\xi_{1+1/2} = x_{1+1/2}$ et qui dont transportées à la vitesse matière à la position $\widetilde{x}_{1+1/2}$ (dans le référentiel eulérien) à l'instant $t^{n+1} = t^n + \Delta t$;
— définition du maillage lagrangien : on considère une cellule lagrangienne $K_i^{\text{Lag}} = (\xi_{1-1/2}, \xi_{1+1/2})$ à laquelle on associe l'état fluide $(\rho_i^n, \mathbf{W}_i^n, \mathbf{\Psi}_i^n) = (\rho_i^{\text{Lag}}, \mathbf{W}_i^{\text{Lag}}, \mathbf{\Psi}_i^{\text{Lag}})$ dans le référentiel lagrangien à l'instant t^n ;
— étape lagrangienne : on met à jour l'état du fluide à la valeur $(\widetilde{\rho}_i, \widetilde{\mathbf{W}}_i, \widetilde{\mathbf{\Psi}}_i)$ en résolvant de manière approchée les équations du mouvement en coordonnées de Lagrange jusqu'à l'instant t^{n+1} ;
— étape de Remap/Projection : on met à jour l'état du fluide à la valeur $(\rho_i^{n+1}, \mathbf{W}_i^{n+1}, \mathbf{\Psi}_i^{n+1})$ en ré-échantillonnant les valeurs lagrangiennes $(\widetilde{\rho}_i, \widetilde{\mathbf{W}}_i, \widetilde{\mathbf{\Psi}}_i)$ dans chaque maille eulérienne K_i, en tenant compte de la nouvelle position $\widetilde{x}_{i+1/2}$ des particules lagrangienne dans le référentiel eulérien.

Pour des problèmes mono-dimensionnels, cette méthode peut s'exprimer comme un schéma classique de type Volumes Finis. Elle découple naturellement les effets liés à la pression (pris en compte dans l'étape lagrangienne) des phénomènes de transport de la matière (pris en compte dans l'étape de Remap/Projection).

Méthode anti-diffusive de capture d'interface
Cette section se rapporte à des travaux publiés dans [20, 18, 15, 15, 13, 10].

L'approche Lagrange-Remap est très utile pour la simulation des problèmes à interface par des méthodes de capture d'interface. On considère le modèle à N composants présenté au chapitre I. Comme on l'a vu, les méthode de capture d'interface tendent à créer des zones où l'interface est épaissie dans une zone de transition (qui à convergence en maillage doit tendre vers une discontinuité). Pour un maillage fixé, la diffusion numérique peut malheureusement envahir le domaine de calcul, ce qui empêche de localiser précisément les interfaces.

Une schéma numérique qui s'inspire des travaux de [DL01, Lag02, JL07] est proposé afin de contrôler cette diffusion numérique pour les modèles de capture d'interface présentés au chapitre I. Pour ce faire, on s'appuie sur la structure très particulière des schémas Lagrange-Remap. Dans la phase Lagrange, les interfaces sont stationnaires. Ainsi, la diffusion numérique liée au transport des interfaces n'intervient-elle que dans la phase de Remap. Dans cette phase, il est possible d'utiliser une technique de transport anti-diffusif pour le traitement des fonctions couleurs. Grâce à un calcul récursif des flux pour l'ensemble des fonctions couleur, il est possible de traiter le cas de $N > 2$ composants tout en satisfaisant la contrainte $Z_0 + \cdots + Z_{N-1} = 1$ au niveau discret.

La méthode obtenue est conservative par rapport à toutes les masses partielles, la quantité de mouvement et l'énergie totale du milieu. La stabilité est garantie sous une contrainte de type Courant-Friedrichs-Lewy (CFL) classique, assurant en particulier un principe du maximum local pour les fonctions couleurs. La méthode étant structurellement mono-dimensionnelle, on peut réaliser des simulations multi-dimensionnelles sur maillage cartésien grâce à un splitting directionnel.

Discrétisation pour les écoulements compressibles par une méthode de splitting acoustique/transport
L'approche Lagrange-Remap pour les cas multi-dimensionnels requiert le suivi d'un maillage lagrangien ce qui est une procédure complexe. Néanmoins, la méthode mono-dimensionnelle est très simple et possède des spécificités très intéressantes :

— elle permet de découpler des phénomènes physiques tels que le transport et l'acoustique ;
— elle permet d'écrire des schémas conservatifs ;
— pour le cas des équation d'Euler, elle permet un découplage des ondes linéaires (transport) et des ondes vraiment non-linéaires (acoustique).

Une autre particularité de la méthode Lagrange-Remap a été exploitée dans [Coq+08, Coq+10]. Rappelons tout d'abord que le nombre de Mach M est un nombre sans dimension qui est défini par $M = u_0/c_0$, où u_0 et c_0 sont respectivement des ordres de grandeur pour la vitesse matière de l'écoulement et la vitesse du son. Dans le cas où $M \ll 1$, un nouveau découplage en terme d'ordre de grandeur des vitesses apparait. En effet les ondes acoustiques sont beaucoup plus rapides que les ondes de transport matériel. Alors que l'étape de Remap restitue les ondes lentes qui pilotent la dynamique de l'écoulement, l'étape Lagrange rend compte des ondes rapides. Ceci suggère comme dans [Coq+08, Coq+10] d'impliciter (en temps) la partie Lagrange du schéma en laissant explicite l'étape Remap.

Toutes ces raisons ont motivé l'élaboration d'une méthode similaire à l'approche Lagrange-Remap mono-dimensionnel qui puisse également être opérationnelle dans un contexte multi-dimensionnel sur maillage non-structuré. Cet effort a abouti à proposer une méthode qui s'appuie sur un splitting d'opérateurs en deux pas : dans le premier pas on considère un sous-système qui ne comporte que les éléments liés à l'acoustique (étape acoustique) et dans le deuxième pas on ne retient

que les opérateurs liés au transport (étape de transport). Sur le système modèle (vii) ceci se traduit de la manière suivante :

$$\begin{cases} \partial_t \rho & + (\partial_{\mathbf{x}} \rho)\mathbf{u} & + \rho \operatorname{div}(\mathbf{u}) & = 0, & \text{(viiia)} \\ \partial_t (\rho \mathbf{W}) & + \partial_{\mathbf{x}} (\rho \mathbf{W})\mathbf{u} & + \rho \mathbf{W} \operatorname{div}(\mathbf{u}) + \mathbf{div}(\mathbf{T}) & = 0, & \text{(viiib)} \\ \partial_t \mathbf{\Psi} & + (\partial_{\mathbf{x}} \mathbf{\Psi})\mathbf{u} & & = 0, & \text{(viiic)} \end{cases}$$

où les termes bleus correspondent au sous-système acoustique et ceux en rouge correspondent au sous-système de transport. Nous avons proposé d'exploiter ce splitting dans le cadre d'une méthode de type Volumes Finis.

L'étape de transport est discrétisée grâce à une simple méthode de décentrement amont (upwind). Pour l'étape acoustique, nous employons une discrétisation de type Volumes Finis pour laquelle les flux doivent être dérivés au cas par cas, selon le système considéré. On voit alors que le schéma complet est conservatif en les variables ρ et $\rho\mathbf{W}$. Dans le cas mono-dimensionnel, il est possible de retrouver la même discrétisation que celle obtenue avec l'approche Lagrange-Remap classique, bien que la méthode soit purement eulérienne : aucun maillage lagrangien n'est nécessaire à sa mise en œuvre.

Splitting acoustique/transport pour les équations d'Euler : méthodes IMEX et régime de Mach
Cette section se rapporte à des travaux publiés dans [5, 7].

Le cas des équations d'Euler est le système sur lequel la méthode de splitting acoustique/transport a été élaborée. On voit dans ce cas que le système acoustique est strictement hyperbolique. En notant c la vitesse du son du fluide, les valeurs propres associées sont $\pm c$ et 0, l'entropie (physique) vérifie $\partial_t s \geq 0$ et le système est invariant par rotation. Ces propriétés sont très similaires au système mono-dimensionnel de la dynamique des gaz en coordonnées Lagrangienne.

La discrétisation de la partie acoustique est réalisée grâce à une relaxation à la Suliciu [Sul90, Bou04, CC08] qui permet de s'affranchir des non-linéarités du système liées à la loi d'état en remplaçant la pression du système par une pression artificielle Π. On obtient un système acoustique approché plus simple pour lequel il est possible de résoudre explicitement le problème de Riemann. La solution du problème de Riemann fournit une formule de mise-à-jour par flux. On voit que le caractère entropique est garanti sous contrainte CFL pour le cas d'un schéma explicite en temps, de même que la positivité de la masse et l'énergie interne. Il est également possible d'opter pour une intégration implicite en temps de l'étape acoustique. On remarque alors qu'un découplage s'opère dans les équations grâce à la relaxation : le système linéaire qui intervient dans le schéma numérique se réduit à un système sur les seules variables $\mathbf{u}$ et Π. Les autres variables : la densité et l'énergie sont mises à jour par une formule qui n'implique pas de système linéaire (bien que cette mise-à-jour soit implicite en temps). Il est possible de montrer que pour des conditions aux limites simples (conditions aux limites périodiques et Neumann homogène), on a existence et unicité de la solution du système linéaire portant sur $(\mathbf{u}, \Pi)$.

La discrétisation de l'étape de transport s'opère grâce à un schéma explicite amont. Ainsi, on obtient au choix : une méthode complètement explicite ou un schéma IMplicite (pour la partie lagrange) et EXplicite (pour la partie transport), souvent abrégé en IMEX. On peut considérer que ce splitting d'opérateurs permet d'isoler dans la méthode IMEX les éléments du système que l'on souhaite impliciter tout en laissant les autres explicites. Pour des écoulements subsoniques, si les ondes acoustiques sont résolues grossièrement du fait de la diffusion numérique, les phénomènes de transport sont approchés plus précisément grâce au choix du pas de temps qui n'est plus contraint que par la vitesse matière.

Dans le contexte d'écoulements subsoniques, la question de la simulation des écoulements à bas nombre de Mach par des méthodes de type Volumes Finis a fait l'objet de très nombreux travaux. Il a été mis en évidence par la communauté que la précision des méthodes de type Godunov s'écroule selon le type de maillage utilisé pour des problèmes multi-dimensionnels lorsque $M \ll 1$. Cette question est toujours un sujet d'actualité pour la communauté. Plusieurs éléments de diagnostic ont été apportés ces dernières années [Tur87, GV99, Cle00, GM04, DOR10, Del10, DOR10, Del+16]. Ces travaux suggèrent que le problème est lié à la discrétisation des termes de gradient de pression qui induisent une diffusion numérique trop importante lorsque $M \ll 1$ (pour une taille de maillage fixée). Fort de ce constat, en transposant ces analyses au cas du schéma splitté acoustique/transport, on voit immédiatement que la discrétisation de ces termes n'intervient que dans la phase acoustique.

En menant une analyse dans le cas mono-dimensionnel on peut mettre en évidence une erreur de troncature du schéma importante pour l'équation d'impulsion. Cette erreur dont l'ordre de grandeur est $O(\Delta x / M)$ provient de la discrétisation de la pression. Plus précisément, cette erreur est issue de la partie décentrée qui intervient lors de l'estimation de la pression aux faces des cellules. Bien que cette estimation ne puisse pas être considérée comme une véritable analyse du problème [2], elle suggère de modifier le décentrement de la pression de sorte à obtenir une erreur uniforme en M. Ceci permet d'écrire un nouveau solveur Volume Finis en modifiant les flux de la seule étape acoustique. La question se pose alors de savoir si le solveur acoustique modifié perd ses bonnes propriétés de stabilité. On peut voir que ce n'est pas le cas. Étant donné la simplicité de la structure du système acoustique (en comparaison au système Euler complet) il est possible d'associer un solveur de Riemann approché à 3 ondes à ce nouveau solveur bas Mach. On voit que ce solveur de Riemann approché dégénère naturellement vers le solveur d'origine lorsque $M \to 1$ et que les contraintes de stabilité sur le choix du pas de temps sont inchangées. Il est à noter cependant que le caractère entropique du schéma bas Mach n'est plus garanti dans la

2. Pour les équations d'Euler, le problème de perte de précision des schémas de type Godunov, en l'absence de termes sources et pour des conditions aux limites périodiques n'apparait pas en 1D. Une analyse réellement multi-dimensionnelle en formulant des hypothèses sur le choix des maillages est nécessaire afin d'obtenir un réel diagnostic comme dans [DOR10, Del10, DOR10].

limite asymptotique $M \to 0$ par les estimations utilisées pour la méthode acoustique/transport d'origine sans correction bas Mach.

La méthode de splitting acoustique/transport combine plusieurs avantages : une simplicité d'analyse et d'implémentation, la conservativité pour la densité, l'impulsion et l'énergie, la possibilité d'implémenter des stratégies d'intégration en temps IMEX et d'utiliser une correction pour augmenter la précision du schéma à bas nombre de Mach. Ainsi, il a semblé intéressant d'utiliser l'approche par splitting acoustique/transport comme une base de travail pour proposer des méthodes de simulation adaptées à d'autres cadres applicatifs.

Schéma préservant l'asymptote pour les équations d'Euler avec gravité et friction
Cette section se rapporte à des travaux publiés dans [11].

On considère ici la simulation d'écoulements mono-dimensionnels en présence de termes de friction et de gravité [3]. Si on se place dans le régime où le terme de friction est très grand et que l'on considère l'évolution du système en temps long, on peut voir que formellement le système adopte un comportement asymptotique très similaire aux équations de Darcy. L'objectif de ce travail est de proposer une méthode IMEX qui préserve ce régime asymptotique pour lequel le rôles des termes sources est déterminant.

Nous choisissons de prendre en compte les termes de friction et de gravité dans l'étape acoustique grâce à une relaxation de type Suliciu et une approche de consistance au sens intégral [Gal02, Gal03, Bou04]. Ceci nous permet de dériver un solveur de Riemann approché mettant en jeu 3 ondes : deux ondes de vitesse $\pm a$, si $a > 0$ est un constante vérifiant les conditions de Whitham, tenant le rôle d'ondes acoustiques approchées et une onde de vitesse nulle à travers laquelle on prescrit des relations de saut qui restituent l'effet des termes sources.

Splitting acoustique/transport pour un modèle bifluide
Cette section se rapporte à des travaux publiés dans [16].

On s'intéresse ici à un système bifluide dont la structure est plus complexe que le système modèle (vii). En effet, ce système met en jeu 3 vitesses de transports : les deux vitesses matières u_1 et u_2 ainsi que la vitesse interfaciale u_I. De plus, le système inclut des termes non-conservatifs liés à la pression interfaciale P_I.

Nous proposons un splitting d'opérateur en 3 sous-systèmes :

— un sous-système acoustique dans lequel l'onde associée à la fraction de volume α_k est stationnaire ;
— un sous-système de transport dans lequel l'onde associée à la fraction de volume α_k est stationnaire ;
— un sous-sytème tenant compte des termes non-conservatifs $u_I \partial_x \alpha_k$ liés au transport de α_k et des termes non-conservatifs liés à la pression interfaciale $(P_k - P_I, u_k P_k - u_I P_I)\partial_x \alpha_k$.

La question des termes non-conservatif est traitée de la manière suivante : il est possible de choisir une discrétisation pour le dernier sous-système qui permet de retrouver une discrétisation complètement conservative lorsque $P_I = 0$ pour les équations d'impulsions $\alpha_k \rho_k u_k$ et d'énergie $\alpha_k \rho_k E_k$.

Cette stratégie nous permet de proposer une discrétisation IMEX pour ce système bifluide. Cette problématique, bien qu'importante pour de nombreuses applications industrielles où les écoulements sont lents n'a été que peu étudiée dans la littérature. Les résultats numériques, bien que cohérents avec les solutions analytiques étudiées peuvent présenter des overshoots et ne sont pas pleinement satisfaisants.

Splitting acoustique/transport pour les équations de Saint-Venant
Cette section se rapporte à des travaux publiés dans [6].

L'adaptation de la méthode de splitting acoustique/transport aux équations de Saint-Venant pose essentiellement deux problèmes : tenir compte du terme source non-conservatif lié aux variations de topographie $x \mapsto \varkappa(x)$ et proposer une un schéma dit «équilibre» (well-balanced scheme) [GL96b, GL96a, Gos00, Bou04]. Dans le cas des équations de Saint-Venant, un schéma équilibre permet de préserver des états stationnaires qui équilibrent les termes de flux convectif et les termes de variation de topographie. Si on note $(x,t) \mapsto h$ le champ de hauteur d'eau, pour une fonction de topographie donnée $x \mapsto \varkappa(x)$, parmi tous les états stationnaires du système nous nous concentrons sur le fameux état du *lac au repos* défini par une vitesse nulle $u = 0$ et $h(x) + \varkappa(z) = \mathrm{c}^{\mathrm{ste}}$.

On choisit comme précédemment d'inclure le terme source dans l'étape acoustique. En utilisant une approche similaire à celle du cas des équations d'Euler avec friction et gravité On propose un solveur de Riemann approché à 3 ondes : deux ondes de vitesse $\pm a$ vérifiant les relations de saut classiques des ondes acoustiques lorsque a est une constante qui satisfait les conditions de Whitham et une onde stationnaire qui porte l'influence du terme non-conservatif de topographie. On peut voir que le solveur ainsi obtenu est consistant au sens intégral [Gal02, Gal03, Bou04]. De plus, il est possible de définir les sauts à travers l'onde stationnaire de sorte à ce que les états du lac au repos soient préservés.

3. Historiquement, ce travail précède l'élaboration de l'approche par splitting acoustique/transport et s'appuyait sur une technique Lagrange-Remap classique. Néanmoins dans le cadre mono-dimensionnel, on peut considérer que les deux approches sont équivalentes.

L'étape de transport est encore une fois traitée par une méthode de décentrement amont et on peut vérifier que le schéma complet est entropique sous condition CFL.

L'étape acoustique peut également être implicitée, de sorte à proposer une version IMEX du schéma qui préserve également l'état du lac au repos.

Schéma conservatif par un splitting acoustique/transport pour les écoulements compressibles avec terme source dérivant d'un potentiel
Cette section se rapporte à des travaux publiés dans [2].

Le cadre initial de ce travail est la simulation d'écoulements compressibles avec termes sources de gravité. On peut considérer un cadre plus large qui est celui des équations d'Euler complétées par un terme source dérivant d'un potentiel $\mathbf{x} \mapsto \Phi(\mathbf{x})$. L'équation d'énergie du système peut être réécrite en utilisant l'énergie totale $(\rho E + \rho\Phi)$ sous une forme complètement conservative. On propose dans ce travail une méthode de discrétisation de type acoustique/transport, qui est conservative par rapport à la densité ρ et l'énergie totale $(\rho E + \rho\Phi)$ et qui préserve les profils de solutions stationnaires statiques définies par $\mathbf{u} = \mathbf{0}$ et $\boldsymbol{\nabla} P = -\rho\boldsymbol{\nabla}\Phi$.

Une adaptation directe de l'approche utilisée pour les équations de Saint-Venant ne permet d'obtenir une schéma conservatif pour $(\rho E + \rho\Phi)$. Pour remédier à ce problème, on introduit un potentiel instationnaire $(\mathbf{x}, t) \mapsto \Psi$ vérifiant l'équation

$$\partial_t(\rho\Psi) + \operatorname{div}(\rho\Psi\mathbf{u}) = \rho\mathbf{u}^T\boldsymbol{\nabla}\Phi + \lambda(\Psi - \Phi(\mathbf{x})), \tag{ix}$$

et une énergie totale relaxée $\mathscr{E} = E + \Psi$, de sorte que quand $\lambda \to +\infty$ on retrouve formellement $\Psi(\mathbf{x}, t) \to \Phi(\mathbf{x})$ et $\mathscr{E} = E + \Phi$. On considère ensuite un système relaxé dans lequel l'équation de conservation d'énergie $\rho(E+\Phi)$ est remplacée par la conservation de $\rho\mathscr{E}$ complétée par l'équation (ix). On applique ensuite la stratégie de splitting acoustique/transport sur le système relaxé en imposant au début de chaque pas de temps que $\Psi(\mathbf{x}, t^n) = \Phi(\mathbf{x})$ afin de reproduire l'équilibre $\lambda \to \infty$.

Le fait d'injecter dans le modèle un potentiel Ψ vérifiant de surcroit une équation plus complexe que celle de Φ semble à première vue déroutant. Néanmoins, il faut bien garder à l'esprit que Ψ peut être considéré comme un simple intermédiaire de calcul que l'on peut faire disparaître totalement de l'expression finale du schéma numérique. Là encore, deux formulations d'intégration en temps sont possibles : une stratégie complètement explicite et une stratégie IMEX.

En effectuant une analyse du comportement en régime bas Mach, on peut faire apparaître sans surprise les mêmes pathologies que dans le cas des équations d'Euler homogènes. Nous appliquons alors la même stratégie de correction de la discrétisation des termes de pression en modifiant le terme de décentrement qui intervient dans l'évaluation de la pression aux faces des cellules. Cette modification permet d'obtenir une erreur de troncature uniforme en M.

Calcul des états d'équilibre pour un modèle de changement de phase
Cette section se rapporte à des travaux publiés dans [19, 14, 17].

Dans cette section, je présente des travaux qui portent sur la résolution du triple équilibre $T_1 = T_2$, $P_1 = P_2$, $g_1 = g_2$ qui se produit au sein d'un mélange diphasique. L'objectif est de calculer les fractions de masse $Y^{\text{eq}}(\tau, e)$, de volume $\alpha^{\text{eq}}(\tau, e)$ et d'énergie $\psi^{\text{eq}}(\tau, e)$ solutions de l'équilibre pour une valeur de (τ, e) donnée. C'est grâce à cette évaluation que l'on peut mettre en œuvre la loi d'état du modèle diphasique HEM. Ce travail d'ingénierie mathématique est important dans une stratégie de simulation car l'utilisation de lois d'état complexes ne peut pas être écartée dans le contexte d'applications industrielles.

La résolution de ce système de trois équations non-linéaires peut se ramener à la résolution d'une seule équation scalaire non-linéaire portant sur la pression [4], dite «équation de changement de phase». L'équation de changement de phase fait intervenir la fonction $P \mapsto T^{\text{sat}}(P)$ qui traduit dans le plan P-T l'équilibre $g_1 = g_2$ et qui définit ce qu'on appelle les *états à saturation*. Malheureusement, il n'est en général pas possible d'obtenir une formule analytique simple pour $T^{\text{sat}}(P)$, y compris dans les cas académiques simples. On considère deux situations : dans le premier cas, on suppose que les deux phases pures sont représentées par des gaz raidis (loi d'état de type Stiffened Gas), dans le deuxième cas les données sont tabulées et on accède directement aux valeurs des états à saturation. Pour chacun de ces cas, on propose de remplacer l'équation de changement de phase par une équation de changement de phase approchée grâce à des approximations polynômiales. C'est cette équation de changement de phase approchée qui est utilisée pour mettre en œuvre des algorithmes itératifs afin de définir les états d'équilibres du système.

Chapitre 3 : Pratique du calcul scientifique

Dans ce très court chapitre, j'évoque une partie de mon travail qui s'apparente à ce que je choisi d'appeler «la pratique du calcul scientifique». Bien que très importante à mes yeux cette activité n'a pas la visibilité académique des publications.

4. On peut également utiliser la température comme inconnue de manière équivalente

L'ingénierie logicielle est importante
Je regroupe tout d'abord un certains nombres d'éléments liés à la programmation et à l'élaboration de codes de calcul scientifique. J'ai appris ces éléments au fil de l'eau en ayant la chance de côtoyer des personnes très compétentes, mais également d'autres moins aguerries qui m'ont permis d'expérimenter et d'améliorer mes méthodes de développement informatique.

Le calcul scientifique comme outil de partage
Outre le fait de rendre possible des simulations numériques, le calcul scientifique est également un outil de communication entre les communautés scientifiques et un outil de partage entre scientifiques. Je rapporte tout d'abord une expérience très enrichissante de travail collectif au CEMRACS 2010. Ensuite, j'évoque une expérience inattendue au cours de laquelle des simulations numériques ont suscité des avancées théoriques. Des calculs réalisés avec des schémas numériques présentés au chapitre II ont mis en défaut des modèles de convection d'atmosphère pour les planètes et les naines brunes. Ces résultats ont suggéré de réviser les mécanismes qui pilotent certaines instabilités dans ces écoulements. Suite à ces études, une nouvelle théorie de la convection des atmosphères à été élaborée et publiée dans [3].

Contributions en calcul scientifique
Je propose ici une liste de codes de calcul auxquels j'ai pu contribuer soit directement en tant que développeur soit à travers l'élaboration de modèles et de méthode numériques.

Chapitre 4 : Perspectives

Dans ce dernier chapitre, je présente les pistes que je souhaite explorer suite aux travaux présentés dans ce mémoire. Une première partie concerne le développement de modèles diphasiques multi-échelle. La seconde concerne l'amélioration des schémas avec splitting d'opérateur acoustique/transport et leur adaptation à de nouveaux modèles d'écoulements.

Chapitre I

Complex flow modeling

In this chapter, I will present results pertaining to the modeling of compressible flows involving several components and physical effects that span across multiple scales. In that sense these flows can be considered as "complex flows".

I chose to gather in the section I.1 many elements that compose a modeling routine that relies on the literature. An important element of this method relies on the definition of Equation of State (EOS) for mixtures, that is examined in section I.4 and I.5. The section I.6 discusses possible dissipative structures for a class of bifluid models. I will show in section I.7 how the proposed modeling routine can be used to design a two-phase model that involves two velocity scales. Finally, I will present models used for simulating flows with an arbitrary number of components separated by sharp interfaces using interface capture methods in section I.8.

I.1 A generic modeling routine

The modeling problems I had to address consists in describing an evolving fluid medium composed of several materials. Within the context of my work, modeling this medium boils down to

— propose a collection of functions $(\mathbf{x}, t) \mapsto b$ that will be referred to as Eulerian representation of fluid parameters,
— exhibit Partial Differential Equations (PDEs) and algebraic closures that connect these fluids parameters and their evolution.

Although a strong intuition of the physical phenomenon at play is a stronger driver to achieve such a task, it is not out of reach for lay applied mathematicians ! I will present a modeling routine that was used in several of my works [23, 22, 1]. This routine is by no means an infallible magic wand for deriving relevant physical models. Nevertheless it enables a step-by-step implementation of the hypotheses that characterize the system during the modeling process. This method is modeled after many works of the literature (see for instance [Her55, Ser59, Gou78, Sal83, Bed85, Geu86, CG89, Gou90, Sal88, GG99, GG00, Rom98, Tru91, GGP97, Gou07, Ber09, GR09, Pes+18]). The following is not a detailed presentation but an overview as many delicate aspects of the methods will not be mentioned.

Let us note $\mathscr{V}(t) \subset \mathbb{R}^d$: the volume of space occupied by a portion of fluid at instant $t \in [t_0, t_1]$ and $\Omega = \{(\mathbf{x}, t) \in \mathbb{R}^d \times [t_0, t_1] \mid \mathbf{x} \in \mathscr{V}(t), t_0 \leq t \leq t_1\}$. I propose to break down this routine into the 3 stages.

1. **Characterizing the system**
   (a) Define a set of m parameters $(\mathcal{T}_1, \dots, \mathcal{T}_m) = \mathcal{T}$ that characterize the system. The (Eulerian) mapping $(\mathbf{x}, t) \mapsto \mathcal{T}$ will be called a transformation of the system.

   > *In this step, one defines by discussing with the specialists (engineers, physicists, etc.) the list of parameters that are required to describe the state of the system.*

   (b) Define the kinematics at play in the system

   > *In this step, one specifies the velocity or velocities at play for transporting matter within the set of parameters $\mathcal{T}$.*

   (c) Postulate constitutive constraints that should be valid for a transformation of the medium in the absence of dissipative processes.

   > *This step aims at expressing constraints that the system parameters should fulfill. Here are some common examples :*
   > — *algebraic constraints like Equations Of States (EOSs)*
   > — *differential constraints like mass conservation or partial mass conservation.*

2. **Modeling the conservative part of the system**

(a) Postulate a kinetic $\mathcal{T} \mapsto E_{\text{kin}}$ energy for the system.

This step exhibit the kinetic energies at play in the system and should rely on the kinematic description.

(b) Postulate a potential energy $\mathcal{T} \mapsto E_{\text{pot}}$ for the system

(c) Define a Lagrangian energy $\mathcal{T} \mapsto \mathscr{L} = E_{\text{kin}} - E_{\text{pot}}$ and the Hamiltonian action $\mathscr{A}$ by setting

$$\mathcal{T} \mapsto \mathscr{A}(\mathcal{T}) = \int_{\Omega} \mathscr{L}(\mathcal{T}(\mathbf{x}, t))\, \mathrm{d}\mathbf{x}\mathrm{d}t \tag{I.1}$$

(d) Apply the **Hamilton principle of stationary action**. This principle postulates that if $\overline{\mathcal{T}}$ is a physically relevant transformation of the system then it is the solution of the following variational problem : consider a family of transformations $(\mathbf{x}, t, \zeta) \mapsto \hat{\mathcal{T}}$ parametrized by $\zeta \in [-1, 1]$, such that

$$\hat{\mathcal{T}}(\mathbf{x}, t, \cdot)_{|\partial\Omega} = \overline{\mathcal{T}}(\mathbf{x}, t), \qquad \hat{\mathcal{T}}(\mathbf{x}, t, \zeta = 0) = \overline{\mathcal{T}}(\mathbf{x}, t), \qquad \hat{\mathcal{T}} \text{ verifies the constitutive constraints.} \tag{I.2}$$

then $\overline{\mathcal{T}}$ is physically relevant if it is a stationary point of $\zeta \mapsto \mathscr{A}(\hat{\mathcal{T}})$, that is to say

$$\frac{\mathrm{d}}{\mathrm{d}\zeta}\Big(\mathscr{A}(\hat{\mathcal{T}})\Big)_{|\zeta=0} = 0. \tag{I.3}$$

In practice, the outcome of this step is a set of PDEs that involve $(\partial\mathscr{L}/\partial\mathcal{T}_k)$ and that express the system evolution.

3. **Modeling the dissipative part of the system**

(a) Exhibit a mathematical entropy $\mathcal{T} \mapsto \eta(\mathcal{T}) \in \mathbb{R}$ and an entropy flux $\mathcal{T} \mapsto \mathbf{g}(\mathcal{T}) \in \mathbb{R}^d$ such that we have an additional conservation law

$$\partial_t \eta + \operatorname{div}(\mathbf{g}) = 0. \tag{I.4}$$

Let us underline that we do not require η to be a strictly convex function (on the contrary of the classic definition of the mathematical literature).

This step is not trivial. It requires to propose an entropy η that is coherent with the constitutive constraints. It may also lead to additional constraints in order to ensure that this additional evolution equation takes the form of a conservation law (see for example [Coq+02, Gui07a, CM20] and section I.6).

The assumption regarding the convexity of η is less strong than what is required in the literature. In practice for many complex systems like multi-component flows, exhibiting an entropy (even a non-convex one) is far from being obvious.

(b) Consider candidate expression for source terms intended to induce dissipation in the system. Complement the conservative system with these source terms.

(c) Refresh the entropy evolution equation (I.4) by accounting for the source terms in the form

$$\partial_t \eta + \operatorname{div}(\mathbf{g}) = \mathcal{Q}, \tag{I.5}$$

(d) Further characterize the source terms in order to ensure that that $\mathcal{Q} \leq 0$.

The additional entropy production $\mathcal{Q}$ accounts for the presence of the additional source terms.

I.2 Basic systems : Euler equations for single component compressible flows

In order to give a clear and concrete example, we propose to retrieve both the barotropic Euler and the non barotropic Euler equations using the previous routine, highlighting each stop of the process.

I.2.1 The barotropic Euler equations

The barotropic Euler equation deals with compressible flows when the EOS only depends on the density so that that energy variables (like the internal energy, the temperature of the entropy) can be considered as passive scalars.

Characterizing the system.

(a) We claim that the medium can be completely characterized by $(\mathbf{x}, t) \mapsto \mathcal{T} = (\rho, \mathbf{u})$, where ρ is the fluid density and $\mathbf{u} \in \mathbb{R}^d$ is the fluid velocity.

(b) The kinematics of the system is (obviously) defined thanks to the velocity field $\mathbf{u}$.

(c) We impose the following constitutive constraints :

— ρ and $\mathbf{u}$ verify the mass conservation equation $\partial_t \rho + \operatorname{div}(\rho\mathbf{u}) = 0$,

— the medium is equipped with an EOS in the form of a barotropic potential energy $\rho \mapsto e^{\text{EOS}}$ so the the pressure P of the medium is defined by $\mathrm{d}e^{\text{EOS}}/\mathrm{d}\rho\ (\rho) = P(\rho)/\rho^2$.

Modeling of the conservative part.

(a) We equip the system with the standard kinetic energy $E_{\text{kin}} = \rho|\mathbf{u}|^2/2$.
(b) We suppose that the potentiel energy of the system is a function of the sole density $E_{\text{pot}} = E_{\text{pot}}(\rho)$.
(c) We define the Lagrangian $\mathscr{L}$ and the action $\mathscr{A}$ by setting

$$\mathscr{L}(\rho, \mathbf{u}) = E_{\text{kin}} - E_{\text{pot}}, \qquad \mathscr{A} = \int_\Omega \mathscr{L}(\rho, \mathbf{u})\, \mathrm{d}x\mathrm{d}t, \tag{I.6}$$

and we note

$$\mathscr{L} + \mathscr{L}^* = \left(\frac{\partial \mathscr{L}}{\partial \rho}\right)_{\mathbf{u}} \rho, \qquad \mathbf{K}^T = \left(\frac{\partial \mathscr{L}}{\partial \mathbf{u}}\right)_{\rho}, \qquad \mathscr{L} + H = \mathbf{K}^T \mathbf{u}. \tag{I.7}$$

,
(d) The Stationary Action Principle yields the following equation of motion

$$\partial_t \mathbf{K} + \mathbf{div}\left(\mathbf{K}\mathbf{u}^T\right) - \boldsymbol{\nabla}\mathscr{L}^* = \mathbf{0}. \tag{I.8}$$

Modeling dissipation .

(a) The motion equation (I.8) also yields an additional conservation law

$$\partial_t H + \mathrm{div}(H\mathbf{u}) - \mathrm{div}(\mathscr{L}^*\mathbf{u}) = 0. \tag{I.9}$$

This suggests to choose respectively $\eta = H$ and $\mathbf{g} = (H - \mathscr{L}^*)\mathbf{u}$ respectively for the entropy and entropy flux of the system.
(b) We suppose that the dissipation occurs by assuming a modified version of (I.8) that reads

$$\partial_t \mathbf{K} + \mathbf{div}\left(\mathbf{K}\mathbf{u}^T\right) - \boldsymbol{\nabla}\mathscr{L}^* = \mathbf{R}, \tag{I.10}$$

where $\mathbf{R}$ is yet to be determined.
(c) Accounting for (I.10) one can compute $\partial_t H$ and obtain

$$\partial_t H + \mathrm{div}(H\mathbf{u}) - \mathrm{div}(\mathscr{L}^*\mathbf{u}) = \mathbf{u}^T\mathbf{R}. \tag{I.11}$$

(d) The entropy budget (I.11) can be used to test different closure definitions for $\mathbf{R}$ so that they will be compatible with an entropy inequality.

> *Let us give two simple classic and simple definitions for* $\mathbf{R}$*. First, a choice that can used for describing wall friction effects in 2D or 1D models is* $\mathbf{R} = -\lambda(\mathbf{u})\mathbf{u}$*, where* $\lambda(\mathbf{u}) > 0$ *is a dissipation coefficient. In this case the entropy flux and entropy production are respectively* $\mathbf{g} = (H - \mathscr{L}^*)\mathbf{u}$ *and* $\mathscr{Q} = -\lambda(\mathbf{u})|\mathbf{u}|^2 < 0$*. A second classic choice is to use a differential definition for* $\mathbf{R}$ *in order to recover viscous dissipation by setting* $\mathbf{R} = \mathbf{div}[\lambda\,\mathrm{div}(\mathbf{u})\,\mathrm{Id} + \mu(\boldsymbol{\nabla}\mathbf{u} + \boldsymbol{\nabla}\mathbf{u}^T)]$ *so that* $\mathbf{g} = [H - \mathscr{L}^* - (\mu + \lambda)\,\mathrm{div}(\mathbf{u})\,\mathrm{Id} - \mu\boldsymbol{\nabla}\mathbf{u}]\mathbf{u}$ *and* $\mathscr{Q} = -(\lambda + \mu)\,\mathrm{div}(\mathbf{u})^2 - \mu\boldsymbol{\nabla}\mathbf{u} : \boldsymbol{\nabla}\mathbf{u} < 0$.

Classic modeling choice : barotropic Euler equations
The classic barotropic Euler equations are recovered by putting classic thermodynamics in play : one sets $E_{\text{pot}}(\rho) = \rho e^{\text{EOS}}(\rho)$, which yields

$$\mathbf{K} = \rho\mathbf{u}, \qquad \mathscr{L}^* = -P, \qquad \eta = H = \rho e^{\text{EOS}}(\rho) + \rho|\mathbf{u}|^2/2, \qquad \mathbf{g} = \left(\rho e^{\text{EOS}}(\rho) + \rho|\mathbf{u}|^2/2 + P\right)\mathbf{u}. \tag{I.12}$$

Equations (I.8) and (I.9) now take the more familiar form

$$\partial_t(\rho\mathbf{u}) + \mathrm{div}(\rho\mathbf{u}\mathbf{u}^T) + \boldsymbol{\nabla}P = 0, \qquad \partial_t(\rho e + \rho|\mathbf{u}|^2/2) + \mathrm{div}\left((\rho e + \rho|\mathbf{u}|^2/2 + P)\mathbf{u}\right) = 0. \tag{I.13}$$

Remark 1 It is important to note that the barotropic case is very interesting as it underlines how the Hamilton principle comes into play in the modeling process. However, it is also misleading. Indeed, the role of the entropy in the modeling is crucial and proposing an entropy for the model is not a simple task. In the barotropic case, this question is simply discarded as the conservation of energy is consequent to the motion equation and yields an entropy for the system.

I.2.2 The Euler equations

I will now present the derivation of the full Euler system for compressible flows. Although the system is quite simple, this case better highlights the hypothesis related to the entropy in the modeling process.

Characterizing the system.

(a) We consider the following parameters : ρ the density of fluid, $(\mathbf{x}, t) \mapsto e$ the specific internal energy of the fluid, s its specific (physical) entropy, p and T respectively the pressure and the temperature of the fluid. The local velocity of the fluid is noted $\mathbf{u} \in \mathbb{R}^d$. All of these parameters are now considered as Eulerian maps $(\mathbf{x}, t) \mapsto b$, $b \in \{\rho, \mathbf{u}, e, p, s, T\}$.
(b) The kinematics of the system is described by $\mathbf{u}$.
(c) We impose several constitutive constraints. First, ρ, p, T, e and s are bounds by thermodynamics hypotheses : we suppose that there is an EOS that connects e, ρ, s, T and p through functions $s = s^{\text{EOS}}(\rho, e)$ and $e = e^{\text{EOS}}(\rho, s)$ so that we have the Gibbs relation

$$T\,\mathrm{d}s = \mathrm{d}e + P\,\mathrm{d}(1/\rho)\,. \tag{I.14}$$

We additionally impose the mass and entropy conservation : $\partial_t\rho + \mathrm{div}(\rho\mathbf{u}) = 0$ and $\partial_t(\rho s) + \mathrm{div}(\rho s\mathbf{u}) = 0$. Accounting for these hypotheses, we propose to reduce the set of independant parameters that governs the system to $(\mathbf{x}, t) \mapsto \mathcal{T} = (\rho, \mathbf{u}, s)$.

Modeling of the conservative part

(a) We equip the system with the standard kinetic energy $E_{\mathrm{kin}} = \rho|\mathbf{u}|^2/2$.
(b) We suppose that the potentiel energy of the system is a function of the density and the physical entropy $E_{\mathrm{pot}} = E_{\mathrm{pot}}(\rho, s)$.
(c) We define the Lagrangian $\mathscr{L}$ and the action $\mathscr{A}$ by setting

$$\mathscr{L}(\rho, \mathbf{u}, s) = E_{\mathrm{kin}} - E_{\mathrm{pot}}, \qquad \mathscr{A} = \int_\Omega \mathscr{L}(\rho, \mathbf{u}, s)\,\mathrm{d}x\mathrm{d}t. \tag{I.15}$$

and we note $\quad \mathscr{L} + \mathscr{L}^* = \left(\frac{\partial \mathscr{L}}{\partial \rho}\right)_{\mathbf{u},s} \rho, \qquad \mathbf{K}^T = \left(\frac{\partial \mathscr{L}}{\partial \mathbf{u}}\right)_{\rho,s}, \qquad \mathscr{L} + H = \mathbf{K}^T\mathbf{u}. \tag{I.16}$

,
(d) The Stationary Action Principle yields the following equation of motion

$$\partial_t\mathbf{K} + \mathbf{div}\left(\mathbf{K}\mathbf{u}^T\right) - \boldsymbol{\nabla}\mathscr{L}^* = \mathbf{0}. \tag{I.17a}$$

The motion equation (I.17a) also provides the following additional conservation law

$$\partial_t H + \mathrm{div}(H\mathbf{u}) - \mathrm{div}(\mathscr{L}^*\mathbf{u}) = 0. \tag{I.17b}$$

Modeling dissipation

(a) In the present case, the mathematical entropy η and its associated flux $\mathbf{g}$ are defined by $\eta = -\rho s$ and $\mathbf{g} = -\rho s\mathbf{u}$. This is consistent with the constitutive constraints $\partial_t(\rho s) + \mathrm{div}(\rho s\mathbf{u}) = 0$.

> *In the case of the Euler equation the choice of the entropy is naturally suggested by the choice of the thermodynamics constitutive relations.*

(b) We suppose that dissipation occurs by assuming a modified version of (I.17) that reads

$$\partial_t\mathbf{K} + \mathbf{div}\left(\mathbf{K}\mathbf{u}^T\right) - \boldsymbol{\nabla}\mathscr{L}^* = \mathbf{R}, \qquad \partial_t H + \mathrm{div}(H\mathbf{u}) - \mathrm{div}(\mathscr{L}^*\mathbf{u}) = \mathcal{M}, \tag{I.18}$$

where $\mathbf{R}$ and $\mathcal{M}$ are yet to be set.
(c) The chain rules yields $\partial_t H = \cdots + (\partial H/\partial s)\partial_t s$ and accounting for (I.18) one obtains the following evolution equation for s

$$\partial_t\eta + \mathrm{div}(\mathbf{g}) = \mathcal{Q}, \qquad \mathcal{Q} = \rho(\mathcal{M} - \mathbf{u}^T\mathbf{R})/\left(\frac{\partial \mathscr{L}}{\partial s}\right)_{\rho,\mathbf{u}}. \tag{I.19}$$

(d) The entropy budget (I.19) can be used as a benchmark equation in order to ensure that candidate models for R and $\mathcal{M}$ yield a negative entropy production $\mathcal{Q} \leq 0$.

Classic modeling choice : Euler equations

In order to recover the classic Euler equations expressed in a more familiar way, the potential energy E_{pot} is defined with the internal energy of the medium $E_{\mathrm{pot}}(\rho, s) = \rho e(\rho, s)$. This leads to

$$\mathbf{K} = \rho\mathbf{u}, \qquad H = \rho e + \rho|\mathbf{u}|^2/2, \qquad \mathscr{L}^* = -P, \qquad \left(\frac{\partial \mathscr{L}}{\partial s}\right)_{\mathbf{u},\rho} = -\rho T, \tag{I.20}$$

so that equations (I.17) read

$$\partial_t(\rho\mathbf{u}) + \mathrm{div}(\rho\mathbf{u}\mathbf{u}^T) + \boldsymbol{\nabla}P = 0, \qquad \partial_t(\rho e + \rho|\mathbf{u}|^2/2) + \mathrm{div}[(\rho e + \rho|\mathbf{u}|^2/2 + P)\mathbf{u}] = 0. \tag{I.21}$$

Remark 2 Within the family of the single material Euler equation, it is possible to derive more complex models like grade n materials by considering a potential energy E_{pot} that depends on differential terms $\nabla\rho$ or ∇s (or even higher order derivatives). This can be used to described capillary effects in the fluid in region of strong gradients of ρ or s [CG89, Gou07].

Remark 3 I need to emphasize that using the derivation routine proposed in section I.1 does (obviously) not guarantee to derive relevant physical models or mathematically well-posed models. The interesting feature of these lines is not that they yield correct models. The interesting feature of this routine is rather that it mostly relies on the definition of energies so the routine can easily produce models. These resulting models may be completely wrong or useless. This routine is a mean to produce a "raw material" that requires to be examined and tested.

> *Roughly speaking, in the routine process that is proposed in section I.1, the Stationary Action Principle acts as a "black box" that takes energies and kinematic definitions as input and outputs momentum evolution equations.*

I.3 A Simple two-phase system : the homogeneous relaxed model

Contributions by the author
This section is related to works that have been published in [23, 24, 22, 21, 19, 17, 14].

I will use the routine proposed in section I.1 to show the derivation of a simple two-phase system that was underlying in several models that I studied over the years.

Characterizing the system
Before going any further, I need to emphasize that the characterization of this two-phase system relies on standard hypotheses. Nevertheless these hypotheses need to considered with care in the sense that they are much stronger than they might seem. These assumptions are further discussed in section I.4.

(a) We consider that the medium is a mixture of two materials $k = 1, 2$ that can be characterized by its density ρ, a specific internal energy e and a specific entropy s. We also assume that the composition of the mixture can be described by 3 additional fluid parameters : the mass fraction Y, the volume fraction α, the energy fraction ψ of the fluid $k = 1$. All of these parameters are now considered as Eulerian maps $(\mathbf{x}, t) \mapsto b$, $b \in \{\rho, e, s, Y, \alpha, \psi\}$.
(b) We consider that both materials share the velocity so that the kinematics of the system is described by a single velocity $(\mathbf{x}, t) \mapsto \mathbf{u}$.
(c) We impose several constitutive constraints :
— the variables ρ, e, s, Y, α, and ψ are not independant. We suppose the mixture is to be equipped with an EOS of the form $e = e^{\text{EOS}}(\rho, e, Y, \alpha, \psi)$,

> *In the case of two-phase system, the definition of the EOS is a very delicate and critical hypothesis. The hypothesis that is formulated here is very strong and we will see in section I.4 how such an EOS can be built.*

— we suppose that the total mass is conserved, *i.e.* $\partial_t \rho + \text{div}(\rho \mathbf{u}) = 0$,
— we suppose that the fraction $b \in \{Y, \alpha, \psi\}$ is evolved by $\partial_t(\rho b) + \text{div}(\rho b \mathbf{u}) = \rho R_b$, where R_b vanishes when no dissipation occurs,
— we suppose that the entropy is conserved : $\partial_t(\rho s) + \text{div}(\rho s \mathbf{u}) = 0$.

Accounting for these hypotheses, we propose to reduce the set of independant parameters that governs the system to $(\mathbf{x}, t) \mapsto \mathcal{T} = (\rho, \mathbf{u}, s, Y, \alpha, \psi)$.

Modeling of the conservative part
The derivation process follows the similar lines as the single component Euler system of section I.2.2. The kinetic energy is defined by $E_{\text{kin}} = \rho|\mathbf{u}|^2/2|$ and the potential energy takes the form $E_{\text{pot}} = E_{\text{pot}}(\rho, s, Y, \alpha, \psi)$. The Lagrangian is set to $\mathscr{L} = E_{\text{kin}} - E_{\text{pot}} = \mathscr{L}(\mathbf{u}, \rho, s, Y, \alpha, \psi)$. With the same definitions for $\mathscr{L}^*$, $\mathbf{K}$ and H as in (I.16), the Stationary Action Principle yields the following equation of motion

$$\partial_t \mathbf{K} + \mathbf{div}\left(\mathbf{K}\mathbf{u}^T\right) - \boldsymbol{\nabla}\mathscr{L}^* = \mathbf{0}, \tag{I.22a}$$

complemented by the conservation equation

$$\partial_t H + \text{div}(H\mathbf{u}) - \text{div}(\mathscr{L}^*\mathbf{u}) = 0. \tag{I.22b}$$

Modeling dissipation
As in the case of the Euler system of section I.2.2, the mathematical entropy η and its associated flux $\mathbf{g}$ are set to $\eta = -\rho s$ and $\mathbf{g} = -\rho s \mathbf{u}$. This time, we do not consider possible dissipation source that may be added to (I.22a) and we focus solely on dissipative processes that are driven by the modification of the mixture composition. Therefore we do not modify (I.22) but we seek for $R_b \neq 0$, $b \in \{Y, \alpha, \psi\}$. Computing $\partial_t H$ and using (I.22) yields this time

$$\partial_t \eta + \text{div}(\mathbf{g}) = \mathcal{Q}, \qquad \mathcal{Q} = \rho\left(\frac{\partial \mathscr{L}}{\partial s}\right)^{-1}\left[\left(\frac{\partial \mathscr{L}}{\partial Y}\right)R_Y + \left(\frac{\partial \mathscr{L}}{\partial \alpha}\right)R_\alpha + \left(\frac{\partial \mathscr{L}}{\partial \psi}\right)R_\psi\right]. \tag{I.23}$$

The entropy evolution (I.23) can also be used as a constraint for choosing the source terms R_b, $b \in \{Y, \alpha, \psi\}$ in order to ensure $\mathcal{Q} \leq 0$. If one additionally demands each term R_b to contribute independently to the entropy production, it is natural to require the stronger constraint that $(\partial \mathscr{L}/\partial s)^{-1}(\partial \mathscr{L}/\partial b)R_b \leq 0$ for each $b \in \{Y, \alpha, \psi\}$. A possible choice for closing the equations that drive the composition is thus

$$R_Y = -\kappa_Y\left(\frac{\partial \mathscr{L}}{\partial Y}\right), \qquad R_\alpha = -\kappa_\alpha\left(\frac{\partial \mathscr{L}}{\partial \alpha}\right), \qquad R_\psi = -\kappa_\psi\left(\frac{\partial \mathscr{L}}{\partial \psi}\right), \tag{I.24}$$

where κ_b is a function such that $\kappa_b(\partial \mathscr{L}/\partial s) > 0$, $b \in \{Y, \alpha, \psi\}$.

Remark 4 The closure relations (I.24) and the entropy budget (I.23) suggest that the two-phase system is driven towards an equilibrium state defined by $(\partial \mathscr{L}/\partial Y) = 0$, $(\partial \mathscr{L}/\partial \alpha) = 0$ and $(\partial \mathscr{L}/\partial \psi) = 0$. We will see at section I.4 that this can be connected to the definition of a new EOS that can define another compressible flow model often referred to as Homogeneous Equilibrium Model (HEM).

Classic modeling choice : Homogeneous Relaxed Model (HRM)
Following similar lines as for the Euler equations the potential energy E_{pot} is defined by the internal energy $E_{\text{pot}}(\rho, s, Y, \alpha, \psi) = \rho e(\rho, s, Y, \alpha, \psi)$. Classic fluid parameters are retrieved for the momentum with $\mathbf{K} = \rho\mathbf{u}$ and the mechanical energy $H = \rho e + \rho|\mathbf{u}|^2/2$. Moreover, the term $\boldsymbol{\nabla}\mathscr{L}^*$ that acts in the momentum equation (I.22a) suggests a definition for the pressure P of the two-phase medium by setting $P = -\mathscr{L}^* = (\partial e/\partial\rho)_{s,Y,\alpha,\psi}$. We will see in section I.4 that this is also coherent with the definition of the two-phase thermodynamics. The dissipative source terms that act on the composition read $R_b = \kappa_b(\partial e/\partial b)$, $b \in \{Y, \alpha, \psi\}$, so that the final dissipative system takes the more familiar form

$$\begin{cases} \partial_t(\rho Y) + \operatorname{div}(\rho Y\mathbf{u}) = \kappa_Y\left(\dfrac{\partial e}{\partial Y}\right), & \text{(I.25a)}\\ \partial_t(\rho\alpha) + \operatorname{div}(\rho\alpha\mathbf{u}) = \kappa_\alpha\left(\dfrac{\partial e}{\partial \alpha}\right), & \text{(I.25b)}\\ \partial_t(\rho\psi) + \operatorname{div}(\rho\psi\mathbf{u}) = \kappa_\psi\left(\dfrac{\partial e}{\partial \psi}\right), & \text{(I.25c)}\\ \partial_t\rho + \operatorname{div}(\rho\mathbf{u}) = 0, & \text{(I.25d)}\\ \partial_t(\rho\mathbf{u}) + \operatorname{div}(\rho\mathbf{u}\mathbf{u}^T) + \boldsymbol{\nabla}P = 0, & \text{(I.25e)}\\ \partial_t\left(\rho e + \rho\dfrac{|\mathbf{u}|^2}{2}\right) + \operatorname{div}\left[\left(\rho e + \rho\dfrac{|\mathbf{u}|^2}{2} + P\right)\mathbf{u}\right] = 0. & \text{(I.25f)} \end{cases}$$

Remark 5 Another possible choice for the definition of R_b can be considered by using the equilibrium values $\alpha^{\text{eq}}(\tau, e)$, $Y^{\text{eq}}(\tau, e)$ and $\psi^{\text{eq}}(\tau, e)$ associated with the composition parameters α, Y and ψ (see section I.4.3). These values described an optimal mixture composition in the sense that they are the solutions of an optimization problem for the mixture entropy s that encompasses the equilibrium $(\partial\mathscr{L}/\partial b) = 0$, $b \in \{Y, \psi, \alpha\}$. In this case, for $b \in \{Y, \psi, \alpha\}$ one can set $R_b = \kappa_b(b - b^{\text{eq}}(\tau, e))$, with $\kappa_b > 0$ (see [HS06, Fac08, 14]).

I.4 Equation of state for a two-phase medium

Contributions by the author
This section covers works that have been published in [23, 24, 22, 21, 19, 14].

In this section, I will present how one can derive an EOS for a mixture of two compressible components using a modeling process that was gradually evolved along the years. I was first involved in the study of a two-phase barotropic model [23, 24, 22]. A non-barotropic two-phase model that assumes thermal equilibrium between phases was also studied in [Car04]. These works rather aimed at deriving phase change related source terms that are compliant with an entropy budget. Analogous arguments were also elaborated independently in [BH05, Hel05, HS06] with a stronger focus on an optimization process of the entropy of the two-phase mixture. A modeling process that combines both approaches was used in [21, 19, 17, 14] to propose and analyze EOS for two-component mixtures that can undergo phase change phenomena.

The models for simulating phase change in compressible flows of the literature can be divided into two categories. A first category involves a single component system with a non-convex EOS like the famous Van der Waals EOS [Van, Kle74]. This type of EOS possesses two stable branches complemented by possible metastable states that represent each pure phase. These pure phase branches are separated by an instable zone (the spinodal zone). Another category of models relies on a two-EOS approach. Each phase is equipped with its own EOS. The mass transfer between each phase should be described thanks to parameters that characterize the composition of the two-phase mixture. I will discuss the latter approach in the following but connections with the first approach will also be discussed.

We consider two materials indexed by $k = 1, 2$ that are both equipped with an EOS in the form of $(\tau_k, e_k) \mapsto s_k^{\text{EOS}}(\tau_k, e_k)$, where $\tau_k = 1/\rho_k$, e_k and s_k denote respectively the specific volume, the specific internal energy and the specific entropy of the material $k = 1, 2$. We furthermore suppose that $\mathrm{d}^2 s_k^{\text{EOS}}$, the Hessian matrix of $(\tau_k, e_k) \mapsto s_k^{\text{EOS}}$ is negative definite, which implies that $(\tau_k, e_k) \mapsto s_k^{\text{EOS}}$ is strictly concave. The temperature T_k and pressure P_k of the material k are positive quantities defined by $(\partial s_k/\partial e_k)_{\tau_k} = 1/T_k > 0$ and $P_k = T_k(\partial s_k/\partial\tau_k)_{e_k} > 0$. We note $g_k = e_k + P_k/\rho_k - T_k s_k$ the free enthalpy (or Gibbs free energy) of the material k.

Moreover, a mass $\mathcal{M}_k$ of fluid k that occupies the volume $\mathcal{V}_k$ with the internal energy $\mathcal{E}_k$ will be endowed with the entropy

$$S_k(\mathcal{M}_k, \mathcal{V}_k, \mathcal{E}_k) = \mathcal{M}_k s_k\left(\mathcal{V}_k/\mathcal{M}_k, \mathcal{E}_k/\mathcal{M}_k\right), \tag{I.26}$$

where the function $(\mathcal{M}_k, \mathcal{V}_k, \mathcal{E}_k) \mapsto S_k$ is strictly concave and first order homogeneous (see *e.g.* [Cal85]).

I.4.1 Two-component mixture : definition

The overall specific volume τ and internal energy e of the two-phase medium need to be related to the phasic quantities τ_k and e_k. I will now present classic modeling lines for describing mixtures using measures defined over the computational

domain. We suppose that $\mathrm{d}m(\mathbf{x},t)$ and $\mathrm{d}e(\mathbf{x},t)$ are respectively the measure of mass and internal energy of the mixture. By assuming the whole space is occupied by the mixture, the measure of volume for the mixture is the Lebesgue measure over $\mathbb{R}^d$ noted $\mathrm{d}\mathbf{x}$. Concerning the phasic quantity : we suppose that $\mathrm{d}m_k(\mathbf{x},t)$, $\mathrm{d}e_k(\mathbf{x},t)$, $\mathrm{d}v_k(\mathbf{x},t)$ are respectively the measures of mass, internal energy and volume of the component $k=1,2$. If one considers a small portion of space $\omega \subset \mathbb{R}^d$, these measures allow to evaluate the following quantities :

$\int_\omega \mathrm{d}\mathbf{x}$: the volume of the mixture in ω ,
$\int_\omega \mathrm{d}m(\mathbf{x},t)$: the mass of the mixture in ω ,
$\int_\omega \mathrm{d}e(\mathbf{x},t)$: the internal energy of the mixture in ω,
$\int_\omega \mathrm{d}v_k(\mathbf{x},t)$: the volume of the component k in ω ,
$\int_\omega \mathrm{d}m_k(\mathbf{x},t)$: the mass of the component k in ω ,
$\int_\omega \mathrm{d}e_k(\mathbf{x},t)$: the internal energy of the component k in ω.

From now on, we shall omit the dependency on $(\mathbf{x},t)$ for the sake of readability. By definition, these measures are related to the specific parameters of the fluids as follows :

$$\mathrm{d}\mathbf{x} = \tau \mathrm{d}m, \qquad \mathrm{d}e = e\mathrm{d}m, \qquad \mathrm{d}v_k = \tau_k \mathrm{d}m_k, \qquad \mathrm{d}e_k = e_k \mathrm{d}m_k. \tag{I.27}$$

From an intuitive point of view $\mathrm{d}m$ *represents the mass of an infinitely small "pinch" of two-component mixture that occupies a volume* $\mathrm{d}\mathbf{x}$ *and has an amount of internal energy* $\mathrm{d}e$*. Likewise a "pinch" of material* k *with mass* $\mathrm{d}m_k$ *occupies the volume* $\mathrm{d}v_k$ *with an internal energy* $\mathrm{d}e_k$*.*

We can now define the fractions of mass Y_k, volume α_k and internal energy ψ_k by setting

$$\mathrm{d}m_k = Y_k \mathrm{d}m, \qquad \mathrm{d}v_k = \alpha_k \mathrm{d}\mathbf{x}, \qquad \mathrm{d}e_k = \psi_k \mathrm{d}e, \tag{I.28}$$

that relate mixtures specific quantities to specific quantities of the component $k=1,2$. Consequently we have

$$\alpha_k \tau = Y_k \tau_k, \qquad \psi_k e = Y_k e_k. \tag{I.29}$$

The assumption that all volumes, energy and mass are positive implies that $Y_k > 0$, $\alpha_k > 0$ and $\psi_k > 0$. Let us now further characterize the mixture : first, we express the additivity of mass by stating that

$$\mathrm{d}m_1 + \mathrm{d}m_2 = \mathrm{d}m. \tag{I.30}$$

We now postulate stronger (but classic) assumptions on the mixture by requiring that ([Cal85, Del03, Hel05]) :

$$\text{the components are immiscible : } \mathrm{d}v_1 + \mathrm{d}v_2 = \mathrm{d}\mathbf{x}, \tag{I.31a}$$
$$\text{the energy of the mixture is the result of energy additivity : } \mathrm{d}e_1 + \mathrm{d}e_2 = \mathrm{d}e. \tag{I.31b}$$

A straightforward consequence of (I.30) and (I.31) is

$$\tau = Y_1\tau_1 + Y_2\tau_2, \qquad e = Y_1 e_1 + Y_2 e_2, \tag{I.32a}$$

$$Y_1 + Y_2 = 1, \qquad \alpha_1 + \alpha_2 = 1, \qquad \psi_1 + \psi_2 = 1. \tag{I.32b}$$

From now one, we shall note $Y = Y_1 = 1 - Y_2$, $\alpha = \alpha_1 = 1 - \alpha_2$, $\psi = \psi_1 = 1 - \psi_2$.

Remark 6 This section does not aim at presenting exhaustively how to characterize mixtures. Many other elements can be brought into play from algebraic closures to differential closures (see for example [Lag02, Del03, Hel05, Mat20]) or energies that are pertaining to surface tension effects [GG00, Gou07] or non-ideal mixture effects [Cor20] and in the broader context of bifluid models the recent results of [BH19, BBL20].

I.4.2 Two-component mixture : an off-equilibrium EOS

The two-phase mixture can be equipped with a first EOS by providing a specific entropy s. In [21, Fac08, 19, 17, 14], we simply used the additivity of entropy and set $s = Y_1 s_1^{\mathrm{EOS}}(\tau_1, e_1) + Y_2 s_2^{\mathrm{EOS}}(\tau_2, e_2)$. This EOS takes the form of a mapping

$$(\tau, e, Y, \alpha, \psi) \mapsto s^{\mathrm{EOS}}(\tau, e, Y, \alpha, \psi) = \begin{cases} s_1^{\mathrm{EOS}}(\tau, e), & \text{if } Y = 1, \\ Y s_1^{\mathrm{EOS}}\left(\frac{\alpha}{Y}\tau, \frac{\psi}{Y}e\right) + (1-Y) s_2^{\mathrm{EOS}}\left(\frac{1-\alpha}{1-Y}\tau, \frac{1-\psi}{1-Y}e\right), & \text{if } 0 < Y < 1, \\ s_2^{\mathrm{EOS}}(\tau, e), & \text{if } Y = 0. \end{cases} \tag{I.33}$$

For the sake of clarity I shall omit hereafter the dependence $(\tau_k, e_k) = (\alpha_k\tau/Y_k, \psi_k e/Y_k)$ of the parameters b_k and note $b_k = b_k(\tau_k, e_k)$ for $b_k \in \{g_k, T_k, P_k\}$, $k=1,2$. A straightforward calculation when $0 < Y < 1$ shows that

$$\mathrm{d}s = \frac{1}{T}\mathrm{d}e + \frac{P}{T}\mathrm{d}\tau + \left[\frac{g_2}{T_2} - \frac{g_1}{T_1}\right]\mathrm{d}Y - \tau\left[\frac{P_2}{T_2} - \frac{P_1}{T_1}\right]\mathrm{d}\alpha - e\left[\frac{1}{T_2} - \frac{1}{T_1}\right]\mathrm{d}\psi, \tag{I.34a}$$

where P and T are defined by

$$\frac{1}{T} = \frac{\psi_1}{T_1} + \frac{\psi_2}{T_2}, \qquad \frac{P}{T} = \alpha_1\frac{P_1}{T_1} + \alpha_2\frac{P_2}{T_2}, \tag{I.34b}$$

As $(\partial s/\partial e) = 1/T > 0$, we see that the mapping between e and s is one-to-one at constant (τ, Y, α, ψ), so the definition (I.33) also enables (up to the change of variable from τ to ρ) an EOS of the form $(\rho, s, Y, \alpha, \psi) \mapsto e^{\mathrm{EOS}}(\rho, s, Y, \alpha, \psi)$.

The two-phase system (I.25) can take the form for $0 < Y < 1$

$$\begin{cases} \partial_t(\rho Y) + \operatorname{div}(\rho Y \mathbf{u}) = \tilde{\kappa}_Y \left[\frac{g_2}{T_2} - \frac{g_1}{T_1}\right], & \text{(I.35a)} \\ \partial_t(\rho\alpha) + \operatorname{div}(\rho\alpha\mathbf{u}) = -\tilde{\kappa}_\alpha \left[\frac{P_2}{T_2} - \frac{P_1}{T_1}\right], & \text{(I.35b)} \\ \partial_t(\rho\psi) + \operatorname{div}(\rho\psi\mathbf{u}) = -\tilde{\kappa}_\psi \left[\frac{1}{T_2} - \frac{1}{T_1}\right], & \text{(I.35c)} \\ \partial_t\rho + \operatorname{div}(\rho\mathbf{u}) = 0, & \text{(I.35d)} \\ \partial_t(\rho\mathbf{u}) + \operatorname{div}(\rho\mathbf{u}\mathbf{u}^T) + \boldsymbol{\nabla} P = 0, & \text{(I.35e)} \\ \partial_t\left(\rho e + \rho\frac{|\mathbf{u}|^2}{2}\right) + \operatorname{div}\left(\rho e\mathbf{u} + \rho\frac{|\mathbf{u}|^2}{2}\mathbf{u} + P\mathbf{u}\right) = 0, & \text{(I.35f)} \end{cases}$$

where $\tilde{\kappa}_b$, $b \in \{Y, \alpha, \psi\}$ are positive coefficients and the pressure P is defined by (I.34b). The source terms that appear (I.35a), (I.35b) and (I.35c) can be considered as relaxation terms that drive the solution towards en equilibrium state. This equilibrium state can be defined thanks to another EOS that will be presented in the section I.4.3.

Remark 7 The system (I.35) is unambiguously defined for $(Y, \alpha, \psi) \in (0,1)^3$. However in the limit case when Y, α or ψ may take the value 0 or 1, the definition of the terms may become delicate. Such an issue requires to be studied on a case-by-case basis depending on the choice of the pure phase EOS and the definition of the parameters $\tilde{\kappa}_b$, $b \in \{Y, \alpha, \psi\}$.

Remark 8 Defining or even quantifying the magnitude order of the parameters $\tilde{\kappa}_b$, $b \in \{Y, \alpha, \psi\}$ is still an active field of research. Providing a definition for the term $\tilde{\kappa}_\alpha$ that pertains to mechanical equilibrium between phases has been investigated in [Gav14, 1].

I.4.3 Two-phase mixture : an equilibrium EOS

The source terms in (I.35) act on the composition variables by inducing a production of entropy in agreement with (I.23). The dissipation stops once the system reaches an equilibrium state such that

$$(T_1, P_1, g_1)\left(\frac{\alpha}{Y}\tau, \frac{\psi}{Y}e\right) = (T_2, P_2, g_2)\left(\frac{1-\alpha}{1-Y}\tau, \frac{1-\psi}{1-Y}e\right) \tag{I.36}$$

According to the definition of the mixture entropy (I.33) and the differential expression (I.34), solving (I.36) is equivalent to seek $(Y, \alpha, \psi) \in (0,1)^3$ such that

$$\frac{\partial s}{\partial Y}(\tau, e, Y, \alpha, \psi) = 0, \qquad \frac{\partial s}{\partial \alpha}(\tau, e, Y, \alpha, \psi) = 0, \qquad \frac{\partial s}{\partial \psi}(\tau, e, Y, \alpha, \psi) = 0, \tag{I.37}$$

for a given value of (τ, e). In other words, the relaxation processes associated with the source terms in (I.35a), (I.35b) and (I.35c) tend to extremize $(Y, \alpha, \psi) \in (0,1)^3 \mapsto s(\tau, e, Y, \alpha, \psi)$ for any fixed (τ, e).

> *This means that for such models, the evolution of the composition evolves in order to optimize the entropy of the mixture for a given overall energy and overall specific volume values e and τ.*

An elegant way of generalizing this problem to $(Y, \alpha, \psi) \in [0,1]^3$ was proposed in [Hel05, HS06] : accouting for the fact that $Y_k s_k(\alpha_k\tau/Y_k, \psi_k e/Y_k) = S_k(Y_k, \alpha_k\tau, \psi_k e)$, we can see that the mixture entropy takes the form

$$s(\tau, e, Y, \alpha, \psi) = S_1(Y, \alpha\tau, \psi e) + S_2(1-Y, (1-\alpha)\tau, (1-\psi)e), \quad (Y, \alpha, \psi) \in [0,1]^3, \tau > 0, e > 0. \tag{I.38}$$

The problem of solving (I.36) is thus extended to seeking the maximum of $s(Y, \alpha, \psi) \in [0,1]^3 \mapsto s(\tau, e, Y, \alpha, \psi)$ for a given (τ, e). A first important consequence of (I.38) is that $(Y, \alpha, \psi) \in [0,1]^3 \mapsto s(\tau, e, Y, \alpha, \psi)$ is strictly concave for a fixed (τ, e). A second important consequence is that for a given (τ, e), the function $(Y, \alpha, \psi) \mapsto s(\tau, e, Y, \alpha, \psi)$ admits a unique maximum value in $[0,1]^3$ that we shall note $(Y^{\text{eq}}(\tau, e), \alpha^{\text{eq}}(\tau, e), \psi^{\text{eq}}(\tau, e))$.

If one assumes that for a given (τ, e) the system reaches equilibrium infinitely fast so that we always have $b = b^{\text{eq}}(\tau, e)$, $b \in \{Y, \alpha, \psi\}$, this implies that the two-phase medium is equipped with a new EOS $(\tau, e) \mapsto s^{\text{eq}}$ defined by

$$s^{\text{eq}}(\tau, e) = s\big(\tau, e, Y^{\text{eq}}(\tau, e), \alpha^{\text{eq}}(\tau, e), \psi^{\text{eq}}(\tau, e)\big). \tag{I.39}$$

Two complementary ways can be used to characterize the new entropy s^{eq}. First, a geometrical argument proposed in [Car04, 23, 22, 21, Fac08, 14] shows that graph of $(\tau, e) \mapsto s^{\text{eq}}$ in the τ-e-s space can be constructed by taking the concave hull of the set $\{(\tau', e', s') \in [0, +\infty)^2 \times \mathbb{R} \mid s' \leq \max(s_1(\tau', e'), s_2(\tau', e'))\}$. The set of points $(\tau, e, s^{\text{eq}}(\tau, e))$ in the τ-e-s space that represent the solution of the equilibrium (I.37) form a so-called "bi-tangent" plane that is tangent to both surfaces $\{(\tau, e, s_k(\tau, e)) \mid (\tau, e) \in [0, +\infty)^2\}$, $k = 1, 2$.

A second argument using convex analysis was shown in [BH05, Hel05, HS06] : the definition (I.39) is equivalent to set

$$s^{\text{eq}}(\tau, e) = (S_1 \square S_2)(1, \tau, e), \tag{I.40}$$

where $(\cdot\square\cdot)$ is the sup-convolution operator defined by $(\mathscr{f}_1\square\mathscr{f}_2)(\mathbf{z}) = \max\{\mathscr{f}_1(\mathbf{z}') + \mathscr{f}_2(\mathbf{z} - \mathbf{z}') \mid \mathbf{z}' \in [0, +\infty)^m\}$ if $\mathscr{f}_1$ and $\mathscr{f}_2$ are real-valued functions defined over $[0, +\infty)^m$, $m \in \mathbb{N}$.

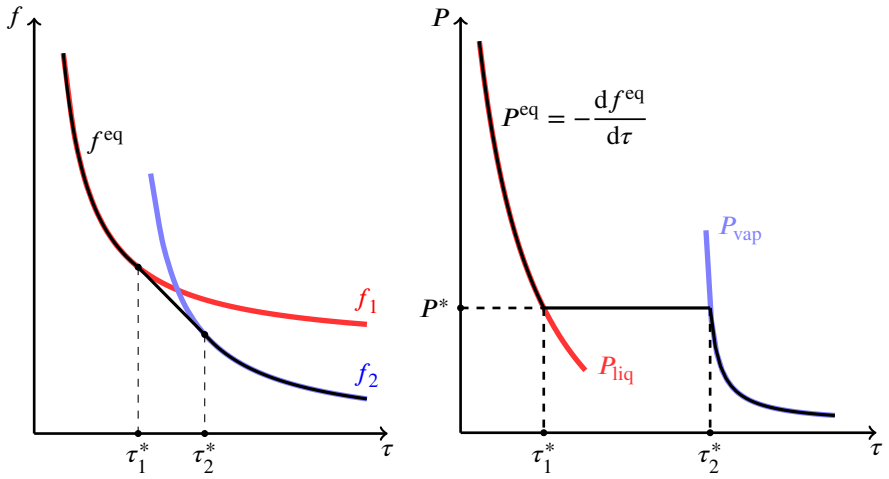

Figure I.1 – Equilibrium EOS obtained by convexification of the free energy for the barotropic HEM model.

Both (I.40) and the concave hull construction imply that the new equilibrium entropy $(\tau, e) \mapsto s^{eq}$ is concave. This resulting EOS can be viewed as the result of a "concavification" process. This idea for modeling material undergoing phase change was studied in [Jao01] within the framework of a single non-concave EOS that describe both phases. Indeed using the construction of s^{eq}, one can recover the Maxwell equilibrium. Therefore this entropy optimization process can be considered as a link between the two-phase and the single phase EOS approaches for describing two-phase media. It is important to note that this approach will discard possible metastable states that can be reached with a non-concave EOS. More recent works [JM16, HJM20, Mat20] have proposed a framework that extends the definition of the equilibrium entropy presented in this section. This work provided remarkable results : it succeeded in connecting the two-EOS approach to the non-concave single-EOS approach and enabled metastability.

In section II.10, I will present algorithms proposed in [19, Fac08, 14, 17] for computing the equilibrium values $Y^{eq}(\tau, e)$, $\alpha^{eq}(\tau, e)$ and $\psi^{eq}(\tau, e)$) with given EOS for the pure phases.

I.5 Study of a two-phase model : Homogeneous Equilibrium Model

Contributions by the author
This section covers works that have been published in [23, 24, 22, 21, 19, 14].

Two-phase flow models can be built using the equilibrium EOS presented in section I.4.3, by considering the compressible single-component Euler equation supplemented with the equilibrium equation of state associated with (I.39). It is common to gather such model into a family called Homogeneous Equilibrium Models (HEM). I will briefly recall here some results concerning the well-posedness of these models.

Barotropic HEM model
A first case was studied in [Car04, 23, 24, 22] using the entropy concavification process described in section I.4.3 under the slightly different framework of two materials equipped with barotropic EOS. In this case the EOS of each phase is given in the form of a free Helmholtz energy function $\tau_k \mapsto f_k$, with $\left(d^2 f_k / d\tau_k^2\right) > 0$. For such EOS, the pressure P_k of the fluid k is given by $P_k = -\left(df_k/d\tau_k\right)$ and the free enthalpy g_k is $g_k = f_k + P_k\tau_k$. The graph of the equilibrium free energy $\tau \mapsto f^{eq}$ is defined by taking the convex hull of the set $\left\{(\tau', f') \in [0, +\infty) \times \mathbb{R} \mid f' \geq \min(f_1(\tau'), f_2(\tau'))\right\}$ as depicted in figure I.1. The matching equilibrium relation of (I.36) for the barotropic case reduces to

$$P_1 = P_2, \qquad g_1 = g_2, \tag{I.41}$$

in the case where both phases are present. Considering one-dimensional problems (for the sake of simplicity), the barotropic HEM model reads

$$\partial_t \rho + \partial_x(\rho u) = 0, \qquad \partial_t(\rho u) + \partial_x(\rho u^2 + P) = 0, \tag{I.42}$$

where $P = P^{eq}(1/\rho) = -(df^{eq}/d\tau)(1/\rho)$.

Clearly, it appears that the resulting free energy function $\tau \mapsto f^{eq}$ is not strictly convex as the part that describes the solution of (I.41) yields a linear behavior in an interval $\tau \in (\tau_1^*, \tau_2^*)$. An unfortunate outcome of this profile is that the pressure law $\tau \mapsto P^{eq}$ associated with f^{eq} becomes constant in $\tau \in (\tau_1^*, \tau_2^*)$ (as shown in figure I.1). In this region the sound velocity vanishes and thus the model (I.42) is no longer hyperbolic. Consequently, well-posedness is not granted for (I.42) using the classic hyperbolic conservation laws theory.

Nevertheless, the system (I.42) was later studied in [GS06] where the Riemann problem associated with (I.42) was shown to possess a unique solution that verifies the Liu entropy criterion [Liu76].

HEM model with energy equation
The case of the HEM including an energy equation is obtained by considering the full Euler equations complemented by the EOS associated with the equilibrium entropy defined by (I.39). More specifically this reads for one-dimensional problems

$$\partial_t \rho + \partial_x(\rho u) = 0, \qquad \partial_t(\rho u) + \partial_x(\rho u^2 + P) = 0, \qquad \partial_t\left(\rho e + \rho\frac{u^2}{2}\right) + \partial_x\left[\left(\rho e + \rho\frac{u^2}{2} + P\right)u\right] = 0, \tag{I.43}$$

where $P = P^{\text{eq}}(1/\rho, e) = [(\partial s^{\text{eq}}/\partial\tau)/(\partial s^{\text{eq}}/\partial e)](1/\rho, e)$. As in the barotropic case, the entropy function $(\tau, e) \mapsto s^{\text{eq}}$ is not strictly convex. However this system is less pathological. Indeed, in [21, Fac08] the sound velocity associated with (I.43) was shown to never vanish so that (I.43) is indeed strictly hyperbolic.

I.6 Dissipative structure for a bifluid system

Contributions by the author
The present elements are not a published contribution of mine. This work was achieved by V. Guillemaud during his PhD [Gui07a] at that was supervised by J.-M. HÉRARD as his EDF and University supervisor and me, as his CEA supervisor. This work appears in [Gui07b].

In this section, I intend to illustrate how the previous may be adapted to equip more complex two-component systems involving several material velocities with dissipative terms.

For the sake of readability I will only consider one-dimensional problems and suppose given two-compressible fluids $k = 1, 2$ that are equipped with an EOS of the form described in section I.4. Using similar notations, we assume that each fluid is transported with the material velocity u_k and we note $E_k = e_k + |u_k|^2/2$ the total energy of the fluid k. I will consider a family of bifluid models of the form

$$\begin{cases} \partial_t \alpha_k + u_I \partial_x \alpha_k = \Lambda_k, & \text{(I.44a)} \\ \partial_t(\alpha_k\rho_k) + \partial_x(\alpha_k\rho_k u_k) = \Gamma_k, & \text{(I.44b)} \\ \partial_t(\alpha_k\rho_k u_k) + \partial_x(\alpha_k\rho_k u_k u_k) + \partial_x(\alpha_k P_k) - P_I\partial_x\alpha_k = D_k + \Gamma_k u_I, & \text{(I.44c)} \\ \partial_t(\alpha_k\rho_k E_k) + \partial_x(\alpha_k\rho_k E_k u_k) + \partial_x(\alpha_k P_k u_k) - P_I u_I \partial_x\alpha_k = \Phi_k + \Gamma_k E_I + D_k u_I - P_I\Lambda_k, & \text{(I.44d)} \end{cases}$$

where the fluid parameters u_I and P_I are homogeneous respectively to a velocity and a pressure usually referred to as interfacial velocity and interfacial pressure. If we note $\theta_k = g_k - (u_k - u_I^2)/2$, we define an interfacial energy e_I to be a convex combination of θ_1 and θ_2 and set $E_I = e_I + |u_I|^2/2$.

This modeling framework encompasses several models that have been studied in the literature like [BN86, GSS96, GSS99, GS02, Coq+02, SGR03, Gui07a, Cro+15, Loc16, Loc+16, Che19, CM20, Cor20]. A key element of the model is to provide a definition for u_I and P_I. Considering a vanishing right-hand term in (I.44d), u_I is an eigenvalue associated with the Jacobian of the system. The nature of the field associated with u_I is intimately connected to the definition of u_I as well as the definition of the non-conservative product $u_I\partial_x\alpha_k$ (see for example [Coq+02, Gui07a]). This question will not be discussed at length here. Let us just mention that the definition proposed in [Coq+02, Gui07a, Gui07b] allows to associate $\mathbf{u}_I$ with a linearly degenerate field and ensure a proper definition of $u_I\partial_x\alpha_k$ in the weak sense.

I propose to examine the definition of the right-hand side terms of (I.44d) and possible constraints upon P_I and u_I in order to enable an entropy inequality for the system. The conservation of total mass, momentum, energy and the saturation relation $\alpha_1 + \alpha_2 = 1$ implies that $\sum_{k=1,2}\Lambda_k = 0$, $\sum_{k=1,2}\Gamma_k = 0$, $\sum_{k=1,2} D_k = 0$ and $\sum_{k=1,2}\Phi_k = 0$.

We then make the structuring assumption that the entropy η and the entropy flux g can be chosen as follows

$$\eta = -(\alpha_1\rho_1 s_1 + \alpha_2\rho_2 s_2), \qquad g = -(\alpha_1\rho_1 s_1 u_1 + \alpha_2\rho_2 s_2 u_2). \tag{I.45}$$

A straightforward (but tedious) calculation yields

$$\partial_t\eta + \partial_x g = +\sum_{k=1,2}\frac{(P_k - P_I)(u_k - u_I)}{T_k}\partial_x\alpha_k - \Phi_2\sum_{k=1,2}\frac{(-1)^k}{T_k} - D_2\sum_{k=1,2}\frac{(-1)^k(u_I - u_k)}{T_k} - \Gamma_2\sum_{k=1,2}\frac{(-1)^k(e_I - \theta_k)}{T_k} + \Lambda_2\sum_{k=1,2}\frac{(-1)^k(P_I - P_k)}{T_k}. \tag{I.46}$$

In order for (I.46) to express an entropy inequality, we need to express the right-hand term of (I.46) as a signed quantity. First, if one assume that the expression of u_I and P_I does not involve any partial differential of the flow parameters, then we necessarily have to impose that

$$\frac{(P_1 - P_I)(u_1 - u_I)}{T_1} = \frac{(P_2 - P_I)(u_2 - u_I)}{T_2}. \tag{I.47}$$

For a given choice of u_I, relation (I.47) sets the definition of a corresponding P_I. Now the remaining terms in the right-hand side of (I.46) can be examined using similar lines as in section I.4.2. We consider that each term is an independent

contribution to the dissipation. This suggests to impose for Φ_2, D_2, Γ_2 and Λ_2 that

$$\Phi_2 \sum_{k=1,2} \frac{(-1)^k}{T_k} \geq 0, \quad D_2 \sum_{k=1,2} \frac{(-1)^k (u_I - u_k)}{T_k} \geq 0, \quad \Gamma_2 \sum_{k=1,2} \frac{(-1)^k (e_I - \theta_k)}{T_k} \geq 0, \quad \Lambda_2 \sum_{k=1,2} \frac{(-1)^k (P_I - P_k)}{T_k} \geq 0. \tag{I.48}$$

In many works of the literature like *e.g.* [BN86, GSS96, GSS99, GS02, Coq+02, Gui07a] the interfacial velocity u_I is defined as a convex combination of u_1 and u_2. The constraint (I.47) then implies that P_I is also a convex combination of P_1 and P_2. In this case, one can see that a possible definition for Φ_2, D_2, Γ_2 and Λ_2 that complies with (I.48) is

$$\Gamma_2 = \kappa_\theta(\theta_1 - \theta_2), \qquad \Lambda_2 = \kappa_P(P_2 - P_1), \qquad D_2 = \kappa_u(u_1 - u_2), \qquad \Phi_2 = \kappa_T(T_1 - T_2), \tag{I.49}$$

where κ_θ, κ_P, κ_u and κ_T are non-negative quantities.

Remark 9 A modeling choice for u_I and P_I that involves $\partial_x \alpha_k$ has been proposed in [SGR03, Che19].

I.7 Multi-scale modeling : a first step

Contributions by the author
This section covers works that have been published in [1].

I will present in this section a model that is a first step towards accounting for multi-scale phenomena in my work. The model is derived by stricly following the routine presented in section I.1.

We consider a two-phase medium that is composed of two compressible materials that are both equipped with a barotropic EOS. As in section I.5 these EOSs take the form of a free energy $\rho_k \mapsto f_k^{\text{EOS}}$, so that the pressure of the fluid k is given by $P_k^{\text{EOS}}(\rho_k) = \rho_k^2 (\mathrm{d} f_k^{\text{EOS}} / \mathrm{d}\rho_k)(\rho_k)$, $k = 1, 2$. Fluid 1 (resp. 2) will represent a gaseous (resp. liquid) phase. The medium is characterized by the following variables :

- the density ρ of the overall mixture,
- the common bulk velocity $\mathbf{u}$ of both phases that are supposed to be at kinematic equilibrium (at the bulk scale),
- the composition of the medium is described by a mass fraction Y and a volume fraction α (both associated with the fluid 1).

Although both fluids are supposed to share the same bulk velocity, we assume that $\mathbf{u}$ is only attached to large scale motions of the fluid and we aim at accounting for small scale kinetic effects that are related to small scale motions of the interface between fluid 1 and fluid 2.

The small scale elements are inserted in the model thanks to the Stationary Action Principle by considering that the system involves two kinetic energies :

- the classic bulk kinetic energy : $E_{\text{kin}}^{\text{large}} = \frac{1}{2}\rho |\mathbf{u}|^2$,
- a small scale kinetic energy : $E_{\text{kin}}^{\text{small}} = \frac{1}{2}\nu(\alpha)(D_t\alpha)^2$,

where $\nu(\alpha) > 0$ is a parameter that is referred to as micro-inertia and $D_t(\cdot) = \partial_t(\cdot) + \partial_{\mathbf{x}}(\cdot)\mathbf{u}$. While the expression of $E_{\text{kin}}^{\text{large}}$ is classic, the definition of $E_{\text{kin}}^{\text{small}}$ is associated with the time derivative variation of α along large scale trajectories associated with the bulk motion. The next step is to provide the model with a mixture potential energy that is supposed to take the form $E_{\text{pot}} = f(\rho, Y, \alpha)$. For the sake of simplicity, I will consider that f is a mixture barotropic potential defined by

$$f(\rho, Y, \alpha) = Y f_1^{\text{EOS}}(\rho Y/\alpha) + f_2^{\text{EOS}}(\rho(1-Y)/(1-\alpha)). \tag{I.50}$$

The Lagrangian $\mathscr{L}$ associated with the state is defined by

$$\mathscr{L}(\rho, \mathbf{u}, Y, \alpha, D_t\alpha) = E_{\text{kin}}^{\text{small}} + E_{\text{kin}}^{\text{small}} - E_{\text{pot}}. \tag{I.51}$$

We postulate the conservation of mass for each of the components, then the Hamilton Stationary Action Principle yields two evolution equations

$$\partial_t(\rho\mathbf{u}) + \operatorname{div}(\rho\mathbf{u}\mathbf{u}^T) + \boldsymbol{\nabla}\left[\rho^2\left(\frac{\partial f}{\partial \rho}\right) + \frac{1}{2}\nu(D_t\alpha)^2\right] = 0, \qquad \partial_t(\nu D_t\alpha) + \operatorname{div}(\mathbf{u}\nu D_t\alpha) - \frac{1}{2}(D_t\nu)(D_t\alpha) = -\rho\frac{\partial f}{\partial \alpha}. \tag{I.52}$$

System (I.52) suggests to define a pressure P for the two-phase medium by setting $P(\rho, Y, \alpha) = \rho^2(\partial f/\partial \rho)$. Accounting for (I.50), this reads

$$P(\rho, Y, \alpha) = \alpha P_1^{\text{EOS}}(\rho Y/\alpha) + (1-\alpha)P_1^{\text{EOS}}(\rho(1-Y)/(1-\alpha)).$$

The system (I.52) puts into play an evolution equation for the bulk momentum and a second order (with respect to time) evolution equation for α. This system can be recast by introducing the variable $\omega = (D_t\alpha)/(\rho Y)$, so that the second order equation of (I.52) on α becomes a two-equation first order system with respect to (α, ω) :

$$D_t\alpha = \rho Y \omega, \qquad D_t\omega = -\frac{1}{2}\frac{\nu'(\alpha)}{\nu(\alpha)}\rho Y \omega^2 + \frac{(P_1 - P_2)}{\nu(\alpha)}. \tag{I.53}$$

We now turn to the study of possible source terms that may be added to the evolution equation of ω in order to account for internal dissipative effects. By computing $\rho D_t(f + |\mathbf{u}|^2/2)$ we obtain that

$$\partial_t\left(\rho f + \rho\frac{|\mathbf{u}|^2}{2}\right) + \mathrm{div}\left(\rho f\mathbf{u} + \rho\frac{|\mathbf{u}|^2}{2}\mathbf{u} + P\mathbf{u}\right) = \mathcal{Q}, \qquad \mathcal{Q} = \rho Y\omega\left(\nu(\alpha)\rho Y D_t\omega + \rho\frac{\partial f}{\partial\alpha} + \frac{1}{2}(\rho Y\omega)^2\nu'(\alpha)\right). \tag{I.54}$$

In order for (I.54) to provide an entropy inequality, this suggests to consider that $\left(\nu(\alpha)\rho Y D_t\omega + \rho\frac{\partial f}{\partial\alpha} + \frac{1}{2}(\rho Y\omega)^2\nu'(\alpha)\right) = -\epsilon Y\omega$ where $\epsilon > 0$ is a parameter called the micro-viscosity coefficient. This system with internal dissipative effects then reads

$$\begin{cases} \partial_t\rho + \mathrm{div}(\rho\mathbf{u}) = 0, & \text{(I.55a)}\\ \partial_t(\rho Y) + \mathrm{div}(\rho Y\mathbf{u}) = 0, & \text{(I.55b)}\\ \partial_t(\rho\mathbf{u}) + \mathrm{div}(\rho\mathbf{u}\mathbf{u}^T) + \boldsymbol{\nabla}\left[P + \frac{1}{2}\nu(\rho Y\omega)^2\right] = 0, & \text{(I.55c)}\\ \partial_t(\rho\alpha) + \mathrm{div}(\rho\alpha\mathbf{u}) = \rho^2 Y\omega, & \text{(I.55d)}\\ \partial_t(\rho Y\omega) + \mathrm{div}(\rho Y\omega\mathbf{u}) = -\frac{\epsilon}{\nu}\rho Y\omega - \frac{1}{2}\frac{\nu'(\alpha)}{\nu(\alpha)}(\rho Y\omega)^2 + \frac{(P_1 - P_2)}{\nu(\alpha)}. & \text{(I.55e)} \end{cases}$$

By examining (I.55), it appears that the Stationnary Action Principle yielded a momentum evolution equation attached to the large scale through the conservation equation for $\rho\mathbf{u}$ and an evolution equation for ω that can be considered as a small scale momentum evolution equation.

In this sense, the effect of the Stationary Action Principle is to provide a momentum conservation equation for each of the kinetic energy involved in the model.

Somehow, one could say that the evolution of α is governed by the values of ω and $D_t\omega$ in the same way that the position of a particle is related to the velocity and acceleration in classical Mechanics.

Connection with interface two-phase flow

The system (I.55) can be connected to several systems of the literature by considering asymptotic limits.

By taking the limit $\nu \to 0$ for a fixed value of $\epsilon = O(\nu^0)$, we obtain a 4-equation model

$$\partial_t\rho + \mathrm{div}(\rho\mathbf{u}) = 0, \quad \partial_t(\rho Y) + \mathrm{div}(\rho Y\mathbf{u}) = 0, \quad \partial_t(\rho\mathbf{u}) + \mathrm{div}(\rho\mathbf{u}\mathbf{u}^T) + \boldsymbol{\nabla}P = 0, \quad \partial_t(\rho\alpha) + \mathrm{div}(\rho\alpha\mathbf{u}) = \rho\frac{(P_1 - P_2)}{\epsilon}, \tag{I.56}$$

that was studied in [CVV02b, CVV02a, Car04].

The limit $\nu \to 0$ and $\epsilon \to 0$ yields a 3-equation model

$$\partial_t\rho + \mathrm{div}(\rho\mathbf{u}) = 0, \qquad \partial_t(\rho Y) + \mathrm{div}(\rho Y\mathbf{u}) = 0, \qquad \partial_t(\rho\mathbf{u}) + \mathrm{div}(\rho\mathbf{u}\mathbf{u}^T) + \boldsymbol{\nabla}P = 0, \qquad P_1 = P_2. \tag{I.57}$$

that was also studied in [CVV02b, CVV02a, Car04].

It is worth noting that both systems (I.56) and (I.57) were used in [CVV02b, CVV02a] for simulating two-phase flows with interface. This type of simulation approach will be discussed in sections I.8 and II.3.

Connection with bubbly flow models

System (I.55) can be related to bubbly flow models. This can be achieved by injecting simple hypotheses pertaining to a mono-disperse flow into the model : we assume that the gaseous phase consists of spherical bubbles of radius $R(\mathbf{x}, t)$ with a number density $n(\mathbf{x}, t)$ function verifying $\partial_t n + \mathrm{div}(n\mathbf{u}) = 0$ and we neglect the density variations of the liquid phase. By noticing that for such disperse flow the volume fraction can be expressed by $\alpha = 4\pi R^3 n/3$, the (I.55d)-(I.55e) yields a second order equation for R :

$$3\alpha(1-\alpha)\nu\frac{D_t(D_tR)}{R} + 3\alpha\nu\left[2 - 5\alpha + \frac{3\alpha(1-\alpha)^2\nu'(\alpha)}{2\nu(\alpha)}\right]\left[\frac{D_tR}{R}\right]^2 + \frac{2\alpha(1-\alpha)}{R}\epsilon D_tR = P_1 - P_2. \tag{I.58}$$

The equation (I.58) shares similarity with a non-linear oscillating system. We proposed in [1] to identify (I.58) with equations of the literature. For the sake of brevity, I will only mention a comparison with the Rayleigh-Plesset equation [Ray17, PP77] that enabled the following estimates for the micro-inertia ν and the micro-viscosity ϵ

$$\nu = \rho_2\frac{(3\alpha)^{-1/3}}{(4\pi n)^{2/3}}, \qquad \epsilon = \frac{4\mu_2}{3\alpha}, \tag{I.59}$$

where μ_2 is the viscosity of the liquid phase. This analysis is coherent with results presented in [GS02, Gav14] for different models.

Other connections can be drawn with model of the literature that I will not fully detail here for the sake of brevity. The idea consists simply in studying the linear regime of the system by considering a first order perturbation of the bubble radius $R = \overline{R}(1 + rz)$ and the liquid pressure $P_2 = \overline{P_2} + r\delta P_2$ for small parameter $0 < r \ll 1$. This study leads to a second

order linear ordinary differential equation on z that has been compared with results of the literature [Pro77, CDL83]. New estimates for ν and ϵ can be identified that take the form

$$\nu = \frac{\rho_2 \overline{R}^2}{\overline{\alpha}}, \qquad \epsilon = \frac{4\mu_2}{3\overline{\alpha}} + \frac{2\rho_2 \overline{R}^2}{3\overline{\alpha}}(\gamma_{\text{th}} + \gamma_{\text{ac}}). \tag{I.60}$$

The coefficients γ_{th} and γ_{ac} characterize the damping in the system due to thermal and acoustic effects. Expressions for both of these coefficients are available in [Pro77, CDL83] and references from previous studies therein.

It is worth mentioning that many models of the literature include relaxation terms like pressure relaxation terms of (I.56) *for which providing an evoluation of the associated stiffness coefficient may be a difficult task. Therefore estimates like* (I.59) *can be quite valuable when one cannot consider the asymptotic regime $\epsilon \to 0$ or $\nu \to 0$.*

A valuable lesson I learned from that experience is that despite the acoustic regime may not be the main motivation in the definition of a model, this regime can be quite useful for understanding the mechanisms at play in the models, for comparing with other models and finally for estimating parameters of the models.

Comparison with experimental results

The study of the acoustic regime also showed that the model was substantially enriched by the small scale information. We performed a study of the dispersion relation associated with a monochromatic wave of system (I.55). The model was able to reproduce resonance phenomena that are missing when the micro-inertia is neglected. Comparisons with a more complex model involving two bulk velocities proposed by [CDL85] and the experimental results of [Sil57, Ler+08] showed a good agreement.

I.8 Modeling N-component flows with sharp interfaces

Contributions by the author

This section covers works that have been published in [20, 18, 10, 15, 13, 15, 8].

A part of my work has been dedicated to the simulation of compressible flows involving $N \geq 2$ separated by sharp interfaces. Although there is no full standard nomenclature regarding these simulation methods, I will refer to these methods as *interface capture methods*.

We consider a collection of N compressible fluids. Each fluid k is supposed to be equipped with an (incomplete) EOS given in the form of a pressure law $P_k^{\text{EOS}} : (\rho_k, e_k) \mapsto P_k$ or equivalently $e_k^{\text{EOS}} : (\rho_k, P_k) \mapsto e_k$ where ρ_k, e_k and P_k denote respectively the density, the specific internal energy and the pressure of the fluid $k = 0 \ldots, N-1$. The sound velocity c_k of the fluid k is defined by $c_k^2 = \left(\partial P_k / \partial \rho_k\right)_{e_k} + (P_k/\rho_k^2)\left(\partial P_k / \partial e_k\right)_{\rho_k}$.

From a coupling problem to an augmented single-fluid problem using color functions

Let $\mathscr{V} \subset \mathbb{R}^d$ be the computational domain. Each fluid k is supposed to evolve in a portion of space $\mathscr{V}_k(t) \subset \mathscr{V}$ separated from the other fluids so that $\mathscr{V}_k(t) \cap \mathscr{V}_{k'}(t) = \emptyset$ when $k \neq k'$ such that $\overline{\cup_{k=0,\ldots,N-1} \mathscr{V}_k(t)} = \overline{\mathscr{V}}$.

In each domain $\mathscr{V}_k(t)$ the medium is governed by the Euler equation supplemented by the EOS of the pure fluid k. Material interfaces defined by $\overline{\mathscr{V}_k(t)} \cap \overline{\mathscr{V}_{k'}(t)}$, $k \neq k'$ are supposed to be surfaces (resp. curves) of three-dimensional (resp two-dimensional) computational domain that form a discontinuity locus for the medium properties. We only consider rather simple kinematics-based jump conditions by requiring the continuity of the pressure and the normal velocity across the material interfaces. These conditions mimic the jump relations associated with classic contact discontinuities in the Euler equations.

A key idea of interface capture is to express the above coupling problem between as a single material problems where the interfaces location along with their associated jump conditions can be recovered using a weak formulation. It is common to represent sharp interfaces to N functions $(\mathbf{x}, t) \mapsto Z_k$ such that $Z_k(\mathbf{x}, t) = 1$ (resp. 0) if the fluid k is present (resp. not present) at the point $\mathbf{x}$ and instant t so that two different fluids cannot share the same location at the same instant (see figure I.2). This hypothesis can be expressed by the relation

$$\sum_{k=0}^{N-1} Z_k(\mathbf{x}, t) = 1. \tag{I.61}$$

The function Z_k is called the color function associated with the fluid k.

As the coupling hypothesis implies that no jump of velocity occurs at the interface, it is then possible to write a simple transport equation for the color functions

$$\partial_t Z_k + \mathbf{u}^T \boldsymbol{\nabla} Z_k = 0, \quad k = 0, \ldots N-1, \tag{I.62}$$

to describe the motion of the interface as the normal velocity to the interface and Z_k cannot experience a jump simultaneously (we shall see later that it is possible to express the evolution of Z_k using a conservation law).

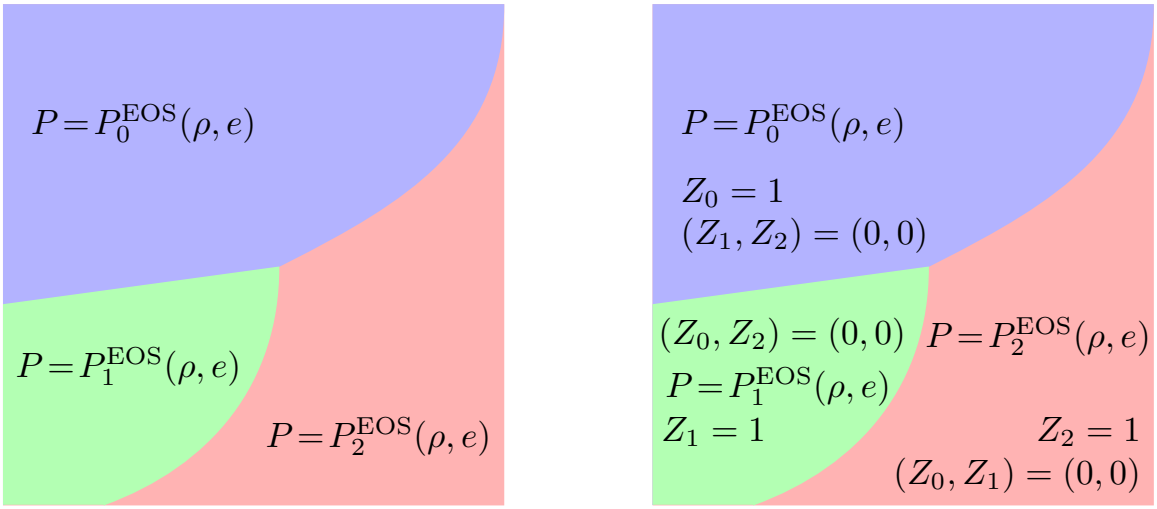

(a) Fluid coupling across sharp interfaces.

(b) The fluid k occupies the portion of space where $Z_k(\mathbf{x}, t) = 1$.

Figure I.2 – Flows with 3 components separated by sharp interfaces.

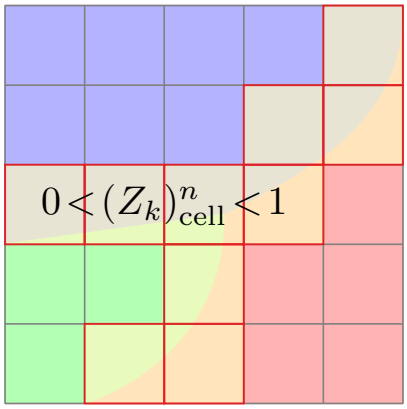

Figure I.3 – Interface capture method : transition area where $0 < Z_k < 1$.

Color function : a convenient numerical tool and a modeling problem

Capturing the motion of the interface now boils down to approximate (I.62). One shall use an initial condition such that $Z_k \in \{0, 1\}$ in each cell of the domain, but most numerical methods will smooth this initial discontinuity by generating intermediate values $0 < Z_k < 1$ in some cells of the computation domain. This situation is similar to what can happen with numerical methods for capturing shocks : a shock is often smeared over a few numerical cells due to numerical diffusion but is expected to converge towards the correct discontinuity as the space step of the discretization tends to 0. Unfortunately, the situation is more complex with the discontinuities carried by Z_k. Indeed, no EOS is *a priori* valid in regions where $0 < Z_k < 1$, so that the model is not fully defined for such values of Z_k. A possible cure can be sought within discretization strategies : some numerical techniques are able to maintain genuine discontinuous color functions throughout the computation, like the level set method [OS88, SSO94, Set99, OF03, LKY03] but fail to ensure conservativity. Another approach, that was used in my work and many others (see for example [QK96, SA99, Shy01]), tries to cope with the numerical diffusion of the interface by proposing a model for the intermediate states $0 < Z_k < 1$.

A model for interface capture

The following model was proposed in [10, 13]. It is an extension of models that were studied during my Ph.D. and published in [27, 26] to the case of flows with $N \geq 2$ component. The density ρ and the internal energy e of the medium verify

$$\rho = \sum_{k=0}^{N-1} Z_k \rho_k, \qquad \rho e = \sum_{k=0}^{N-1} Z_k \rho_k e_k^{\mathrm{EOS}}(\rho_k, P_k). \tag{I.63}$$

We introduce Y_k the mass fraction of fluid k that is defined by

$$Y_k = \rho_k Z_k / \rho. \tag{I.64}$$

Accounting for $\rho Y_0 = \rho - \sum_{k=1}^{N-1} \rho Y_k$ and $Z_0 = 1 - \sum_{k=1}^{N-1} Z_k$, the interface capture model reads

$$\begin{cases} \partial_t Z_k + \mathbf{u}^T \boldsymbol{\nabla} Z_k = 0, \quad k = 1, \dots, N-1, & \text{(I.65a)} \\ \partial_t(\rho Y_k) + \operatorname{div}(\rho Y_k \mathbf{u}) = 0, \quad k = 1, \dots, N-1, & \text{(I.65b)} \\ \partial_t \rho + \operatorname{div}(\rho \mathbf{u}) = 0, & \text{(I.65c)} \\ \partial_t(\rho u) + \operatorname{div}(\rho \mathbf{u}\mathbf{u}^T) + \boldsymbol{\nabla} P = 0, & \text{(I.65d)} \\ \partial_t(\rho E) + \operatorname{div}(\rho E \mathbf{u} + P\mathbf{u}) = 0, & \text{(I.65e)} \end{cases}$$

where $E = e + |\mathbf{u}|^2/2$ and the pressure $(\rho, e, Y_0, \dots Y_{N-1}, Z_0, \dots Z_{N-1},) \mapsto P$ is defined by assuming that we have a pressure equilibrium between all components. More precisely, for given values of e, Y_k and Z_k, $k = 0, \dots N-1$, P is the solution of

$$e = \sum_{k=0}^{N-1} Y_k e_k^{\mathrm{EOS}}\left(\frac{\rho Y_k}{Z_k}, P\right). \tag{I.66}$$

The system (I.65) can be viewed as a Euler system complemented by conservation and transport equations for the mass fractions Y_k and the color functions Z_k (with a strong coupling through the pressure law). Under simple hypotheses one can see that the pressure law is well-defined in the sense that (I.66) admits a unique solution. Considering one-dimensional problems, the wave structure of (I.65) is composed of two genuinely nonlinear waves of celerity $u \pm c$ and $2N+1$ linearly degenerate waves of celerity u, where

$$\left(\sum_k \xi_k Z_k\right) c^2 = \sum_k Y_k \xi_k c_k^2, \qquad \xi_k = \rho_k \left(\frac{\partial e_k}{\partial P_k}\right)_{\rho_k}. \tag{I.67}$$

One can see that the system is hyperbolic and a complete set of Rankine-Hugoniot conditions is available for (I.65) so that it is possible to define unambiguously weak solutions.

Remark 10 Actually an equivalent fully conservative form can be considered by replacing (I.65b) by a conservation equation $\partial_t(\rho Z_k) + \operatorname{div}(\rho Z_k \mathbf{u}) = 0$.

It is important to note that a key feature is missing in the model (I.65) : in the general case the system has no known entropy. As a consequence there is no straightforward definition of a mixture temperature, although it is possible to compute a temperature for each component.

The model (I.65) *seems reasonable for handling the dynamics of the flow when it involves mostly inertial effects. When one deals with effects that requires a stronger consistency with thermodynamics, for instance motions driven by variations of temperature and phase change the model* (I.65) *needs to be considered with caution.*

A numerical method for solving system (I.65) while preserving an accurate location of the interface will be described in section II.3.

Chapitre II

Numerical methods for compressible flows

A large part of my work is dedicated to propose numerical methods for simulating fluid flows. I will present a near-exhaustive overview of these numerical schemes in the present chapter. The section II.2 presents a Lagrange-Remap approach for a one-dimensional template system that encompasses several systems I have studied. This Lagrange-Remap strategy follows closely the standard method of the literature. In section II.3, I will present how this approach can be equipped with an anti-diffusive numerical scheme for proposing interface capture methods that control the numerical smearing of the interface. In sections II.4, I will propose a general presentation of an operator splitting procedure that revisits the Lagrange-Remap approach without involving genuine Lagrangian coordinates. These ideas set the ground for a series of sequel works that showed that this approach can be adapted to different systems and tackle several issues. In section II.5, I will present how this approach was modified in order to derive all-Mach regime accurate schemes and Implicit-Explicit (IMEX) methods so that the choice of the time step is no longer constrained by the sound velocity. I section II.6, I will show that this approach can be used to derive a numerical scheme that accounts for gravity and friction stiff source terms and that features Asymptotic Preserving (AP) properties with respect to a limit system in the large friction regime. This splitting strategy can also be applied to complex systems involving several material velocities : an application to a class of two-velocity two-pressure bifluid models is shown in section II.7. The method can also be adapted to the case of systems involving non-conservative source terms induced by a potential energy. Two examples are given in section II.8 for the shallow water equations and in section II.9 for the gas dynamics equations. The resulting schemes feature well-balanced properties with respect to specific stationary states. I will present a final work in section II.10 that deals with computing and approximating equilibrium states for the systems that can undergo phase change presented in section I.4.3.

II.1 Target system and notations

I will consider a target template system that can be expressed as follows

$$\partial_t \rho + \mathrm{div}(\rho \mathbf{u}) = 0, \qquad \partial_t(\rho \mathbf{W}) + \mathrm{div}(\rho \mathbf{W}\mathbf{u}^T + \mathbf{T}) = \mathbf{R}_\mathbf{W}, \qquad \partial_t \mathbf{\Psi} + (\partial_x \mathbf{\Psi})\mathbf{u} = \mathbf{R}_\mathbf{\Psi}, \tag{II.1}$$

with an initial condition $(\rho, \mathbf{W}, \mathbf{\Psi})(\mathbf{x}, t = t^n) = (\rho^n, \mathbf{W}^n, \mathbf{\Psi}^n)(\mathbf{x})$. The form of system (II.1) singles out the role of the mass variable and the material velocity $\mathbf{u}$ in the system (II.1).

Let us remark that most systems of the chapter I fits the generic form of system (II.1) (the bifluid system of section I.6 does not). In particular, the multi-component model (I.65) fit the target system if one chooses

$$\rho\mathbf{W} = \begin{bmatrix} \rho Y_1 \\ \vdots \\ \rho Y_{N-1} \\ \rho u_1 \\ \rho u_2 \\ \rho u_3 \\ \rho E \end{bmatrix}, \qquad \mathbf{\Psi} = \begin{bmatrix} Z_1 \\ \vdots \\ Z_{N-1} \end{bmatrix}, \qquad \mathbf{T} = P \left[\begin{array}{ccc} 0 & 0 & 0 \\ \vdots & \vdots & \vdots \\ 0 & 0 & 0 \\ \hline 1 & 0 & 0 \\ 0 & 1 & 0 \\ 0 & 0 & 1 \\ \hline u_1 & u_2 & u_3 \end{array}\right] \tag{II.2}$$

II.2 Classic Lagrange-Remap algorithm for a one-dimensional problem

This section is a brief refresher to the Lagrange-Remap method for one-dimensional problems (for a most complete presentation, the reader can refer to [GR96, Des17]) In the following I will consider only one-dimensional problems for system (II.1) without source terms, namely

$$\partial_t \rho + \partial_x(\rho u) = 0, \qquad \partial_t(\rho \mathbf{W}) + \partial_x(u\rho\mathbf{W} + \mathbf{T}) = \mathbf{0}, \qquad \partial_t \mathbf{\Psi} + u\partial_x \mathbf{\Psi} = 0, \tag{II.3}$$

and I will review the main lines of the classic Lagrange-Remap algorithm for approximating (II.3).

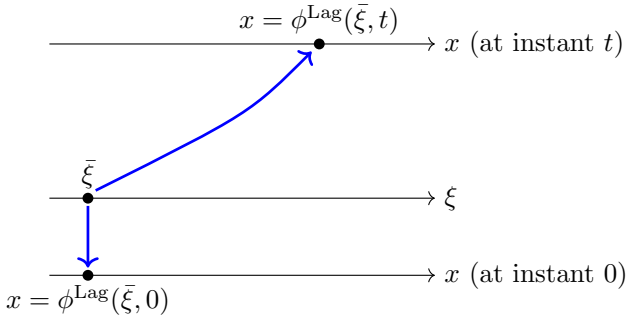

Figure II.1 – Mapping from the Lagrangian coordinates to the Eulerian coordinates.

Figure II.2 – Spatial mass coordinate (on a block of butter) are also very helpful for cooking !

Lagrangian coordinates (for one-dimensional problems)

We first need to introduce the Lagrangian formulation of (II.3). For $t \geq t^n$, we note $\phi^{\mathrm{Lag}}(\xi, t)$ the position of a fluid particle at instant t that was at position ξ at the initial instant $t = t^n$ (see figure II.1) and $J^{\mathrm{Lag}}(\xi, t) \overset{\text{def}}{=} \left(\partial\phi^{\mathrm{Lag}}/\partial\xi\right)_t$. We suppose the flow to be non-singular in the sense that we assume that $\phi^{\mathrm{Lag}}(\cdot, t)$ is one-to-one so that we consider loosing generality that $J^{\mathrm{Lag}} > 0$.

For any Eulerian mapping $(x, t) \mapsto b$, we can associate a Lagrangian mapping $(\xi, t) \mapsto b^{\mathrm{Lag}}$ defined by

$$b^{\mathrm{Lag}}(\xi, t) \overset{\text{def}}{=} b\big(\phi^{\mathrm{Lag}}(\xi, t), t\big). \tag{II.4}$$

The material velocity u is connected to the mapping ϕ^{Lag} by the assumption that

$$u^{\mathrm{Lag}}(\xi, t) = \left(\frac{\partial\phi^{\mathrm{Lag}}}{\partial t}\right)_{\xi}(\xi, t), \tag{II.5}$$

and the conservation of total mass in Lagrangian coordinates can be expressed by

$$\rho^n(\xi) = \rho^{\mathrm{Lag}}(\xi, t) J^{\mathrm{Lag}}(\xi, t). \tag{II.6}$$

One-dimensional flow equation in Lagrangian coordinates

System (II.3) can be expressed using Lagrangian coordinates as follows

$$\rho^{\mathrm{Lag}} J^{\mathrm{Lag}} = \rho^n, \qquad \rho^n(\xi)\,\partial_t \tau^{\mathrm{Lag}} - \partial_\xi u^{\mathrm{Lag}} = 0, \qquad \rho^n(\xi)\,\partial_t \mathbf{W}^{\mathrm{Lag}} + \partial_\xi \mathbf{T}^{\mathrm{Lag}} = \mathbf{0}, \qquad \partial_t \mathbf{\Psi}^{\mathrm{Lag}} = 0, \tag{II.7}$$

We consider an alternate but equivalent formulation of (II.7) that reads

$$\partial_t(\rho^{\mathrm{Lag}} J^{\mathrm{Lag}}) = 0, \qquad \partial_t J^{\mathrm{Lag}} - \partial_\xi u^{\mathrm{Lag}} = 0, \qquad \partial_t(\rho^{\mathrm{Lag}} \mathbf{W}^{\mathrm{Lag}} J^{\mathrm{Lag}}) + \partial_\xi \mathbf{T}^{\mathrm{Lag}} = \mathbf{0}, \qquad \partial_t \mathbf{\Psi}^{\mathrm{Lag}} = 0. \tag{II.8}$$

Remark 11 Another popular form of (II.7) can be obtained by changing the space coordinate : if we set $m(\xi) = \int_0^\xi \rho^n(\xi)\,\mathrm{d}\xi$ then all fields can be expressed with respect to (m, t) instead of (ξ, t). Up to an abuse of notation, (II.7) can be recast into

$$\partial_t(\rho^{\mathrm{Lag}} J^{\mathrm{Lag}}) = 0, \qquad \partial_t \tau^{\mathrm{Lag}} - \partial_m u^{\mathrm{Lag}} = 0, \qquad \partial_t \mathbf{W}^{\mathrm{Lag}} + \partial_m \mathbf{T}^{\mathrm{Lag}} = \mathbf{0}, \qquad \partial_t \mathbf{\Psi}^{\mathrm{Lag}} = 0. \tag{II.9}$$

Using the spatial m-coordinate to replace the x-coordinate for a one-dimensional problem may be at first a bit awkward. However, if one thinks of cooking instructions for cakes, it is quite natural. Indeed, on a block of butter, the length is usually shown with mass unit as shown in figure II.2 !

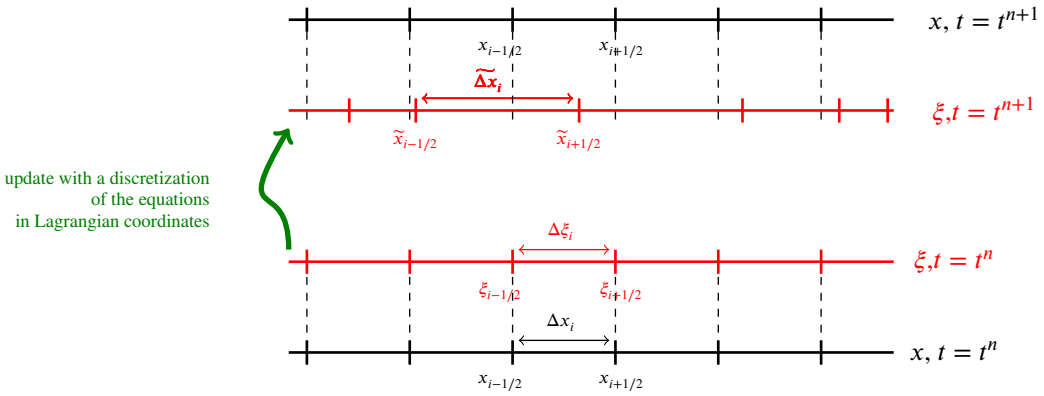

Figure II.3 – One-dimensional Lagrange-Remap discretization. Eulerian and Lagrangian mesh.

Lagrangian and Eulerian meshes

Using classic notations, let $\left(x_{i+1/2}\right)_{i\in\mathbb{Z}} \subset \mathbb{R}$ be a strictly increasing sequence so that $(K_i)_{i\in\mathbb{Z}}$ is an Eulerian mesh where $K_i = (x_{i+1/2}, x_{i-1/2})$. We will now "attach" a Lagrangian mesh frame to the Eulerian reference : we consider a sequence of fluid particles with an position initial position $\xi_{i+1/2} = x_{i+1/2}$ at the instant $t = t^n$. At the instant $t^{n+1} = t^n + \Delta t$, these particles have been transported with the flow at the position $\widetilde{x}_{i+1/2} = \phi^{\text{Lag}}(\xi_{i+1/2}, t^{n+1})$. We suppose that Δt is small enough so that the trajectories $\phi^{\text{Lag}}(\xi_{i+1/2}, t^{n+1})$ do not cross each other, *i.e.* $\widetilde{x}_{i-1/2} < \widetilde{x}_{i+1/2}$ for $i \in \mathbb{Z}$. We can now define a Lagrangian cell $K_i^{\text{Lag}} = (\xi_{i-1/2}, \xi_{i+1/2})$ that corresponds to a portion of fluid that occupies the volume $(\phi^{\text{Lag}}(\xi_{i-1/2}, t), \phi^{\text{Lag}}(\xi_{i+1/2}, t))$ for $t \in [t^n, t^{n+1})$, as depicted in figure II.3. Finally, we note $\Delta x_i = x_{i+1/2} - x_{i-1/2}$ the space step of the Eulerian mesh and $\widetilde{\Delta x_i} = \widetilde{x}_{i+1/2} - \widetilde{x}_{i-1/2}$ the volume of the Lagrangian cell K_i^{Lag} at instant t^{n+1} in the Eulerian frame.

Lagrange-Remap : discretization strategy

Let $(x, t) \mapsto b$ be an Eulerian field, we note b_i^n an approximate value of $b(x, t^n)$ for $x \in K_i$, and $\widetilde{b}_i$: an approximate value of $b^{\text{Lag}}(\xi, t^{n+1})$ for $\xi \in K_i^{\text{Lag}}$.

Let $(\rho_i^n, \mathbf{W}_i^n, \mathbf{\Psi}_i^n)_{i\in\mathbb{Z}}$ be the set of discretized variable at instant t^n over the Eulerian mesh, The Lagrange-Remap algorithm is an update from the instant t^n to instant t^{n+1} that can be summed up as follows :

— Step 1 : $(\rho_i^n, \mathbf{W}_i^n, \mathbf{\Psi}_i^n) \longrightarrow (\rho_i^{\text{Lag}}, \mathbf{W}_i^{\text{Lag}}, \mathbf{\Psi}_i^{\text{Lag}})$.
Attach a Lagrangian reference frame to the Eulerian frame at instant $t = t^n$ and build the discretized Lagrangian variable by setting $(\rho_i^{\text{Lag}}, \mathbf{W}_i^{\text{Lag}}, \mathbf{\Psi}_i^{\text{Lag}}) = (\rho_i^n, \mathbf{W}_i^n, \mathbf{\Psi}_i^n)$, for $i \in \mathbb{Z}$,

— Step 2 : $(\rho_i^{\text{Lag}}, \mathbf{W}_i^{\text{Lag}}, \mathbf{\Psi}_i^{\text{Lag}}) \longrightarrow (\widetilde{\rho}_i, \widetilde{\mathbf{W}}_i, \widetilde{\mathbf{\Psi}}_i)$.
Update the Lagrangian variable $(\rho_i^{\text{Lag}}, \mathbf{W}_i^{\text{Lag}}, \mathbf{\Psi}_i^{\text{Lag}})$ to its state $(\widetilde{\rho}_i, \widetilde{\mathbf{W}}_i, \widetilde{\mathbf{\Psi}}_i)$ by approximating the solution of (II.8) between $[t^n, t^{n+1})$,

— Step 3 : $(\widetilde{\rho}_i, \widetilde{\mathbf{W}}_i, \widetilde{\mathbf{\Psi}}_i) \longrightarrow (\rho_i^{n+1}, \mathbf{W}_i^{n+1}, \mathbf{\Psi}_i^{n+1})$.
Resample (remap) the Lagrangian variable $(\widetilde{\rho}_i, \widetilde{\mathbf{W}}_i, \widetilde{\mathbf{\Psi}}_i)$ onto the Eulerian mesh by accounting for the motion of the Lagrangian mesh in order to obtain the updated Eulerian variables $(\rho_i^{n+1}, \mathbf{W}_i^{n+1}, \mathbf{\Psi}_i^{n+1})$, for $i \in \mathbb{Z}$.

Discretization of the Lagrange step

For the step 2, I will describe a generic approach without completely specifying the space discretization. Let us suppose that $\left\{\partial_\xi u^{\text{Lag}}\right\}_i$ and $\left\{\partial_\xi \mathbf{T}^{\text{Lag}}\right\}_i$ are respectively a discretization of $\partial_\xi u^{\text{Lag}}(\xi, t)$ and $\partial_\xi \mathbf{T}^{\text{Lag}}(\xi, t)$ for $(\xi, t) \in K_i^{\text{Lag}} \times [t^n, t^n + \Delta t)$, so that we discretize system (II.8) by

$$\widetilde{J_i^{\text{Lag}}}\,\widetilde{\rho_i^{\text{Lag}}} = \rho_i^n, \quad \widetilde{J_i^{\text{Lag}}} - 1 = \Delta t \left\{\partial_\xi u^{\text{Lag}}\right\}_i, \quad \widetilde{J_i^{\text{Lag}}}\,\widetilde{\rho_i^{\text{Lag}}}\,\widetilde{\mathbf{W}_i^{\text{Lag}}} - \rho_i^n \mathbf{W}_i^n + \Delta t \left\{\partial_\xi \mathbf{T}^{\text{Lag}}\right\}_i = 0, \quad \widetilde{\mathbf{\Psi}_i^{\text{Lag}}} = \mathbf{\Psi}_i^n. \tag{II.10}$$

The portion of fluid within K_i^{Lag} is evolved by the flow into the volume $\phi^{\text{Lag}}(K_i^{\text{Lag}}, t^{n+1})$. We make the approximation that $\phi^{\text{Lag}}(K_i^{\text{Lag}}, t^{n+1}) = (\widetilde{x}_{i-1/2}, \widetilde{x}_{i+1/2})$. According to the definition of J^{Lag} we have

$$\widetilde{x}_{i+1/2} - \widetilde{x}_{i-1/2} = \phi^{\text{Lag}}(\xi_{i+1/2}, t^{n+1}) - \phi^{\text{Lag}}(\xi_{i-1/2}, t^{n+1}) = \int_{K_i^{\text{Lag}}} J^{\text{Lag}}(\xi, t^{n+1})\, \mathrm{d}\xi.$$

This suggests to evaluate $\widetilde{\Delta x}_i$ by the relation

$$\widetilde{\Delta x}_i = \widetilde{x}_{i+1/2} - \widetilde{x}_{i-1/2} = \widetilde{J_i^{\text{Lag}}} \Delta\xi_i = \widetilde{J_i^{\text{Lag}}} \Delta x_i. \tag{II.11}$$

Discretization of the Remap step

For the step 3, consider an Eulerian field $(x,t) \mapsto b$. As $\widetilde{b}_i$ is an approximate value of b^{Lag} within cell $\xi \in K_i^{\text{Lag}}$, we set $\widetilde{b}(x) = \widetilde{b}_i$ if $x \in (\widetilde{x}_{i-1/2}, \widetilde{x}_{i+1/2})$, so that $x \mapsto \widetilde{b}$ is an approximation of $x \mapsto b(x, t^{n+1})$. We can use $\widetilde{b}$ to express an update of b within cell K_i thanks to the Chasles relation, we have

$$\int_{x_{i-1/2}}^{x_{i+1/2}} \widetilde{b}(x)\,\mathrm{d}x = \underbrace{\int_{\widetilde{x}_{i-1/2}}^{\widetilde{x}_{i+1/2}} \widetilde{b}(x)\,\mathrm{d}x}_{=\widetilde{\Delta x}_i \widetilde{b}_i} - \int_{x_{i+1/2}}^{\widetilde{x}_{i+1/2}} \widetilde{b}(x)\,\mathrm{d}x + \int_{x_{i-1/2}}^{\widetilde{x}_{i-1/2}} \widetilde{b}(x)\,\mathrm{d}x. \tag{II.12}$$

Let us now note

$$u_{i+1/2} = \frac{\widetilde{x}_{i+1/2} - x_{i+1/2}}{\Delta t} \quad \text{and} \quad (\widetilde{ub})_{i+1/2} \text{ an approximate of } \frac{1}{\Delta t}\int_{x_{i+1/2}}^{x_{i+1/2}+u_{i+1/2}\Delta t} \widetilde{b}(x)\mathrm{d}x.$$

Relation (II.12) suggests to resample the variable b over the Cartesian mesh through the following update relation

$$\Delta x_i b_i^{n+1} - \widetilde{\Delta x}_i \widetilde{b}_i + \Delta t\Big[(\widetilde{b}\,u)_{i+1/2} - (\widetilde{b}\,u)_{i-1/2}\Big] = 0. \tag{II.13}$$

The resampling formula (II.13) is very similar to an update by means of a flux formula except for the fact that it involves two different space steps Δx_i and $\widetilde{\Delta x}_i$.

Using (II.11), we can recast the remap relation (II.13) into

$$\Delta x_i(b_i^{n+1} - \widetilde{J_i^{\text{Lag}} b_i}) + \Delta t\Big[(\widetilde{b}\,u)_{i+1/2} - (\widetilde{b}\,u)_{i-1/2}\Big] = 0. \tag{II.14}$$

Overall Lagrange-Remap numerical scheme

Using the Lagrange step (II.10), the evolution of the Lagrangian cell volume (II.11), the remap step (II.13) and $\Delta\xi_i = \Delta x_i$, the overall Lagrange-Remap numerical scheme reads

$$\begin{cases} \Delta x_i(\rho_i^{n+1} - \rho_i^n) + \Delta t\big((\widetilde{\rho u})_{i+1/2} - (\widetilde{\rho u})_{i-1/2}\big) = 0, & \text{(II.15a)} \\ \Delta x_i\big((\rho\mathbf{W})_i^{n+1} - (\rho\mathbf{W})_i^n\big) + \Delta t\Big((\widetilde{\rho\mathbf{W}u})_{i+1/2} - (\widetilde{\rho\mathbf{W}u})_{i-1/2}\Big) + \Delta t\Delta x_i\left\{\partial_\xi \mathbf{T}^{\text{Lag}}\right\}_i = 0, & \text{(II.15b)} \\ \Delta x_i(\mathbf{\Psi}_i^{n+1} - \mathbf{\Psi}_i^n) + \Delta t\Big((\widetilde{\mathbf{\Psi}}\,u)_{i+1/2} - (\widetilde{\mathbf{\Psi}}\,u)_{i-1/2}\Big) - \mathbf{\Psi}_i^n \Delta t\Delta x_i\left\{\partial_\xi u^{\text{Lag}}\right\}_i = 0. & \text{(II.15c)} \end{cases}$$

It is worth noting that if $\left\{\partial_\xi \mathbf{T}^{\text{Lag}}\right\}_i$ is a conservative approximation of $\partial_\xi \mathbf{T}^{\text{Lag}}$ then the overall numerical scheme is conservative with respect to ρ and $\rho\mathbf{W}$.

This method in this form is intrinsically limited to one-dimensional problems. The extension to multi-dimensional problems was performed over Cartesian grids by means of a dimensional splitting.

II.3 Anti-diffusive interface capture numerical scheme

Contributions by the author
This section covers works that have been published in [20, 18, 15, 15, 13, 10].

The general guideline presented in section II.2 has been exploited in several articles I contributed to for simulating flows with $N \geq 2$ components. I will present in this section the numerical methods proposed in these papers.

The interface capture method proposes to capture the location of the material interfaces between the multiple components within a transition zone that is meant to converge towards a contact discontinuity although it is smeared by numerical diffusion. Therefore, limiting the numerical diffusion associated with the contact discontinuity that carries the interface location is a key issue within this context.

Following seminal ideas introduced in [DL01, Lag02, JL07] we take advantage of the structure of the Lagrange-Remap solver to introduce anti-diffusive mechanisms into the numerical scheme. Indeed, during the Lagrange step, color functions are stationary, therefore no numerical diffusion can be generated during this stage by the motion of the interface. The discretization of contact discontinuities in the model only comes into play during the Remap step. Therefore the numerical diffusion of the interface needs to be controlled during this stage.

Lagrange step for the multi-component model

The Lagrangian step was performed using the acoustic solver [Des97, Des10]. In our context, this reads

$$a_{i+\frac{1}{2}}=\sqrt{\min_{j=i,i+1}(\rho_j^n)\max_{j=i,i+1}(\rho c^2)_j^n},\qquad P_{i+\frac{1}{2}}=\frac{P_i^n+P_{i+1}^n}{2}-\frac{a_{i+\frac{1}{2}}}{2}(u_{i+1}^n-u_i^n),\quad u_{i+\frac{1}{2}}=\frac{u_i^n+u_{i+1}^n}{2}-\frac{(P_{i+1}^n-P_i^n)}{2a_{i+\frac{1}{2}}},\tag{II.16a}$$

$$\{\partial_\xi u\}_i=\frac{1}{\Delta x_i}(u_{i+\frac{1}{2}}-u_{i-\frac{1}{2}}),\qquad \{\partial_\xi \mathbf{T}\}_i=\frac{1}{\Delta x_i}(\mathbf{T}_{i+\frac{1}{2}}-\mathbf{T}_{i-\frac{1}{2}}),\qquad \mathbf{T}_{i+\frac{1}{2}}=\left[0,\dots,0,P_{i+\frac{1}{2}},P_{i+\frac{1}{2}}u_{i+\frac{1}{2}}\right]^T.\tag{II.16b}$$

The stability of the acoustic solver is obtained by chosing Δt in agreement with the CFL condition

$$\Delta t\max(a_{i+1/2},|u_{i+1/2}|)\le C^{\mathrm{CFL}}\min(\Delta x_i,\Delta x_{i+1}),\tag{II.17}$$

where in practice C^{CFL} is a constant chosen $C^{\mathrm{CFL}}\le 0.8$ (see [Des97]).

Remark 12 The acoustic scheme can be obtained using a Suliciu-type relaxation approach [Sul90, Bou04, CC08] or HLLC solver [TSS94, Tor09] for the Lagrangian gas dynamics system (II.9).

Remap step for the multi-component model

Before going any further, let us first define the upwind flux $b^{\mathrm{up}}_{i+1/2}$ and downwind flux $b^{\mathrm{down}}_{i+1/2}$ with respect to the velocity $u_{i+1/2}$ by

$$b^{\mathrm{up}}_{i+1/2}=\begin{cases}b_i, & \text{if } u_{i+1/2}>0,\\ b_{i+1}, & \text{otherwise,}\end{cases}\qquad b^{\mathrm{down}}_{i+1/2}=\begin{cases}b_{i+1}, & \text{if } u_{i+1/2}>0,\\ b_i, & \text{otherwise.}\end{cases}$$

For the Remap step, the numerical flux $(\widetilde{bu})_{i+1/2}$ is defined by setting $(\widetilde{bu})_{i+1/2}=\widetilde{b}_{i+1/2}u_{i+1/2}$ and

$$\widetilde{\rho}_{i+1/2}=\sum_{k=0}^{N-1}(\widetilde{\rho_k})_{i+1/2}(\widetilde{Z_k})_{i+1/2},\quad \widetilde{(\rho e)}_{i+1/2}=\sum_{k=0}^{N-1}(\widetilde{\rho_k e_k})_{i+1/2}(\widetilde{Z_k})_{i+1/2},\quad \widetilde{(\rho Y_k)}_{i+1/2}=(\widetilde{\rho_k})_{i+1/2}(\widetilde{Z_k})_{i+1/2},\tag{II.18a}$$

$$\widetilde{(\rho u)}_{i+1/2}=\widetilde{\rho}_{i+1/2}\widetilde{u}_{i+1/2},\qquad \widetilde{(\rho E)}_{i+1/2}=\widetilde{(\rho e)}_{i+1/2}+\frac{1}{2}\widetilde{\rho}_{i+1/2}(\widetilde{u}_{i+1/2})^2\tag{II.18b}$$

where we choose

$$\left(\widetilde{u},\widetilde{\rho_k},\widetilde{(\rho_k e_k)}\right)_{i+1/2}=\left(\widetilde{u}^{\mathrm{up}}_{i+1/2},\widetilde{\rho_k}^{\mathrm{up}}_{i+1/2},\widetilde{(\rho_k e_k)}^{\mathrm{up}}_{i+1/2}\right),\tag{II.18c}$$

so that the full definition of the Remap numerical scheme boils down to define the numerical flux $(Z_k)_{i+1/2}$ of the color functions.

Choice of the flux $(Z_k)_{i+1/2}$ for the color functions

An obvious and simple choice for $(Z_k)_{i+1/2}$ is the upwind value :

$$(Z_k)_{i+1/2}=\widetilde{(Z_k)}^{\mathrm{up}}_{i+1/2}.\tag{II.19}$$

The choice (II.19) yields a very robust scheme, however the overall numerical method is unsurprisingly very diffusive. Indeed, the interfaces get smeared into large regions where $0<Z_k<1$ in the computational domain. As shown in figure II.4, after a few time steps the geometric features of the interface can no longer be accurately described by the variations of Z_k. In order to cope with this difficulty, we chose to adapt the approach proposed by [DL01, Lag02, JL07] to the multi-component models (I.65). The strategy relies on the definition of so-called "trust intervals" $\left(I_k^n\right)_{i+1/2}$ and can be summed up in the following table.

$u_{i+1/2}>0$		$u_{i+1/2}<0$	
$u_{i-1/2}>0$	$u_{i-1/2}<0$	$u_{i+3/2}<0$	$u_{i+3/2}>0$
choose $\widetilde{(Z_k)}_{i+1/2}$ as close as possible to the the downwind value $\widetilde{(Z_k)}^{\mathrm{down}}_{i+1/2}$ within a "trust interval" $(I_k^n)_{i+1/2}$	choose the default "safe" upwind value $(Z_k)_{i+1/2}=\widetilde{(Z_k)}^{\mathrm{up}}_{i+1/2}$	choose $\widetilde{(Z_k)}_{i+1/2}$ as close as possible to the the downwind value $\widetilde{(Z_k)}^{\mathrm{down}}_{i+1/2}$ within a "trust interval" $(I_k^n)_{i+1/2}$	choose the default "safe" upwind value $(Z_k)_{i+1/2}=\widetilde{(Z_k)}^{\mathrm{up}}_{i+1/2}$

Defining the numerical scheme now narrows down to defining the trust intervals. I will start by the case $N=2$ that was investigated in [18] and then explain the modified method that was presented in [10] for the case $N>2$.

Case $N=2$

We only need to consider $\widetilde{(Z_1)}_{i+1/2}$ as the complementary color function is retrieved by $Z_0=1-Z_1$. Under the CFL condition

$$\max_{i\in\mathbb{Z}}|u_{i+1/2}|\frac{\Delta t}{\Delta x}\le\frac{1}{2},\tag{II.20}$$

one can show that

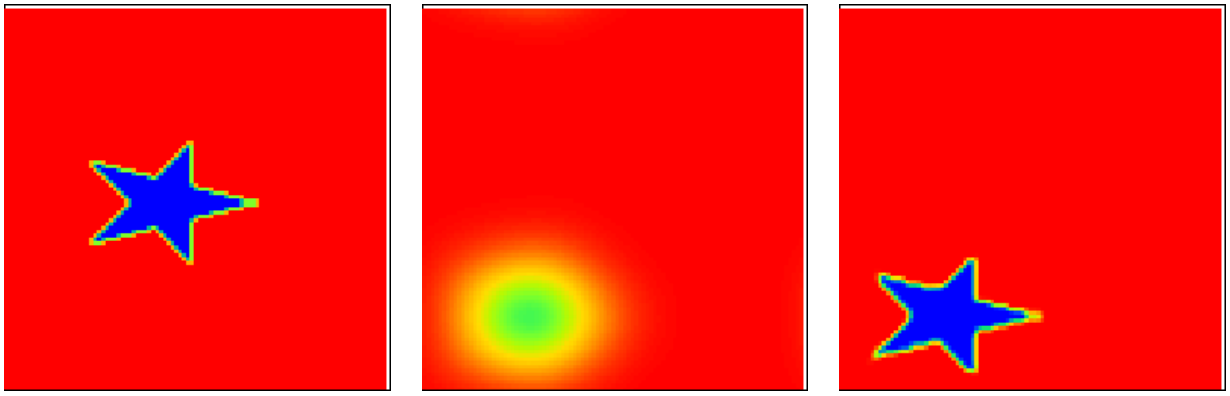

Profile at $t = 0$ | Profile at $t = 1$s with the upwind scheme | Profile at $t = 1$s with the anti-diffusive scheme

Figure II.4 – Mapping of the color functions for the transport of a star-shaped interface by Lagrange-Remap methods interface capture methods.

— when $u_{i+1/2} > 0$ and $u_{i-1/2} > 0$, it is possible to explicitly construct a non-empty interval $(I_1^n)_{i+1/2}$ such that $(Z_1)_{i+1/2}$ is a consistent flux and such that we have a local maximum principle in the cell i for Z_1, in the sense that $\min[(Z_1)_{i-1}^n, (Z_1)_i^n] \leq (Z_1)_i^{n+1} \leq \max[(Z_1)_{i-1}^n, (Z_1)_i^n]$,
— when $u_{i+1/2} < 0$ and $u_{i+3/2} < 0$, it is possible to explicitly construct a non-empty interval $(I_1^n)_{i+1/2}$ such that $(Z_1)_{i+1/2}$ is a consistent flux and such that we have a local maximum principle in the cell $i+1$ for Z_1, in the sense that $\min[(Z_1)_{i+2}^n, (Z_1)_{i+1}^n] \leq (Z_1)_{i+1}^{n+1} \leq \max[(Z_1)_{i+2}^n, (Z_1)_{i+1}^n]$.

Case $N > 2$

When $N > 2$, it is possible to follow the exact same lines as for the case $N = 2$, unfortunately this will not ensure that

$$(Z_k)_i^{n+1} \in [0,1] \quad \text{and} \quad \sum_{k=0}^{N-1} (Z_k)_i^{n+1} = 1. \tag{II.21}$$

To correct this issue, we proposed in [13, 10] to use the algorithm introduced in [JL07] for the multi-component model (I.65). The idea consists in computing a first sequence of trust intervals $(I_k)_{i+1/2}$ as in the $N = 2$ case. Then one builds recursively new trust intervals $(J_k^n)_{i+1/2} \subset (I_k^n)_{i+1/2}$ enforcing for each $k = 0, \dots, N-1$ that (II.21) is verified. If we note $(I_k^n)_{i+1/2} = [\omega_{k,i+1/2}^n, \Omega_{k,i+1/2}^n]$ the procedure reads

(i) For $k = 0$, set

$$(J_0^n)_{i+1/2} = \left[\max\left(\omega_{1,i+1/2}^n, 1 - \sum_{l=1}^{N-2} \Omega_{l,i+1/2}^n \right), \min\left(\Omega_{1,i+1/2}^n, 1 - \sum_{l=1}^{N-2} \omega_{l,i+1/2}^n \right) \right].$$

(ii) For $k = 1, \dots, N-2$, we suppose that $\widetilde{(Z_k)}_{i+1/2}$ are already known for $l \leq k$ and set

$$(J_k^n)_{i+1/2} = \left[\max\left(\omega_{k,i+1/2}^n, 1 - \sum_{l=0}^{k-1} \widetilde{(Z_l)}_{i+1/2} - \sum_{l=k+1}^{N-2} \Omega_{l,i+1/2}^n \right), \min\left(\Omega_{k,i+1/2}^n, 1 - \sum_{l=0}^{k-1} \widetilde{(Z_l)}_{i+1/2} - \sum_{l=k+1}^{N-2} \omega_{l,i+1/2}^n \right) \right].$$

(iii) For $k = N-1$, suppose that $\widetilde{(Z_l)}_{l+1/2}$ are already known for $l < N-1$ and set for the last flux

$$(J_{N-1}^n)_{i+1/2} = \left[\max\left(\omega_{N-1,i+1/2}^n, 1 \sum_{l=0}^{N-2} \widetilde{(Z_l)}_{i+1/2} \right), \min\left(\Omega_{N-1,i+1/2}^n, 1 - \sum_{l=0}^{N-2} \widetilde{(Z_l)}_{i+1/2} \right) \right].$$

Remark 13 In the two-component case studied in [18], the numerical scheme that was proposed had slightly stronger stability and consistency results. Indeed we showed that it was possible to construct trust intervals that also ensured consistency and stability for the mass fractions Y_k.

As shown in figure II.4 for a pure transport test and in figure II.5 with a three-component Kelvin-Helmholtz test, the anti-diffusive interface capture method succeeds in controlling the numerical diffusion. However, it is important to keep in mind that the overall flow is approximated with the same accuracy as a classic first order scheme. Indeed, far from the interface in pure fluid region, the numerical scheme degenerates to a classic upwind solver. Moreover, although the scheme succeeds in capturing small details of the interface it does not necessarily mean that these pertain to a genuine relevant fine description of the interface. These may be numerical artefacts.

The control of the numerical smearing of the interface in this method relies on the ability to exhibit a stability criterion for the transport equation. This task is achieved in a simple manner thanks to the one-dimensional setting. For multi-dimensional problems that can be discretized over a Cartesian grid, a dimensional splitting allows to take advantage of the good properties of the method. For unstructured meshes, an extension has been proposed in [Des+10] that was also used

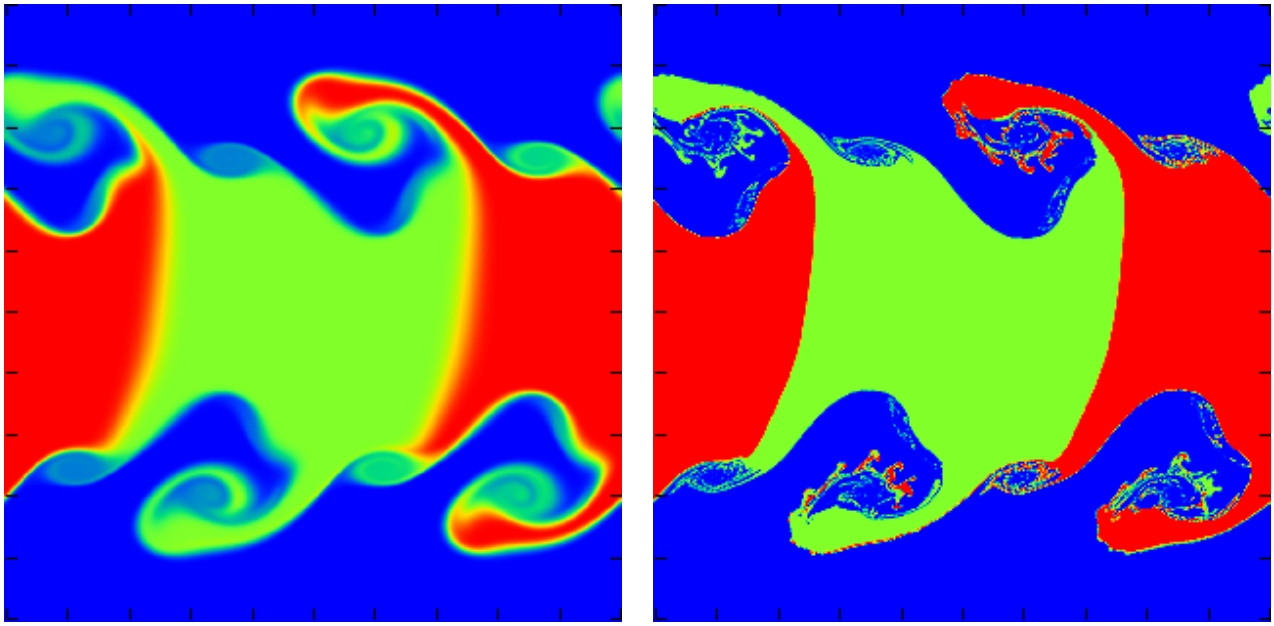

Upwind scheme Anti-diffusive scheme

Figure II.5 – Mapping of the color functions for a three-component Kelvin-Helmholtz instability by Lagrange-Remap interface capture methods.

in [12]. In this case, the stability argument is much more sophisticated and the numerical method the choice of mesh can (unsurprisingly) substantially impact the results.

Implementations of the present method I was involved in that were achieved in different simulation codes are present in section III.3.

CEMRACS 2010 : Towards more accuracte interface capture methods

A strategy designed for improving the accuracy of the interface capture method in the case $N = 2$ was proposed during the CEMRACS 2010 by the SIMCAPIAD project (see [15] and also section III.2). The driving idea was to use a MUSCL-limited spatial slope reconstruction supplemented with an order 2 Runge-Kutta time update far from the interface, while letting the anti-diffusive mechanism drive the flow update in the vicinity of the interface. The numerical results showed a significant improvement of the accuracy for a given mesh, although moderate overshoots could appear near the interface.

II.4 Discretization strategy for compressible fluid flows by means of an acoustic/transport operator splitting : general approach

In this section, I will present a general guideline to perform an operator splitting between acoustic and transport operators for discretizing compressible fluid flows. These ideas were implemented, extended and adapted in a series of works I co-authored. These schemes have been developed over the past years and my views on these methods have slightly evolved during this period of time. These numerical schemes have a strong connection with the classic Lagrange-Remap strategy presented in section II.2 whose features were driving influence in the design of these splitting schemes.

II.4.1 Motivations and influences

My interest in the Lagrange-Remap approach stemmed from the study of the work of F. Lagoutière and B. Després. At the time it was frustrating to see that, up to my knowledge, the classic Lagrange-Remap method seemed constrained to one-dimensional problems or Cartesian meshes with dimensional splitting. Indeed, the extension of the classic Lagrange-Remap method for two or three-dimensional problems seemed quite complex as it implies handling a moving mesh in a multi-dimensional setting.

Attractive features of the classic Lagrange-Remap approach

The one-dimensional case described in section II.2 seems a bit restrictive for most applications. However, the Lagrange-Remap method shows very interesting features :

— it decouples transport and other propagation phenomena like acoustic,
— in the case of the Euler equations it decouples linear (transport) and nonlinear waves (acoustic),
— it is compliant with the design of conservative numerical schemes as the problem boils down to propose a conservative discretization of $\partial_\xi \mathbf{T}^{\mathrm{Lag}}$.

I need to underline a very motivating and remarkable feature of the Lagrange-Remap procedure that was exploited in pioneering work of [Coq+08, Coq+10] : if one considers the case of the gas dynamics system for subsonic flows $|u| \ll c$, the Lagrange-Remap procedure allows also to decouple propagation phenomena with respect to their magnitude. More precisely :

— the Lagrange system (II.7) will account for fast (acoustic) phenomena,
— the remap step will account for slow phenomena by resampling the variable after the (slow) material motion.

If ones uses an explicit numerical discretization, the CFL constraint will be imposed by the fastest waves, *i.e.* the sound velocity c in our example. This imposes time steps that are too small for practical use in many industrial situations. This problem was addressed in [Coq+08, Coq+10] where they propose to use an implicit time-integration for the Lagrange/acoustic step and an explicit time-integration for the remap step.

The overall method proposed in [Coq+08, Coq+10] is very elegant as it allows to separate phenomena according to their propagation nature and also according to the magnitude of the propagation velocity. It also allows to build numerical methods that are both very efficient and simple. These methods are often referred to as IMEX (IMplicit-EXplicit) in the literature.

Taking another look at the moving mesh

When one looks at the numerical scheme of section II.2 one can remark that the moving mesh is not present in relations (II.15), neither is it present in the Lagrange step (II.10). The moving mesh is only involved in the Remap step (II.13). Using the relation (II.11) and (II.10), we see that $\widetilde{\Delta x}_i = \Delta x_i \left(1 + \Delta t \left\{\partial_\xi u^{\mathrm{Lag}}\right\}_i\right)$. The Remap step (II.13) then reads

$$\frac{b_i^{n+1} - \widetilde{b}_i}{\Delta t} + \frac{1}{\Delta x_i}\left[(\widetilde{b}\,u)_{i+1/2} - (\widetilde{b}\,u)_{i-1/2}\right] - \widetilde{b}_i \left\{\partial_\xi u^{\mathrm{Lag}}\right\}_i = 0. \tag{II.22}$$

The term $\left\{\partial_\xi u^{\mathrm{Lag}}\right\}_i$ features a derivative with respect to the Lagrangian coordinate ξ that is performed on a fixed mesh with respect to the ξ. The leftmost term of (II.22) is consistent with $\partial b/\partial t$, the middle term is consistent with $\partial(bu)/\partial x$ and the rightmost one with $u(\partial b/\partial x)$. We can see that the overall equation (II.22) seems consistent with the transport equation $(\partial b/\partial t) + u(\partial b/\partial x) = 0$.

These observations motivated seeking for numerical schemes with similar valuable features but without resorting to the Lagrangian point of view.

II.4.2 Mimicking Lagrange-Remap by splitting operators

We will now see that how to sketch an algorithm that shares many features with the Lagrange-Remap algorithm but without involving any moving mesh. The target problem we shall consider is once again the system (II.1) presented in section II.1 with vasnishing source terms :

$$\partial_t \rho + \mathrm{div}(\rho \mathbf{u}) = 0, \qquad \partial_t(\rho \mathbf{W}) + \mathbf{div}(\rho \mathbf{W}\mathbf{u}^T + \mathbf{T}) = \mathbf{0}, \qquad \partial_t \mathbf{\Psi} + (\partial_{\mathbf{x}} \mathbf{\Psi})\mathbf{u} = \mathbf{0}, \tag{II.23}$$

Acoustic/transport splitting

Let us suppose that the solutions are regular so we can recast the system (II.23) as follows

$$\begin{cases} \partial_t \rho & + (\partial_{\mathbf{x}} \rho)\mathbf{u} & + \rho \operatorname{div}(\mathbf{u}) & = 0, & \text{(II.24a)} \\ \partial_t (\rho \mathbf{W}) & + \partial_{\mathbf{x}} (\rho \mathbf{W})\mathbf{u} & + \rho \mathbf{W} \operatorname{div}(\mathbf{u}) + \mathbf{div}(\mathbf{T}) & = 0, & \text{(II.24b)} \\ \partial_t \mathbf{\Psi} & + (\partial_{\mathbf{x}} \mathbf{\Psi})\mathbf{u} & & = 0. & \text{(II.24c)} \end{cases}$$

We then consider two subsystems : a first subsystem composed of the blue terms

$$\partial_t \rho + \rho \operatorname{div}(\mathbf{u}) = 0, \qquad \partial_t (\rho \mathbf{W}) + \rho \mathbf{W} \operatorname{div}(\mathbf{u}) + \mathbf{div}(\mathbf{T}) = 0, \qquad \partial_t \mathbf{\Psi} = 0, \qquad \text{(II.25)}$$

that will be referred to as the acoustic subsystem and a second system composed of the red terms

$$\partial_t \rho + (\partial_{\mathbf{x}} \rho)\mathbf{u} = 0, \qquad \partial_t (\rho \mathbf{W}) + \partial_{\mathbf{x}} (\rho \mathbf{W})\mathbf{u} = 0, \qquad \partial_t \mathbf{\Psi} + (\partial_{\mathbf{x}} \mathbf{\Psi})\mathbf{u} = 0, \qquad \text{(II.26)}$$

that will be called the transport subsystem. The discretization strategy we propose is a two-step procedure [1] :

- Step 1 : update the state variable from its value $(\rho^n, \mathbf{W}^n, \mathbf{\Psi}^n)$ at the instant $t = t^n$ to $(\widetilde{\rho}, \widetilde{\mathbf{W}}, \widetilde{\mathbf{\Psi}})$ by approximating the solution of the acoustic subsystem (II.25),
- Step 2 : update the state variable from $(\widetilde{\rho}, \widetilde{\mathbf{W}}, \widetilde{\mathbf{\Psi}})$, to the value $(\rho^{n+1}, \mathbf{W}^{n+1}, \mathbf{\Psi}^{n+1})$ that describe the fluid at the instant $t = t^{n+1}$ by approximating the solution of the transport subsystem (II.26).

Acoustic subsystem : properties and approximations

After simple manipulations (II.25) can be expressed as

$$\rho(\mathbf{x}, t)\partial_t \tau - \operatorname{div}(\mathbf{u}) = 0, \qquad \rho(\mathbf{x}, t)\partial_t \mathbf{W} + \mathbf{div}(\mathbf{T}) = 0, \qquad \partial_t \mathbf{\Psi} = 0. \qquad \text{(II.27)}$$

System (II.27) bears a resemblance to (II.7). In this sense we can say it is a (pseudo) Lagrangian system or acoustic system. Moreover, we will see that for the classic cases, the eigenstructure of (II.27) mimics the eigenstructure of an acoustic system.

It is important to note that the density that appears as a cofactor of the time derivative depends on $(\mathbf{x}, t)$ and not solely $\mathbf{x}$ as it is the case for the genuine Lagrangian system (II.7). This matter is delicate as (II.27) is not in conservative form, so that the definition of weak solutions may be difficult. Nevertheless, that situation is not desperate. Indeed, let us not forget that the purpose of (II.27) is only to approximate some parts of the original system (II.23). Then we propose to approximate (II.27) by a relaxed system that reads

$$\partial_t \varkappa = \lambda(\varkappa - \rho), \qquad \varkappa \partial_t \tau - \operatorname{div}(\mathbf{u}) = 0, \qquad \varkappa \partial_t \mathbf{W} + \mathbf{div}(\mathbf{T}) = 0, \qquad \partial_t \mathbf{\Psi} = 0, \qquad \text{(II.28}_\lambda\text{)}$$

so that formally in the limit regime $\lambda \to +\infty$ we recover the acoustic system (II.27). At each time step, using classic lines, we will simulate this limit regime by enforcing an initial value $\varkappa(\mathbf{x}, t = t^n) = \rho(\mathbf{x}, t^n)$ and solving (II.28$_\lambda$) with $\lambda = 0$, namely

$$\partial_t \varkappa = 0, \qquad \varkappa \partial_t \tau - \operatorname{div}(\mathbf{u}) = 0, \qquad \varkappa \partial_t \mathbf{W} + \mathbf{div}(\mathbf{T}) = 0, \qquad \partial_t \mathbf{\Psi} = 0, \qquad \text{(II.29)}$$

so that now $\varkappa$ only depends on $\mathbf{x}$ in (II.29).

> *The variable $\varkappa(\mathbf{x})$ now acts as a "frozen density" so that (II.29) can be viewed as assuming that $\rho(\mathbf{x}, t)\partial_t \cdot \simeq \rho(\mathbf{x}, t^n)\partial_t \cdot$ in (II.27).*

If one introduces a new variable $L(\mathbf{x}, t)$ defined by

$$L(\mathbf{x}, t)\rho(\mathbf{x}, t) = \varkappa(\mathbf{x}), \qquad \text{(II.30)}$$

the system (II.29) now takes the form

$$\partial_t (L\rho) = 0, \qquad \partial_t L - \operatorname{div}(\mathbf{u}) = 0, \qquad \partial_t (L\rho \mathbf{W}) + \mathbf{div}(\mathbf{T}) = 0, \qquad \partial_t \mathbf{\Psi} = 0. \qquad \text{(II.31)}$$

The approximate acoustic system (II.31) is the system that will be chosen for evolving the flow variables in step 1.

This system is quite similar to the Lagrangian equation (II.8). An interesting feature is that it is expressed using a conservative form, therefore enabling the definition of weak solutions. Moreover, the jump relations obtained by considering pure shock solutions of (II.31) are the same as the jump relations of the genuine Lagrangian system (II.8).

Remark 14 As in the case of the genuine equations in Lagrangian coordinates, for one-dimensional problems it is also possible to introduce a spatial mass coordinate $m(x) = \int_0^x \varkappa(x')\,\mathrm{d}x'$ and recast (up to an abuse of notation) the approximate acoustic equation (II.29) into

$$\partial_t \tau - \partial_m u = 0, \qquad \partial_t \mathbf{W} + \partial_m \mathbf{T} = 0, \qquad \partial_t \mathbf{\Psi} = 0, \qquad \text{(II.32)}$$

so that we retrieve the system of gas dynamics in Lagrangian coordinates (II.9).

Properties of the transport subsystem

While the properties of the acoustic system may vary from one system to another, the properties of the transport system (II.26) are quite straightforward. The system is hyperbolic involving only transport at velocity $\mathbf{u}$.

1. The notations $(\rho^n, \mathbf{W}^n, \mathbf{\Psi}^n)$ and $(\widetilde{\rho}, \widetilde{\mathbf{W}}, \widetilde{\mathbf{\Psi}})$ are yet vague but they will of course refer to discrete values defined over a mesh.

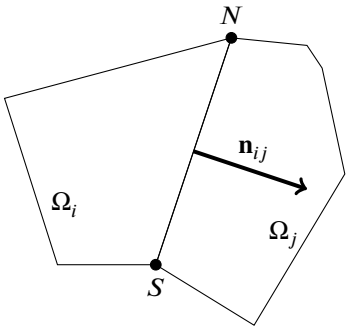

Figure II.6 – the face $\Gamma_{ij} = \overline{\Omega_i} \cap \overline{\Omega_j}$ defined by the segment (NS) has a unit normal vector $\mathbf{n}_{ij}$ oriented from Ω_i to Ω_j.

II.4.3 Finite volume discretization for the acoustic/transport splitting for multi-dimensional problems

I will present in this section a general finite-volume framework for discretizing (II.25)-(II.26). A distinctive feature from the classic Lagrange-Remap is that handling multi-dimensional problems using unstructured meshes does not require any specific processing. Before going any further, let us introduce notations pertaining to the multi-dimensional discretization. We suppose that $\Omega \subset \mathbb{R}^d$ with $d = 2$ ($d = 3$) is a polygonal (resp. polyhedral) domain that is covered by a set of N polygonal (resp. polyhedral) cells $(\Omega_i)_{1\leq i\leq N}$. We note $\Gamma_{ij} = \overline{\Omega_i} \cap \overline{\Omega_j}$, so that Γ_{ij} can either be empty, a vertex, an edge (for the case $d = 3$) or a single face of the mesh. We note $\mathcal{N}(i) = \{1 \leq j \leq N \mid \Gamma_{ij} \text{ is a face of } \Omega_i\}$, the set of indices of the neighbour cells of Ω_i. The unit normal vector to the face Γ_{ij} of a cell Ω_i, pointing from Ω_i to Ω_j is noted $\mathbf{n}_{ij}$, $j \in \mathcal{N}(i)$ (see figure II.6) and we set $\sigma_{ij} = |\Gamma_{ij}|/|K_i|$.

Discretization of the acoustic system

We suppose that u_{ij} and $\mathbf{T}_{ij}$ are numerical fluxes so that

$$u_{ij} \text{ is an approximate for } \frac{1}{\Delta t|\Gamma_{ij}|}\int_{t^n}^{t^{n+1}}\int_{\Gamma_{ij}} (\mathbf{u}^T\mathbf{n}_{ij})\,\mathrm{d}\gamma\,\mathrm{d}t \quad \text{and} \quad \mathbf{T}_{ij} \text{ is an approximate for } \frac{1}{\Delta t|\Gamma_{ij}|}\int_{t^n}^{t^{n+1}}\int_{\Gamma_{ij}} (\mathbf{T}\mathbf{n}_{ij})\,\mathrm{d}\gamma\,\mathrm{d}t.$$

We propose to use the following discretization for (II.25)

$$\widetilde{(L\rho)}_i = \rho_i^n, \qquad \widetilde{L}_i - 1 - \Delta t\sum_{j\in\mathcal{N}(i)}\sigma_{ij}u_{ij} = 0, \qquad \widetilde{(L\rho\mathbf{W})}_i - (\rho\mathbf{W})_i^n + \Delta t\sum_{j\in\mathcal{N}(i)}\sigma_{ij}\mathbf{T}_{ij} = 0, \qquad \widetilde{\mathbf{\Psi}}_i = \mathbf{\Psi}_i^n. \tag{II.33}$$

Discretization of the transport step for multi-dimensional problems

For the transport step, we consider a generic flux formula defined by

$$(\widetilde{bu})_{ij} \text{ is an approximate of } \frac{1}{\Delta t|\Gamma_{ij}|}\int_{t^n}^{t^{n+1}}\int_{\Gamma_{ij}} \widetilde{b}\,(\mathbf{u}^T\mathbf{n}_{ij})\,\mathrm{d}\gamma\,\mathrm{d}t, \tag{II.34}$$

and we use a generic discretization of (II.26) as follows

$$b_i^{n+1} - \widetilde{b}_i + \Delta t\sum_{j\in\mathcal{N}(i)}\sigma_{ij}(\widetilde{bu})_{ij} - \Delta t\,\widetilde{b}_i\sum_{j\in\mathcal{N}(i)}\sigma_{ij}u_{ij} = 0. \tag{II.35}$$

Overall algorithm

If one substitutes the update relation (II.33) of step 1 into (II.35), the overall numerical scheme reads

$$\begin{cases} \rho_i^{n+1} - \rho_i^n + \Delta t\sum_{j\in\mathcal{N}(i)}\sigma_{ij}(\widetilde{\rho u})_{ij} = 0, & \text{(II.36a)}\\ (\rho\mathbf{W})_i^{n+1} - (\rho\mathbf{W})_i^n + \Delta t\sum_{j\in\mathcal{N}(i)}\sigma_{ij}[(\widetilde{\rho\mathbf{W}\,u})_{ij} + \mathbf{T}_{ij}] = 0, & \text{(II.36b)}\\ \mathbf{\Psi}_i^{n+1} - \mathbf{\Psi}_i^n + \Delta t\sum_{j\in\mathcal{N}(i)}\sigma_{ij}(\widetilde{\mathbf{\Psi}\,u})_{ij} - \Delta t\,\mathbf{\Psi}_i^n\sum_{j\in\mathcal{N}(i)}\sigma_{ij}u_{ij} = 0. & \text{(II.36c)}\end{cases}$$

An important feature is that the numerical scheme (II.36) is conservative with respect to ρ and $\rho\mathbf{W}$.

Regarding stability, if one performs an explicit time update for both the acoustic step (II.33) and the transport step (II.35) it is natural to expect two CFL-type constraints in the form

$$\Delta t\max_{j\in\mathcal{N}(i)}\sigma_{ij}\Lambda_{ij}^{\text{acoustic}} \leq \frac{1}{2}, \qquad i = 0,\dots,N-1, \tag{II.37a}$$

$$\Delta t\max_{j\in\mathcal{N}(i)}\sigma_{ij}\Lambda_{ij}^{\text{transport}} \leq \frac{1}{2}, \qquad i = 0,\dots,N-1, \tag{II.37b}$$

where $\Lambda_{ij}^{\text{acoustic}}$ (resp. $\Lambda_{ij}^{\text{transport}}$) is expected to be an upper bound for the characteristic velocities associated with the acoustic system (II.31) (resp. transport system (II.35)) in the vicinity of the interface Γ_{ij}. It is then natural to anticipate that

$\Lambda_{ij}^{\text{transport}}$ should only involve estimates of the material velocity while $\Lambda_{ij}^{\text{transport}}$ may implicate the spectrum of the acoustic operator.

Remark 15 In the one-dimensional case, we can see that up to the choice of the numerical fluxes it is possible to build the exact same scheme as the original Lagrange-Remap scheme without considering any moving mesh.

II.5 Acoustic/transport splitting scheme for the Euler equations : IMEX strategies and Mach regime

Contributions by the author
This section covers works that have been published in [5, 7].

In many applications, the acoustic CFL (II.37) is very restrictive when the sound velocity c is large in comparison to the propagation phenomena of interest. This may be the case for simulation when the magnitude of the material velocity $\mathbf{u}$ is relatively small compared to c. In this case, the splitting between the acoustic system and the transport system allows to decouple the propagation phenomena according to their magnitude. It is then possible to use the seminal ideas proposed by [Coq+10] for a classic Lagrange-Remap framework for one-dimensional systems by using a time-implicit (resp. time-explicit) scheme for the system that deals with the fast (resp. slow) waves.

The compressible Euler equations fit the target model (II.1) using the notations of section I.2.2, by assuming regular solutions the system reads

$$\begin{cases} \partial_t \rho + (\partial_x \rho)\mathbf{u} + \rho \operatorname{div}(\mathbf{u}) = 0, & \text{(II.38a)} \\ \partial_t(\rho\mathbf{u}) + \partial_x(\rho\mathbf{u})\mathbf{u} + \rho\mathbf{u}\operatorname{div}(\mathbf{u}) + \boldsymbol{\nabla} P = \mathbf{0}, & \text{(II.38b)} \\ \partial_t(\rho E) + \partial_x(\rho E)\mathbf{u} + \rho E \operatorname{div}(\mathbf{u}) + \operatorname{div}(P\mathbf{u}) = 0, & \text{(II.38c)} \end{cases}$$

so that the acoustic system reads

$$\rho\partial_t\tau - \operatorname{div}(\mathbf{u}) = 0, \qquad \rho\partial_t\mathbf{u} + \boldsymbol{\nabla} P = 0, \qquad \rho\partial_t E + \operatorname{div}(P\mathbf{u}) = 0, \tag{II.39}$$

and the transport system is

$$\partial_t\rho + (\partial_{\mathbf{x}}\rho)\mathbf{u} = 0, \qquad \partial_t(\rho\mathbf{u}) + \partial_{\mathbf{x}}(\rho\mathbf{u})\mathbf{u} = 0, \qquad \partial_t(\rho E) + \partial_{\mathbf{x}}(\rho E)\mathbf{u} = 0. \tag{II.40}$$

Properties of the acoustic system for the Euler equations
I will now briefly recall the main properties of the acoustic system. We have that

(i) the acoustic system (II.39) is rotational invariant,
(ii) the pressure P verifies
$$\rho\partial_t P + (\rho c)^2 \operatorname{\mathbf{div}}(\mathbf{u}) = 0 \tag{II.41}$$
(iii) $(\tau, e) \mapsto s$ is a strictly convex entropy associated with the (II.39) that verifies the evolution equation $\partial_t s \geq 0$,
(iv) system (II.39) admits three ordered eigenvalues $-c, 0, c$,
(v) system (II.39) is strictly hyperbolic,
(vi) the field associated with the eigenvalue $\pm c$ (resp. 0) is genuinely nonlinear (resp. linearly degenerate).

We can see that the properties of the acoustic system are very similar to the properties of the one-dimensional Lagrangian system (II.8).

Approximations of the acoustic system : frozen density and Suliciu-type relaxation
In [7] we used a classic Suliciu-type relaxation approach [Sul90, Bau+04, Bou04, CC08] to build the Finite Volume approximation of the acoustic system. This relies on replacing the pressure P by a surrogate pressure Π in the system. The new pressure Π is imposed to verify a simplified mock-up of (II.41). I will present this approximation by inserting the pressure relaxation variable Π into the system along with the relaxation variable $\varkappa$ introduced in (II.28$_\lambda$), so that we consider

$$\partial_t\varkappa = \lambda(\varkappa - \rho), \quad \varkappa\partial_t\tau - \operatorname{div}(\mathbf{u}) = 0, \quad \varkappa\partial_t\mathbf{u} + \boldsymbol{\nabla}\Pi = 0, \quad \varkappa\partial_t E + \operatorname{div}(\Pi\mathbf{u}) = 0, \quad \varkappa\partial_t\Pi + a^2 \operatorname{div}(\mathbf{u}) = \lambda(\Pi - P), \tag{II.42$_\lambda$}$$

in the limit regime $\lambda \to +\infty$ as an approximation of (II.39). The parameter a is chosen in agreement with the Whitham sub-characteristic condition

$$a > \max \rho c, \tag{II.43}$$

for the sake of stability. The limit regime $\lambda \to \infty$ is classically achieved by enforcing at each time step $(\varkappa, \Pi)_i^n = \left(\rho_i^n, P^{\text{EOS}}(\tau_i^n, e_i^n)\right)$ and then solving (II.42$_\lambda$) with $\lambda = 0$. If we set define L by (II.30), the approximate acoustic system for $\lambda = 0$ reads

$$\partial_t(L\rho) = 0, \quad \partial_t L - \operatorname{div}(\mathbf{u}) = 0, \quad \partial_t(L\rho\mathbf{u}) + \boldsymbol{\nabla}\Pi = 0, \quad \partial_t(L\rho E) + \operatorname{div}(\Pi\mathbf{u}) = 0, \quad \partial_t(L\rho\Pi) + \operatorname{div}(a^2\mathbf{u}) = 0. \tag{II.44}$$

By comparing with the Lagrangian system (II.8) one can see that L plays the role of a surrogate J.

Finite volume approximation

The acoustic approximate system (II.44) inherits from the rotational invariance of the acoustic system (II.39). Therefore, one can easily build a multi-dimensional Finite Volume approximation of (II.44) by considering a one-dimensional Riemann problem in a reference frame attached to each face Γ_{ij}. This yields the following acoustic update

$$\widetilde{(L\rho)}_i = \rho_i^n, \tag{II.45a}$$

$$\widetilde{L}_i = 1 + \Delta t \sum_{j\in\mathcal{N}(i)} \sigma_{ij} u_{ij}^*, \tag{II.45b}$$

$$\widetilde{(L\rho\mathbf{u})}_i = (\rho\mathbf{u})_i^n - \Delta t \sum_{j\in\mathcal{N}(i)} \sigma_{ij} \Pi_{ij}^* \mathbf{n}_{ij}, \tag{II.45c}$$

$$\widetilde{(L\rho E)}_i = (\rho E)_i^n - \Delta t \sum_{j\in\mathcal{N}(i)} \sigma_{ij} \Pi_{ij}^* \mathbf{u}_{ij}^*, \tag{II.45d}$$

supplemented with a discretization of the evolution equation for Π

$$\widetilde{(L\rho\Pi)}_i = (\rho\Pi)_i^n - \Delta t \sum_{j\in\mathcal{N}(i)} (a_{ij})^2 u_{ij}^*, \tag{II.45e}$$

with numerical fluxes u_{ij}^* and Π_{ij}^* defined by

$$u_{ij}^* = \frac{1}{2}\mathbf{n}_{ij}^T(\mathbf{u}_i^\sharp + \mathbf{u}_j^\sharp) + \frac{1}{2a_{ij}}(\Pi_j^\sharp - \Pi_i^\sharp), \qquad \Pi_{ij}^* = \frac{1}{2}(\Pi_i^\sharp + \Pi_j^\sharp) + \frac{a_{ij}}{2}\mathbf{n}_{ij}^T(\mathbf{u}_j^\sharp - \mathbf{u}_i^\sharp), \qquad a_{ij} = \mathcal{K}\max_{k=i,j}(\rho_k^n c_k^n), \tag{II.46}$$

where $\mathcal{K} > 1$. Choosing $(\mathbf{u}_i^\sharp, \Pi_i^\sharp) = (\mathbf{u}_i^n, \Pi_i^n)$ yields a time-explicit scheme while $(\mathbf{u}_i^\sharp, \Pi_i^\sharp) = (\widetilde{\mathbf{u}}_i, \widetilde{\Pi}_i)$ leads to a time-implicit discretization.

For the transport step, we simply use the scheme (II.35) presented for the generic case that reads here

$$b_i^{n+1} - \widetilde{b}_i + \Delta t \sum_{j\in\mathcal{N}(i)} \sigma_{ij}(\widetilde{bu})_{ij} - \Delta t\, \widetilde{b}_i \sum_{j\in\mathcal{N}(i)} \sigma_{ij} u_{ij}^* = 0, \qquad b \in \{\rho, \rho u_1, \rho u_2, \rho u_3, \rho E\}, \tag{II.35}$$

with the upwind choice

$$\widetilde{b}_{ij} = \frac{(\widetilde{b}_i + \widetilde{b}_j)}{2} - \mathrm{sign}(u_{ij}^*)\frac{\widetilde{b}_j - \widetilde{b}_i}{2}, \qquad (\widetilde{bu})_{ij} = \widetilde{b}_{ij} u_{ij}^*. \tag{II.47}$$

Finally the overall acoustic/splitting scheme reads

$$\begin{cases} \rho_i^{n+1} - \rho_i^n + \Delta t \sum_{j\in\mathcal{N}(i)} \sigma_{ij}(\widetilde{\rho u})_{ij} = 0, & \text{(II.48a)} \\ (\rho\mathbf{u})_i^{n+1} - (\rho\mathbf{u})_i^n + \Delta t \sum_{j\in\mathcal{N}(i)} \sigma_{ij}\left[\widetilde{(\rho\mathbf{u})}_{ij}\, u_{ij}^* + \Pi_{ij}^*\mathbf{n}_{ij}\right] = 0, & \text{(II.48b)} \\ (\rho E)_i^{n+1} - (\rho E)_i^n + \Delta t \sum_{j\in\mathcal{N}(i)} \sigma_{ij}\left[\widetilde{(\rho E)}_{ij}\, u_{ij}^* + \Pi_{ij}^* u_{ij}^*\right] = 0. & \text{(II.48c)} \end{cases}$$

Properties of the acoustic/transport scheme

The numerical acoustic/transport splitting scheme has several nice features. First, the overall scheme is conservative with respect to ρ, $\rho\mathbf{u}$ and ρE. The time-explicit version of the scheme can be shown to be positivity preserving with respect to density and internal energy and also satisfies a discrete entropy inequality under classic CFL conditions that involve the sound velocity of the fluid.

The scheme obtained by considering a time-implicit discretization of the acoustic system and a time-explicit discretization of the transport system is referred to as an IMplicit-EXplicit (IMEX) scheme. In this case, the stability is guaranteed for the transport step under the CFL condition $\Delta t \max_i \left[\sum_{j\in\mathcal{N}(i)} \sigma_{ij}|u_{ij}^*|\right] \leq 1$. Unfortunately, this inequality does not provide a direct estimate for the time step as the calculation of u_{ij} requires a known value for Δt.

The system (II.45) is implicit with respect to the variables $\widetilde{\mathbf{u}}_i$, $\widetilde{\Pi}_i$, $\widetilde{L}_i$, $\widetilde{\rho}_i$ and $\widetilde{E}_i$. However, one can see that it only involves a solve the linear system composed of (II.45c)-(II.45e) with respect to the variable $\widetilde{\mathbf{u}}_i$ and $\widetilde{\Pi}_i$ and then the update of the other variables through (II.45b), (II.45a), (II.45d) is performed thanks to a direct evaluation.

The linear system formed by (II.45c)-(II.45e) is consistent with the subsystem

$$\rho^n \partial_t \mathbf{u} + \boldsymbol{\nabla}\Pi = 0, \qquad \rho^n \partial_t \Pi + \mathrm{div}(a^2\mathbf{u}) = 0, \tag{II.49}$$

that features in (II.44), which is nothing but a first order linear wave propagation system. In this sense, one can see that the acoustic/splitting algorithm really decouples the resolution of acoustic phenomena from the other effects of the Euler system. Let us also mention that for any $\Delta t > 0$ the linear system (II.45c)-(II.45e) supplemented with Neumann boundary conditions or periodic boundary conditions admits a single solution.

Low Mach behavior of the scheme acoustic/transport splitting scheme and modified scheme

Many applications involve flows where the fluid motion is relatively slow compared to the sound velocity of the medium. The common use to characterize such flow behavior is to rescale the Euler equations (II.38c) thanks to the following characteristic magnitude parameters

length	time	density	velocity	pressure	internal energy	sound velocity	Mach number
L	T	ρ_0	$u_0 = L/T$	P_0	$e_0 = P_0\rho_0$	$c_0 = \sqrt{P_0/\rho_0}$	$M = u_0/c_0$

that yield the following non-dimensional variables

$$\widehat{\mathbf{x}} = \mathbf{x}/L, \quad \widehat{t} = t/T, \quad \widehat{\rho} = \rho/\rho_0, \quad \widehat{\mathbf{u}} = \mathbf{u}/u_0, \quad \widehat{e} = e/e_0, \quad \widehat{P} = P/P_0, \quad \widehat{c} = c/c_0, \quad \widehat{E} = \widehat{e} + |\widehat{\mathbf{u}}|^2/2. \tag{II.50}$$

It is common to use the non-dimensional Mach number M to characterize this particular flow behavior. If we set $\boldsymbol{\nabla}_{\widehat{\mathbf{x}}}\cdot$, $\mathrm{div}_{\widehat{\mathbf{x}}}(\cdot)$ and $\mathbf{div}_{\widehat{\mathbf{x}}}(\cdot)$ to be the gradient and divergence operators with respect to the space variable $\widehat{\mathbf{x}}$, the Euler system (II.38c) can be recast into the non-dimensional formulation

$$\partial_{\widehat{t}}\widehat{\rho} + \mathrm{div}_{\widehat{\mathbf{x}}}(\widehat{\rho}\widehat{\mathbf{u}}) = 0, \qquad \partial_{\widehat{t}}(\widehat{\rho}\widehat{\mathbf{u}}) + \mathbf{div}_{\widehat{\mathbf{x}}}(\widehat{\rho}\widehat{\mathbf{u}}\widehat{\mathbf{u}}^T) + \frac{1}{M^2}\boldsymbol{\nabla}_{\widehat{\mathbf{x}}}\widehat{P} = 0, \qquad \partial_{\widehat{t}}(\widehat{\rho}\widehat{E}) + \mathrm{div}_{\widehat{\mathbf{x}}}(\widehat{\rho}E\widehat{\mathbf{u}} + \widehat{P}\widehat{\mathbf{u}}) = 0. \tag{II.51}$$

Mach regimes

System (II.51) shows that when M becomes very small, the equations become singular. If one considers small M values, this suggests to distinguish two different cases :

- the case when $\boldsymbol{\nabla}_{\widehat{\mathbf{x}}}\widehat{P}$ will always remain of magnitude $O(M^2)$, so that $\widehat{\rho}$, $\widehat{\mathbf{u}}$, $\widehat{E}$ will also remain $O(M^0)$. In this case, we will say that the system is in the *low Mach regime*,
- the case when $\boldsymbol{\nabla}_{\widehat{\mathbf{x}}}\widehat{P}$ will not remain of magnitude $O(M^2)$. Then the magnitude of $\widehat{\rho}\widehat{\mathbf{u}}$ may experience large variations from $O(M^0)$ to $O(M^{-1})$ or $O(M^{-2})$, so that M may grow significantly and the Mach regime may change. In case of such change of the Mach regime, one usually talk about all Mach-regime or simply *all-regime flows*.

The behavior of the Euler equations in the low Mach regime and adapted simulation strategies have been intensively investigated since many years by many authors. These topics are still very actively studied in the community. Over the years many questions have been raised by puzzling simulation results that show a great discrepancy in the performance of Godunov-type methods in the low Mach regime :

- on a triangular mesh with periodic boundary conditions, classic Godunov-type methods seem to perform normally ,
- on a quadrangular mesh with periodic boundary conditions, Godunov-type methods perform very poorly in low Mach regime,
- for one-dimensional problems with periodic (or Neumann) boundary conditions, the Godunov-type methods perform normally in low Mach regime.

I intentionally use the vague word "seem" as the situation depends on the boundary condition and the possible presence of source terms. While it is not my intention to provide a full overview of these topics in this document, I will try to briefly sketch typical lines that have been used to investigate and possibly cure the low Mach performance problem of Godunov-type methods.

Different diagnosis elements have been highlighted by many authors over the years [Tur87, GV99, Cle00, GM04]. Many of these contributions establish a link between the poor performance of the Godunov-type schemes and the role of the numerical viscosity of the scheme. In particular, a very accurate study of this question was brought by S. Dellacherie in [DOR10, Del10, DOR10, Del+16] where a connection is drawn between a space of near-incompressible solutions and a discrete equivalent space for approximated solutions. While the near-incompressible space contains functions whose velocity is near divergence-free, the characteristics of its discrete equivalent space strongly depends on the mesh choice and the numerical diffusion of the scheme. In the case of Godunov-type methods with quadrangle (resp. hexahedral) meshes in 2D (resp. 3D), this discrete space provides a very poor approximation of the near-incompressible velocity fields.

Truncation error of the acoustic/transport scheme in the low Mach regime

In order to investigate the low Mach behavior of the acoustic/transport splitting scheme, we considered a non-dimensional expression of the solver for one-dimensional problems (for the sake of simplicity) to highlight the role of the Mach number in the truncation error of the scheme. This analysis showed that for initial conditions that comply with the low Mach regime condition in a discrete form, the truncation error for all variables has the form $O(\Delta\widehat{x}) + O(\Delta\widehat{t}) + O(M\Delta\widehat{x})$ except for the momentum equation whose truncation error takes the form $O(\Delta\widehat{x}) + O(\Delta\widehat{t}) + O(M\Delta\widehat{x}) + O(\Delta\widehat{x}/M)$. This shows that the control of the error is not uniform with respect to M and that it may significantly degrade the accuracy of the scheme when $M \ll 1$ if $\Delta\widehat{x}$ is not small enough.

A modified scheme for a Mach-uniform truncation error

When analyzing the numerical scheme one can see that the source of the $O(\Delta\widehat{x}/M)$ error terms lies in the acoustic step. This can be highlighted using the equivalent equation associated with the acoustic step update (II.45). We get

$$\partial_{\widehat{t}}\widehat{u} + \frac{\widehat{\tau}}{M^2}\partial_{\widehat{x}}\widehat{P} = O(\Delta\widehat{t}) + O(\Delta\widehat{x}/M). \tag{II.52}$$

More precisely, it is possible to track the origin of the $O(\Delta\hat{x}/M)$ to the upwind term that features in the def of $\Pi_{i+1/2}$ in (II.46). We suggested in [7, 5] to adopt a new pressure flux definition as follows

$$\Pi^{*,\theta}_{i+1/2} = \frac{1}{2}(\Pi^{\sharp}_i + \Pi^{\sharp}_{i+1}) - \theta_{i+1/2}\frac{a_{i+1/2}}{2}(u^{\sharp}_{i+1} - u^{\sharp}_i), \tag{II.53}$$

where $\theta_{i+1/2} \in [0,1]$ is a user-defined parameter and $b^{\sharp}_i = b^n_i$ (resp. $b^{\sharp}_j = \widetilde{b_j}$) in the case of an explicit scheme (resp. IMEX scheme), $b \in \{u, \Pi\}$. If one note $x \mapsto \theta$ a smooth function so that $\theta(x_i) = \theta_{i+1/2}$ and one performs the study of the truncation error in the low Mach regime associated with the modified numerical scheme we get

$$\partial_{\hat{t}}\hat{u} + \frac{\hat{\tau}}{M^2}\partial_{\hat{x}}\hat{P} = O(\Delta\hat{t}) + O(\theta\Delta\hat{x}/M). \tag{II.54}$$

Therefore, in the case $M \ll 1$ if one chooses $\theta = O(M)$, the truncation error of the modified acoustic/transport scheme becomes uniform with respect to the Mach number.

Approximate Riemann solver for the modified scheme

The flux modification (II.53) that consists in "centering" the pressure value at the face of the cell is a standard technique of the literature [DOR10, Del10, DOR10, Del+16, TKP99, Pai+00, Dau+08]. Unfortunately, the stability estimates that can be derived thanks to the relaxation procedure are no longer valid. Nevertheless, in our special case, it is possible to exhibit an approximate Riemann solver $\mathbf{U}^{\theta}_{\mathrm{RP}}$ that allows to recover the modified flux formula (II.53). One can remark two important features of the low Mach modified approximate Riemann solver : $\mathbf{U}^{\theta=1}_{\mathrm{RP}} = \mathbf{U}_{\mathrm{RP}}$, so that we retrieve the unmodified approach for $\theta = 1$ and the speed of the waves involved with $\mathbf{U}^{\theta}_{\mathrm{RP}}$ are the same as those of $\mathbf{U}_{\mathrm{RP}}$. This suggests that stability is obtained under the same CFL constraints as the unmodified solver $\mathbf{U}_{\mathrm{RP}}$. More precisely, one can see that under the same CFL conditions the all-Mach solver is positivity-preserving with respect to the density, with the internal energy and is entropy-satisfying for $\theta > 0$. It is important to note that the in the limit $M \to 0$ it is not guaranteed that the numerical scheme will satisfy a discrete entropy inequality when $\theta = O(M)$.

All-Mach regime simulations

I present here a few results obtained with both the explicit and IMEX strategies with and without low Mach correction. The figure II.7 displays the velocity profile obtained for the test of the Gresho vortex with a reference Mach number $M \sim 10^{-2}$. This illustrates the important accuracy gain of the low Mach adapted scheme on a coarse grid. The table II.1 shows the required number of time steps and CPU time to perform the simulation, that favors the IMEX method.

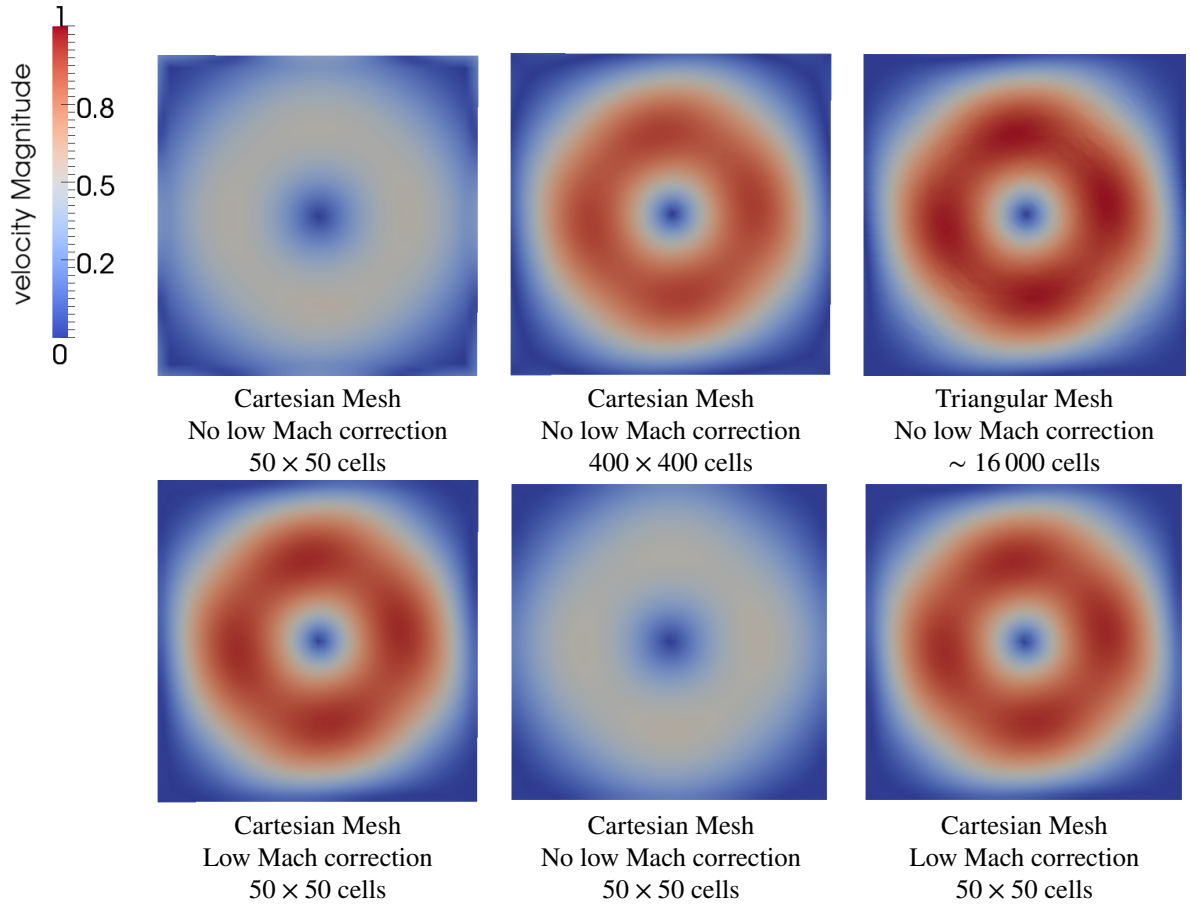

Figure II.7 – Profile of the velocity for the vortex simulation.

Table II.1 – Vortex in a box test case for $M \sim 10^{-2}$ with a Cartesian mesh. Comparison of the number of iterations and CPU time of EX($\theta = 1$), EX($\theta = O(M)$), IMEX($\theta = 1$) and IMEX($\theta = O(M)$) schemes to obtain solutions of figure II.7.

Numerical scheme	EX($\theta = 1$)	EX($\theta = 1$)	EX($\theta = O(M)$)	IMEX($\theta = 1$)	IMEX($\theta = O(M)$)
Mesh	400×400	50×50	50×50	50×50	50×50
Number of iterations	18 457	2 306	2 305	43	56
CPU time (s)	9 263.04 (2h 34 min)	17.14	19.3	3.75	5.77

II.6 Asymptotic Preserving acoustic/transport splitting scheme for the Euler equations with gravity and friction

Contributions by the author
This section covers works that have been published in [11].

The acoustic/transport splitting strategy can also be used when the system involves stiff source terms. This work was an early study so that the method was designed using the legacy Lagrange-Remap approach, that can be interpreted using the acoustic/transport splitting. We consider a one-dimensional compressible flow with friction terms and gravity that reads

$$\partial_t \rho + \partial_x(\rho u) = 0, \qquad \partial_t(\rho u) + \partial_x(\rho u^2 + P) = \rho(g - \alpha_f u), \qquad \partial_t(\rho E) + \partial_x(\rho E u + P u) = \rho(g - \alpha_f u)u, \tag{II.55}$$

where g is the gravity acceleration and α_f is a friction coefficient. The question consists in studying the long time behavior of (II.55) when the friction parameter α_f becomes very large. The limit regime can be obtained by considering a dimensionless form of the equations and by supposing (up to a slight abuse of notations) that

$$\alpha_f = \alpha_f'/\epsilon, \qquad t = t'/\epsilon, \qquad u = u^{(0)} + \epsilon u^{(1)} + O(\epsilon^2). \tag{II.56}$$

By letting $\epsilon \to 0$, we see that the long time behavior of (II.55) is governed by

$$\partial_{t'}\rho + \partial_x(\rho u^{(1)}) = 0, \qquad \partial_x P = \rho\Big(g - \alpha_f' u^{(1)}\Big), \qquad \partial_{t'}(\rho e) + \partial_x\big(\rho e u^{(1)} + P u^{(1)}\big) = \rho\Big(g - \alpha_f' u^{(1)}\Big)u^{(1)}. \tag{II.57}$$

By noticing that (II.57) implies (formally) $\partial_{t'}\rho + \partial_x\Big((\rho g - \partial_x P)/\alpha_f'\Big) = 0$, one can see that the asymptotic model (II.57) can be considered as a diffusive or parabolic limit of (II.55). This type of limit regime has been studied in the literature in the case of the gas dynamics equations limit towards the Darcy law (see for example [MM90, HL92, CG06]).

Performing simulation of (II.55) in the limit regime defined by both large friction and long time behavior sets two challenges : the first challenge is the ability to use large time steps while remaining stable and the second challenge consists in preserving the scheme accuracy for a given space step with very small values of ϵ. The first issue was tackled by developing an IMEX scheme and the second matter was addressed by ensuring that the numerical scheme verifies an Asymptotic Preserving (AP) property (see *e.g.* [Jin95, JL96, Kla98, JP00, GT04, BLT10, Deg+09, FJ10, DP11, DBF12]) with respect to the limit system (II.57).

Supposing that the solution is smooth, (II.55) can be expressed as follows

$$\begin{cases} \partial_t \rho & + \partial_x(\rho) u & + \rho \partial_x(u) & = 0, & \text{(II.58a)} \\ \partial_t(\rho u) & + \partial_x(\rho u) u & + \rho u \partial_x u + \partial_x P & = \rho(g - \alpha_f u), & \text{(II.58b)} \\ \partial_t(\rho E) & + \partial_x(\rho E) u & + \rho E \partial_x u + \partial_x(P u) & = \rho(g - \alpha_f u)u, & \text{(II.58c)} \end{cases}$$

Following the idea that the transport step just advects the matter at a prescribed velocity, we choose to account for the source terms within the acoustic step so that the resulting velocity may express a balance between pressure effects, friction and gravity. The acoustic system reads

$$\rho \partial_t \tau - \partial_x u = 0, \qquad \rho \partial_t u - \partial_x P = \rho(g - \alpha u), \qquad \rho \partial_t E - \partial_x(P u) = \rho(g - \alpha u)u. \tag{II.59}$$

We then carry out the approximations presented in section II.5 : we performed a Suliciu-type approximation for the pressure and density terms are "frozen" at their value at instant t^n (as in section II.5) so that we obtained the following approximate acoustic system using a spatial mass coordinate (see remark 11 and 14) :

$$\partial_t \tau - \partial_m u = 0, \qquad \partial_t u - \partial_m \Pi = (g - \alpha u), \qquad \partial_t E - \partial_m(\Pi u) = (g - \alpha u)u, \qquad \partial_t \Pi - \partial_m(a^2 u) = 0. \tag{II.60}$$

Following [Coq+08, Coq+10] we exploited another specific feature of this one-dimensional problem : noting $w^\pm = \Pi \pm a u$ the strong Riemann invariants associated with the wave $\pm a$, system (II.60) takes the equivalent form

$$\partial_t \tau - \partial_m u = 0, \qquad \partial_t E - \partial_m(\Pi u) = (g - \alpha u)u, \qquad \partial_t w^\pm \pm \partial_m(a w^\pm) = \pm\big[a g - \alpha_f (w^+ - w^-)/2\big]. \tag{II.61}$$

A final key ingredient is the consistency in the integral sense [Gal02, Gal03, Bou04]. This approach allowed to propose an approximate Riemann solver for (II.60) that accounts for the presence of the source term. The resulting ARS involves 3 waves. A first pair of waves of velocity $\pm a$ acts as artificial acoustic waves and set to verify the classic Rankine-Hugoniot jump conditions of (II.60) when the source terms are omitted. The third wave has a null velocity and is used to impose a jump of pressure that accounts for source terms (instead of ensuring pressure continuity for the homogeneous system) and enforcing continuity for the velocity.

The resulting scheme takes the form of a classic Finite Volume method involving numerical fluxes and centered source

terms, more precisely

$$\begin{cases} \rho_i^n \dfrac{\widetilde{u}_i - u_i^n}{\Delta t} + \dfrac{\Pi^*_{i+1/2} - \Pi^*_{i-1/2}}{\Delta x_i} = \{\rho(g - \alpha_f u)\}_i, & \text{(II.62a)} \\ \rho_i^n \dfrac{\widetilde{\Pi}_i - \Pi_i^n}{\Delta t} + a^2 \dfrac{u^*_{i+1/2} - u^*_{i-1/2}}{\Delta x_i} = 0, & \text{(II.62b)} \\ \rho_i^n \dfrac{\widetilde{\tau}_i - \tau_i^n}{\Delta t} - \dfrac{u^*_{i+1/2} - u^*_{i-1/2}}{\Delta x_i} = 0, & \text{(II.62c)} \\ \rho_i^n \dfrac{\widetilde{E}_i - E_i^n}{\Delta t} + \dfrac{u^*_{i+1/2}\Pi^*_{i+1/2} - u^*_{i-1/2}\Pi^*_{i-1/2}}{\Delta x_i} = \{\rho(g - \alpha_f u)u\}_i & \text{(II.62d)} \end{cases}$$

where

$$\Pi^*_{i+1/2} = \frac{(w^+)_i^\sharp + (w^-)_{i+1}^\sharp}{2}, \quad u^*_{i+1/2} = \frac{(w^+)_i^\sharp - (w^-)_{i+1}^\sharp + g\Delta m_{i+1/2}}{2a + \alpha_f \Delta m_{i+1/2}}, \quad \Delta m_{i+1/2} = \frac{\rho_i^n \Delta x_i + \rho_{i+1}^n \Delta x_{i+1}}{2}. \tag{II.63}$$

$$\{\rho(g - \alpha_f u)\}_i = g\frac{\Delta m_{i+1/2} + \Delta m_{i-1/2}}{2\Delta x_i} - \alpha \frac{u^*_{i+1/2}\Delta m_{i+1/2} + u^*_{i-1/2}\Delta m_{i-1/2}}{2\Delta x_i} \tag{II.64}$$

$$\{\rho(g - \alpha_f u)u\}_i = g\frac{u^*_{i+1/2}\Delta m_{i+1/2} + u^*_{i-1/2}\Delta m_{i-1/2}}{2\Delta x_i} - \alpha_f \frac{\left(u^*_{i+1/2}\right)^2 \Delta m_{i+1/2} + \left(u^*_{i-1/2}\right)^2 \Delta m_{i-1/2}}{2\Delta x_i} \tag{II.65}$$

If $(w^\pm)_i^\sharp = (w^\pm)_i^n$ we obtain an explicit method and if $(w^\pm)_i^\sharp = \widetilde{(w^\pm)}_i$ we obtain an implicit method for the acoustic step.

The discretization of the transport is performed using a standard upwind method as proposed in section II.5. This approach yields both an explicit and an IMEX method. One can show that the IMEX methods is asymptotic preserving with respect to the limit system (II.57) and that under classic CFL conditions the explicit scheme is positivity-preserving for the density and satisfies a discrete entropy inequality.

II.7 Acoustic/transport splitting scheme for a bifluid model

Contributions by the author
This section covers works that have been published in [16].

Bifluid systems like the model mentioned in section I.6 have been widely studied in the literature and numerous numerical schemes have been proposed for their discretization. However, most of these schemes pertain to the simulation of fast phenomena and little attention has been given to derive large time step stable numerical methods for these type of bifluid models.

The numerical scheme that I will briefly describe in this section can be considered as a first attempt to elaborate an acoustic/transport splitting scheme for a bifluid model. We only consider one-dimensional problems and write the two-pressure two-velocity bifluid model presented in section I.6 using the following compact form

$$\partial_t \alpha_k + u_I \partial_x \alpha_k = 0, \quad \partial_t(\alpha_k \rho_k) + \partial_x(\alpha_k \rho_k u_k) = 0, \quad \partial_t(\alpha_k \rho_k \mathbf{W}_k) + \partial_x(\alpha_k \rho_k \mathbf{W}_k u_k) + \partial_x(\alpha_k \mathbf{T}_k) - \mathbf{T}_I \partial_x \alpha_k = 0, \tag{II.66}$$

where

$$\mathbf{W}_k = (u_k, E_k)^T, \qquad \mathbf{T}_k = (P_k, P_k u_k)^T \qquad \mathbf{T}_I = (P_I, P_I u_I)^T. \tag{II.67}$$

In order to design an operator splitting, we consider smooth solutions and split up operators in (II.66) as follows

$$\begin{cases} \partial_t \alpha_k & & & +u_I \partial_x \alpha_k & = 0, & \text{(II.68a)} \\ \partial_t(\alpha_k \rho_k) & +u_k \partial_x(\alpha_k \rho_k) & + \alpha_k \rho_k \partial_x u_k & & = 0, & \text{(II.68b)} \\ \partial_t(\alpha_k \rho_k \mathbf{W}_k) & + u_k \partial_x(\alpha_k \rho_k \mathbf{W}_k) & + (\alpha_k \rho_k \mathbf{W}_k)\partial_x u_k + \alpha_k \partial_x \mathbf{T}_k & + (\mathbf{T}_k - \mathbf{T}_I)\partial_x \alpha_k & = 0. & \text{(II.68c)} \end{cases}$$

A particular feature of this system is that it suggests to consider three subsystems : a first subsystem dedicated to the acoustic effects

$$\partial_t \alpha_k = 0, \qquad \partial_t(\alpha_k \rho_k) + (\alpha_k \rho_k)\partial_x u_k = 0, \qquad \partial_t(\alpha_k \rho_k \mathbf{W}_k) + (\alpha_k \rho_k \mathbf{W}_k)\partial_x u_k + \alpha_k \partial_x \mathbf{T}_k = 0, \tag{II.69}$$

a second subsystem for transport effects

$$\partial_t \alpha_k = 0, \qquad \partial_t b + u_k \partial_x b = 0, \qquad b \in \{\alpha_k \rho_k, \alpha_k \rho_k u_k, \alpha_k \rho_k E_k\}, \tag{II.70}$$

and a third system, referred to as α-step, that accounts for non-conservative terms

$$\partial_t \alpha_k + u_I \partial_x \alpha_k = 0, \qquad \partial_t(\alpha_k \rho_k) = 0, \qquad \partial_t(\alpha_k \mathbf{W}_k) + (\mathbf{T}_k - \mathbf{T}_I)\partial_x \alpha_k = 0. \tag{II.71}$$

Eigenstructure of the subsystems
All three subsystems (II.69), (II.70) and (II.71) are hyperbolic with the following eigenstructure :

— the eigenvalues for the acoustic subsystem (II.69) are $\pm c_k$ (associated with genuinely nonlinear waves) and 0 (linearly degenerate waves),
— the eigenvalues for the transport subsystem (II.70) are u_k and 0 (all associated with linearly degenerate waves),
— the eigenvalues for the non-conservative subsystem (II.71) are u_I and 0 (all associated with linearly degenerate waves).

Approximating the acoustic subsystem
The subsystem (II.69) is composed of two independent acoustic systems for each fluid $k = 1, 2$ while parameters α_k act as stationary fields. It can be expressed as follows

$$\partial_t \alpha_k = 0, \qquad \rho_k \partial_t \tau_k - \partial_x u_k = 0, \qquad \rho_k \partial_t \mathbf{W}_k + \partial_x \mathbf{T}_k = 0. \tag{II.72}$$

It is easy to apply the approximations proposed for the single-component acoustic system in section II.5 fluid by fluid : the densities ρ_k are "frozen" in the $\rho_k \partial_t(\cdot)$ terms so that it is possible to introduce two mass coordinates m_k defined by $\mathrm{d}m_k(x) = \rho_k(x, t^n)\,\mathrm{d}x$ and use a Suliciu-type relaxation procedure by introducing two surrogate pressures Π_k. This yields (up to a slight abuse of notation) the approximate acoustic system

$$\partial_t \alpha_k = 0, \quad \partial_t \tau_k - \partial_{m_k} u_k = 0, \quad \partial_t u_k + \partial_{m_k} \Pi_k = 0, \quad \partial_t E_k + \partial_{m_k}(\Pi_k u_k) = 0, \quad \partial_t \Pi_k + a_k^2 \partial_{m_k} u_k = 0, \tag{II.73}$$

where the constant a_k is an upper bound for $\rho_k c_k$ in agreement with the Whitham conditions. We exploit the advantage of one-dimensional context by expressing (II.73) into a partially diagonal form. We set $w_k^{\pm} = \Pi_k \pm a_k u_k$, $I_k = \Pi_k + a_k^2 \tau_k$ and then (II.73) takes the form

$$\partial_t \alpha_k = 0, \quad \partial_t I_k = 0, \quad \partial_t w_k^+ + a_k \partial_{m_k} w_k^+ = 0, \quad \partial_t w_k^- - a_k \partial_{m_k} w_k^- = 0, \quad \partial_t E_k + \partial_{m_k}(\Pi_k u_k) = 0. \tag{II.74}$$

Finite volume discretization
The evolution of $w_k^{\pm}$ in acoustic step (II.74) is discretized as follows

$$\widetilde{(w_k^{\pm})}_i - (w_k^{\pm})_i^n \pm a_k \frac{\Delta t}{\Delta m_k}\Big((w_k^{\pm})_{i+1/2}^{\sharp} - (w_k^{\pm})_{i-1/2}^{\sharp}\Big) = 0, \qquad (w_k^+)_{i+1/2}^{\sharp} = (w_k^+)_i^{\sharp}, \qquad (w_k^-)_{i+1/2}^{\sharp} = (w_k^-)_{i+1}^{\sharp}, \tag{II.75}$$

where $(w_k^{\pm})_i^{\sharp} = (w_k^{\pm})_i^n$ yields an explicit update and $(w_k^{\pm})_i^{\sharp} = \widetilde{(w_k^{\pm})}_i$ yields an implicit update of the acoustic step (II.74). We then set

$$(\Pi_k)_{i+1/2}^{\sharp} = \frac{(w_k^+)_i^{\sharp} + (w_k^-)_{i+1}^{\sharp}}{2}, \qquad (u_k)_{i+1/2}^{\sharp} = \frac{(w_k^+)_i^{\sharp} - (w_k^-)_{i+1}^{\sharp}}{2a_k}, \qquad (\Pi_k u_k)_{i+1/2}^{\sharp} = (\Pi_k)_{i+1/2}^{\sharp}(u_k)_{i+1/2}^{\sharp}, \tag{II.76}$$

and update the remaining variables in the acoustic step (II.74) as follows

$$\widetilde{(\alpha_k^{\pm})}_i = (\alpha_k^{\pm})_i^n, \qquad \widetilde{(I_k^{\pm})}_i = (I_k^{\pm})_i^n, \qquad \widetilde{(E_k)}_i = (E_k)_i^n - \frac{\Delta t}{\Delta m_k}\Big((\Pi_k u_k)_{i+1/2}^{\sharp} - (\Pi_k u_k)_{i-1/2}^{\sharp}\Big). \tag{II.77}$$

The transport step (II.70) is discretized using an upwind scheme. Finally for the α-step (II.71), the update of α_k is achieved with an upwind strategy and the discretization of $\partial_t(\alpha_k \mathbf{W}_k) + (\mathbf{T}_k - \mathbf{T}_I)\partial_x \alpha_k$ is designed in order to ensure that the overall scheme provide a conservative discretization of the fluxes $\alpha_k \mathbf{T}_k$, $\alpha_k \rho_k \mathbf{W}_k u_k$ and $\alpha_k \rho_k u_k$.

Under classic CFL conditions, the explicit scheme is positivity preserving for α_k, ρ_k, e_k. A CFL condition can also be expressed for the IMEX scheme that provide these positivity results, however it cannot be exploited for choosing the time step as it involves quantities that are computed with a given time step during the acoustic step.

The numerical results show mixed performances. While some variables show a good agreement with the reference solution, some other may experience overshoots or undershoots. These numerical defects seem to wear off as the space step goes to zero. These flaws need yet to be corrected (if it is possible) to obtain a numerical method that can be reliably exploited for numerical simulations.

II.8 Acoustic/transport splitting scheme for the Shallow water equations

Contributions by the author
This section covers works that have been published in [6].

The acoustic/transport splitting method was adapted to the Shallow Water Equations (SWE). This system reads for one-dimensional problems

$$\partial_t h + \partial_x(hu) = 0, \qquad \partial_t(hu) + \partial_x(hu^2 + gh^2/2) = -gh\partial_x \varkappa, \qquad \partial_t \varkappa = 0, \tag{II.78}$$

where $x \mapsto \varkappa$ is a given smooth function that describes the topography while h, u and g respectively denote water height, velocity and gravity acceleration. The system (II.78) can be supplemented with an entropy inequality

$$\partial_t\left(\frac{hu^2}{2} + \frac{gh^2}{2}\right) + \partial_x\left[\left(\frac{hu^2}{2} + \frac{gh^2}{2}\right)u\right] \leq -ghu\partial_x \varkappa. \tag{II.79}$$

A particular steady solution of (II.78) is the so-called "lake at rest" solution that is defined by

$$h + \varkappa = \text{constant}, \qquad u = 0. \tag{II.80}$$

A specific goal of our work was to propose a numerical scheme that enables a well-balanced treatment [GL96b, GL96a, Gos00, Bou04] of the non-conservative terms so that it can preserve the lake at rest solution (II.80) while inheriting from the good properties of the original scheme for the Euler equations. For smooth solutions, the (SWE) reads

$$\begin{cases} \partial_t h & +(\partial_x h)u & +h(\partial_x u) & = 0, & \text{(II.81a)} \\ \partial_t(hu) & +\partial_x(hu)u & +hu(\partial_x u)+\partial_x(gh^2/2) & = -gh\partial_x\varkappa, & \text{(II.81b)} \\ \partial_t\varkappa & & & = 0. & \text{(II.81c)} \end{cases}$$

We choose to consider the following acoustic subsystem

$$h\partial_t(1/h)+\partial_x u = 0, \qquad h\partial_t u+\partial_x(gh^2/2) = -gh\partial_x\varkappa, \qquad \partial_t\varkappa = 0. \tag{II.82}$$

and the transport subsystem

$$\partial_t h-(\partial_x h)u = 0, \qquad \partial_t(hu)+\partial_x(hu)u = 0, \qquad \partial_t\varkappa = 0. \tag{II.83}$$

We followed similar lines as in the case of the Euler equation with friction (presented in section II.6) for deriving an approximate acoustic system : the water height terms are frozen at the time t^n so that $h\partial_t(\cdot)$ can be replaced with $h^n\partial_t(\cdot)$ and we introduce a mass spatial coordinate variable m. By linearizing the pressure term using a Suliciu-like relation we obtain

$$\partial_t(1/h)-\partial_m u = 0, \qquad \partial_t u+\partial_m\Pi = -gh\partial_m\varkappa, \qquad \partial_t\Pi+a^2\partial_m u = 0, \qquad \partial_t\varkappa = 0, \tag{II.84}$$

where the pressure term is reset to $\Pi_i^n = g\left(h_i^n\right)^2/2$ at each time step $t = t^n$. The constant a is chosen in compliance with the Whitham subcharacteristic condition that takes here the form $a > h\sqrt{gh}$, where h spans the value of the solution for $[t^n, t^{n+1})$.

The approximate acoustic system (II.82) involves four linearly degenerate characteristic fields associated with the characteristic velocities $\{-a, 0, 0, +a\}$ and it is strictly hyperbolic. The non-conservative term is well-defined for smooth $\varkappa$. The construction of a numerical solver for (II.82) relies on a three-wave approximate Riemann solver that accounts for the non-conservative terms in the integral sense [Gal02, Gal03, Bou04] in the same spirit as for the Euler system with friction and gravity that was presented in section II.6. The approximate Riemann solver is composed of a pair of waves with velocity $\pm a$ where standard jump relations associated with (II.82) are imposed by supposing that $\varkappa$ is constant across these waves. The third wave is a null velocity wave : we suppose continuity for the velocity across this wave and we enforce a pressure jump that is meant to account for the influence of the non-conservative term. In the end, the complete definition of the scheme boils down to provide an expression for the pressure jump. This jump value can be set in order to ensure that : the scheme is consistent in the integral sense, it preserves left and right states verifying the lake at rest conditions (II.80) and in the case of a constant topography $\varkappa$, it degenerates into a classic Suliciu relaxation scheme.

The resulting scheme for the acoustic step can be viewed as a flux-based Finite Volume scheme with centered source terms that reads

$$\begin{cases} h_i^n\dfrac{1/\widetilde{h}_i-1/h_i^n}{\Delta t}-\dfrac{1}{\Delta x_i}\left(u^*_{i+1/2}-u^*_{i-1/2}\right) = 0, & \text{(II.85a)} \\ h_i^n\dfrac{\widetilde{u}_i-u_i^n}{\Delta t}+\dfrac{1}{\Delta x_i}\left(\Pi^*_{i+1/2}-\Pi^*_{i-1/2}\right) = h_i^n\{gh\partial_m\varkappa\}_i, & \text{(II.85b)} \\ h_i^n\dfrac{\widetilde{\Pi}_i-\Pi_i^n}{\Delta t}+\dfrac{a^2}{\Delta x_i}\left(u^*_{i+1/2}-u^*_{i-1/2}\right) = 0. & \text{(II.85c)} \end{cases}$$

where $\Delta m_{i+1/2} = (h_i^n\Delta x_i + h_{i+1}^n\Delta x_{i+1})/2$ and

$$u^*_{i+1/2} = \frac{u_i^\sharp+u_{i+1}^\sharp}{2}-\frac{\Pi_{i+1}^\sharp-\Pi_i^\sharp}{2a}-\frac{\Delta m_{i+1/2}}{2a}\{gh\partial_m\varkappa\}_{i+1/2}, \qquad \Pi_{i+1/2} = \frac{\Pi_{i+1}^\sharp-\Pi_i^\sharp}{2}-\frac{a}{2}(u_{i+1}^\sharp-u_i^\sharp) \tag{II.86a}$$

$$\{gh\partial_m\varkappa\}_i^n = \frac{\Delta m_{i+1/2}}{2h_i^n\Delta x_i}\{gh\partial_m\varkappa\}^n_{i+1/2}+\frac{\Delta m_{i-1/2}}{2h_i^n\Delta x_i}\{gh\partial_m\varkappa\}^n_{i-1/2}, \quad \{gh\partial_m\varkappa\}_{i+1/2} = \frac{g}{2}(h_i^n+h_{i+1}^n)\frac{\varkappa_{i+1}-\varkappa_i}{\Delta m_{i+1/2}}. \tag{II.86b}$$

Once again, two options are available for the time discretization : choosing $(u_i^\sharp, \Pi_i^\sharp) = (u_i^n, \Pi_i^n)$ yields an explicit scheme and $(u_i^\sharp, \Pi_i^\sharp) = (\widetilde{u}_i, \widetilde{\Pi}_i)$ provides an IMEX scheme. It is important to note that for the IMEX scheme, the source term is evaluated at instant t^n.

Both explicit and IMEX schemes are shown to be well-balanced with respect to lake at rest initial conditions. The linear system for (u, Π) involved in the IMEX was studied using the variables $w^\pm = \Pi \pm au$: it was shown to that this system admits a unique solution for any $\Delta t > 0$ with Dirichlet boundary conditions.

The explicit scheme inherits from the stability properties that were obtained in the Euler case. Indeed, under classic CFL conditions, it is positive preserving for the water height h, and satisfies a discrete entropy inequality that is consistent with (II.79).

II.9 Fully conservative acoustic/transport splitting scheme for compressible flows with source terms that derive from a potential

Contributions by the author
This section covers works that have been published in [2].

The original goal of this work was to propose a numerical scheme for the Euler equations with gravity source terms in the context of astrophysical flows of planets atmosphere. The target simulations require to accurately capture near-hydrostatic flows while possibly accounting for important variations of the Mach number. Another important feature is that the numerical scheme needs to be consistent with the conservation of the total energy $(\rho E + \rho\Phi)$ where $\mathbf{x} \mapsto \Phi(\mathbf{x})$ is the gravity potential energy. Supposing now Φ to be a general potential (not necessarily gravity), we consider the following system

$$\partial_t \rho + \operatorname{div}(\rho\mathbf{u}) = 0, \qquad \partial_t(\rho\mathbf{u}) + \operatorname{div}(\rho\mathbf{u}\mathbf{u}^T) + \boldsymbol{\nabla} P = -\rho\boldsymbol{\nabla}\Phi, \tag{II.87a}$$

$$\partial_t(\rho E + \rho\Phi) + \operatorname{div}(\rho E\mathbf{u} + \rho\Phi\mathbf{u} + P\mathbf{u}) = 0, \qquad \partial_t\Phi = 0. \tag{II.87b}$$

The goal is to derive an all-Mach accurate, conservative scheme with respect to the density ρ, momentum $\rho\mathbf{u}$ and total energy $(\rho E + \rho\Phi)$ that is well-balanced [GL96b, GL96a, Gos00, Bou04] with respect to the stationary profiles

$$\mathbf{u} = \mathbf{0}, \qquad \boldsymbol{\nabla} P = -\rho\boldsymbol{\nabla}\Phi. \tag{II.88}$$

A first method would be to follow the lines of the numerical scheme developed for the shallow water equations [6] that was discussed in section II.8. Unfortunately these lines cannot be applied directly unless one sacrifices the conservation of $(\rho E + \rho\Phi)$. This problem can be circumvented as follows : first, let us remark that $\rho\Phi$ verifies the unstationary equation $\partial_t(\rho\Phi) + \operatorname{div}(\rho\Phi\mathbf{u}) = \rho\mathbf{u}^T\boldsymbol{\nabla}\Phi$, let us introduce a surrogate unstationary gravitational potential $(\mathbf{x}, t) \mapsto \Psi$ and an energy $\mathscr{E} = e + |\mathbf{u}|^2/2 + \Psi$ that verifies $\partial_t(\rho\Psi) + \operatorname{div}(\rho\Psi\mathbf{u}) = \rho\mathbf{u}^T\boldsymbol{\nabla}\Phi + \lambda(\Psi - \Phi(\mathbf{x}))$, so when $\lambda \to +\infty$ we formally have $\Psi(\mathbf{x}, t) \to \Phi(\mathbf{x})$. Now we consider

$$\partial_t \rho + \operatorname{div}(\rho\mathbf{u}) = 0, \tag{II.89a}$$

$$\partial_t(\rho\mathbf{u}) + \operatorname{div}(\rho\mathbf{u}\mathbf{u}^T) + \boldsymbol{\nabla} P = -\rho\boldsymbol{\nabla}\Phi, \tag{II.89b}$$

$$\partial_t(\rho\mathscr{E}) + \operatorname{div}(\rho\mathscr{E}\mathbf{u} + P\mathbf{u}) = 0, \tag{II.89c}$$

$$\partial_t(\rho\Psi) + \operatorname{div}(\rho\Psi\mathbf{u}) = \rho\mathbf{u}^T\boldsymbol{\nabla}\Phi + \lambda(\Psi - \Phi(\mathbf{x})), \tag{II.89d}$$

$$\partial_t\Phi = 0. \tag{II.89e}$$

Consequently if one considers (II.89) in the limit regime $\lambda \to +\infty$ we retrieve (formally) the original system (II.87b).

Once again, the limit λ is mimicked by enforcing $\Psi(\mathbf{x}, t^n) = \Phi(\mathbf{x})$ at each time step and by evolving ρ, $\rho\mathbf{u}$ and $\rho\mathscr{E}$ by solving (II.89) with $\lambda = 0$. Supposing a smooth solution, the system reads

$$\partial_t\rho \quad + (\partial_x\rho)\mathbf{u} \quad + \rho\operatorname{div}(\mathbf{u}) \quad = 0, \tag{II.90a}$$

$$\partial_t(\rho\mathbf{u}) \quad + \partial_x(\rho\mathbf{u})\mathbf{u} \quad + \rho\mathbf{u}\operatorname{div}(\mathbf{u}) + \boldsymbol{\nabla} P \quad = -\rho\boldsymbol{\nabla}\Phi, \tag{II.90b}$$

$$\partial_t(\rho\mathscr{E}) \quad + \partial_x(\rho\mathscr{E})\mathbf{u} \quad + \rho\mathscr{E}\operatorname{div}(\mathbf{u}) + \operatorname{div}(P\mathbf{u}) = 0, \tag{II.90c}$$

$$\partial_t(\rho\Psi) \quad + (\partial_x\rho\Psi)\mathbf{u} \quad + \rho\Psi\operatorname{div}(\mathbf{u}) \quad = \rho\mathbf{u}^T\boldsymbol{\nabla}\Phi, \tag{II.90d}$$

$$\partial_t\Phi \quad = 0. \tag{II.90e}$$

This suggests to isolate the following acoustic subsystem

$$\rho\partial_t\tau - \operatorname{div}(\mathbf{u}) = 0, \qquad \rho\partial_t u - \boldsymbol{\nabla} P = -\rho\boldsymbol{\nabla}\Phi, \qquad \rho\partial_t\mathscr{E} + \operatorname{div}(P\mathbf{u}) = 0, \qquad \rho\partial_t\Psi = \rho\mathbf{u}^T\boldsymbol{\nabla}\Phi, \qquad \partial_t\Phi = 0, \tag{II.91}$$

and the transport subsystem

$$\partial_t b + (\partial_x b)\mathbf{u} = 0, \qquad \text{for } b \in \{\rho, \rho\mathbf{u}, \rho\mathscr{E}, \rho\Psi\}. \tag{II.92}$$

Acoustic susbystem and its approximation

The system (II.91) is hyperbolic and involves a pair of acoustic waves of velocity $\pm c$ associated with genuinely nonlinear fields complemented by 3 waves of velocity 0 (that are obviously linearly degenerate).

We propose to proceed using similar lines as in section II.8 by partially freezing the density and introducing an artificial pressure Π through a Suliciu-type relaxation. For the sake of simplicity, we present the resulting system for one-dimensional problems using spatial mass coordinate m, which gives

$$\partial_t\tau - \partial_m u = 0, \qquad \partial_t u - \partial_m\Pi = -(1/\tau)\partial_m\Phi, \qquad \partial_t\mathscr{E} + \partial_m(\Pi u) = 0, \tag{II.93a}$$

$$\partial_t\Psi = (u/\tau)\partial_m\Phi, \qquad \partial_t\Pi + a^2\partial_m u = 0, \qquad \partial_t\Phi = 0. \tag{II.93b}$$

Once again, the approximate acoustic problem (II.93) is solved thanks to an approximate Riemann solver that accounts for the non-conservative terms $(\partial_m\Phi)/\tau$ and $(u/\tau)\partial_m\Phi$ in the integral sense [Gal02, Gal03, Bou04] following similar lines as the numerical solver elaborated for the shallow water equations presented in section II.8. The resulting Finite Volume

update for the acoustic step reads

$$\begin{cases} \widetilde{L}_i = 1 + \dfrac{\Delta t}{\Delta x}\Big(u^*_{i+1/2} - u^*_{i-1/2}\Big), & \text{(II.94a)} \\ \widetilde{(L\rho u)}_i = (\rho u)^n_i - \dfrac{\Delta t}{\Delta x}\Big(\Pi^*_{i+1/2} - \Pi^*_{i-1/2}\Big) - \dfrac{\Delta t}{\Delta x}\{\rho\delta\Phi\}^n_i & \text{(II.94b)} \\ \widetilde{(L\rho\mathscr{E})}_i = (\rho\mathscr{E})^n_i - \dfrac{\Delta t}{\Delta x}\Big(u^*_{i+1/2}\Pi^*_{i+1/2} - u^*_{i-1/2}\Pi^*_{i-1/2}\Big), & \text{(II.94c)} \\ \widetilde{(L\rho\Psi)}_i = (\rho\Psi)^n_i + \dfrac{\Delta t}{\Delta x}\{u\rho\delta\Phi\}^n_i & \text{(II.94d)} \\ \widetilde{(L\rho\Pi)}_i = (\rho\Pi)^n_i - a^2\dfrac{\Delta t}{\Delta x}\Big(u^*_{i+1/2} - u^*_{i-1/2}\Big), & \text{(II.94e)} \end{cases}$$

where

$$u^*_{i+1/2} = \frac{u^\sharp_{i+1} + u^\sharp_i}{2} - \frac{1}{2a}\Big(\Pi^\sharp_{i+1} - \Pi^\sharp_i + \{\rho\delta\Phi\}^n_{i+1/2}\Big), \qquad \Pi^*_{i+1/2} = \frac{\Pi^\sharp_{i+1} + \Pi^\sharp_i}{2} - \frac{a}{2}\Big(u^\sharp_{i+1} - u^\sharp_i\Big), \tag{II.95}$$

$$\{\rho\delta\Phi\}^n_i = \frac{\{\rho\delta\Phi\}^n_{i-1/2} + \{\rho\delta\Phi\}^n_{i+1/2}}{2}, \qquad \{\rho\delta\Phi\}^n_{i+1/2} = \frac{\rho^n_i + \rho^n_{i+1}}{2}\big(\Phi_{i+1} - \Phi_i\big), \tag{II.96}$$

and

$$\{\rho u\delta\Phi\}^n_i = \frac{u^*_{i-1/2}\{\rho\delta\Phi\}^n_{i-1/2} + u^*_{i+1/2}\{\rho\delta\Phi\}^n_{i+1/2}}{2}. \tag{II.97}$$

Finite Volume discretization

A complete numerical scheme for (II.87b) is obtained by adding a discrete transport step to (II.94) that is performed using an upwind technique as (II.47) for the variables ρ, $\rho\mathbf{u}$, $\rho\mathscr{E}$ and $\rho\Psi$. The final step of the numerical scheme consists in resetting the value of Ψ by imposing $\Psi^{n+1}_i = \Phi_i$. Following the analysis described in section II.5, a low Mach correction is implemented by replacing $\Pi^*_{i+1/2}$ with

$$\Pi^{*,\theta}_{i+1/2} = \frac{\Pi^\sharp_{i+1} + \Pi^\sharp_i}{2} - \frac{a\theta}{2}\Big(u^\sharp_{i+1} - u^\sharp_i\Big), \tag{II.98}$$

where $\theta = O(M)$. The effects of both the well-balanced feature and the low Mach correction on the accuracy of the

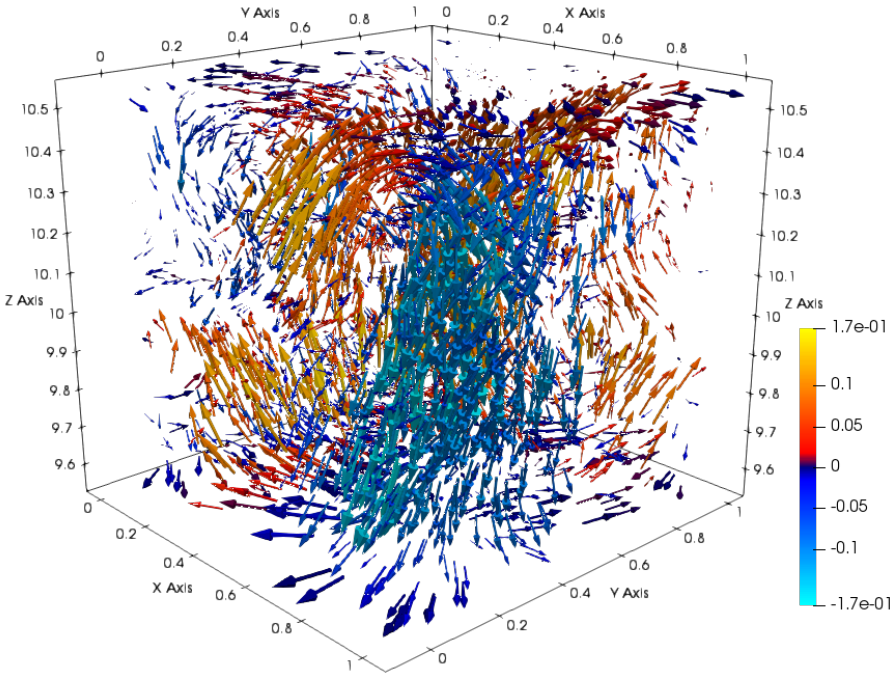

Figure II.8 – Velocity profile of a 3D Rayleigh-Bénard instability simulations.The length of an arrow is scaled using the magnitude of the local velocity. The colorbar represents the vertical component of the velocity showing the direction of the flow. The simulation was performed by T. PADIOLEAU with the code ARK.

scheme turned out to be quite substantial. For instance, the numerical scheme was able to preserve unstable equilibrium initial conditions so that it was necessary to seed (even very small) perturbations to trigger the instability. As mentioned in section III.2 this property led to (unexpected) developments concerning the theory of convection in the atmosphere of Brown Dwarfs and planets[3]. I display in figure II.8 results issued from the simulation of a 3D Rayleigh-Bénard instability.

II.10 Computation of phase change equilibrium states

Contributions by the author
This section covers works that have been published in [19, 14, 17].

In this section, I will present a method for computing the fluid parameters of a two-phase mixture governed by the equilibrium EOS presented in section I.4.3. We suppose given two pure phase $k = 1, 2$ EOS in the form of entropy laws $(\tau_k, e_k) \mapsto s_k$. The question boils down to compute τ_k, e_k, and all composition variables Y_k, α_k and ψ_k satisfying the equilibrium (I.36) recalled below

$$(T_1, P_1, g_1)\left(\frac{\alpha}{Y}\tau, \frac{\psi}{Y}e\right) = (T_2, P_2, g_2)\left(\frac{1-\alpha}{1-Y}\tau, \frac{1-\psi}{1-Y}e\right), \tag{I.36}$$

for a given value of the mixture internal energy e and the specific volume τ.

A single equation for computing phase change equilibrium states

I will show that the system (I.36) can be reduced to a 2×2 system using the pair of variables (P, T). This choice of variables may also help dealing with tabulated EOS that are often parameterized in the (P, T)-plane. Let ut consider the pure phase EOS in the form of functions $(P_k, T_k) \mapsto \tau_k$ and $(P_k, T_k) \mapsto e_k$. By the definition (I.32) of e and τ, the mass fraction of phase 1 verifies $Y_1 = (\tau - \tau_1)/(\tau_2 - \tau_1)$ and $Y_1 = (e - e_1)/(e_2 - e_1)$. Therefore (I.36) is equivalent to search for P and T such that

$$\frac{\tau - \tau_1(P,T)}{\tau_2(P,T) - \tau_1(P,T)} = \frac{e - e_1(P,T)}{e_2(P,T) - e_1(P,T)}, \tag{II.99a}$$

$$g_1(P,T) = g_2(P,T). \tag{II.99b}$$

In the (T, P)-plane, the locus of points verifying (II.99b) is called the coexistence curve. This curve is the graph of the function $P \mapsto T^{\text{sat}}(P)$. Let us now suppose that for a given pair of function $(P, T) \mapsto g_1$ and $(P, T) \mapsto g_2$, we can actually solve (II.99b) with respect to T for a given P so that the definition of $P \mapsto T^{\text{sat}}(P)$ is known. Then the 2×2 system (II.99) reduces to the nonlinear equation scalar with respect to P :

$$\frac{\tau A(P) - 1}{B(P) - 1} = \frac{eC(P) - 1}{D(T) - 1}, \tag{II.100}$$

with

$$A(P) = 1/\tau_1(P, T^{\text{sat}}(P)), \qquad B(P) = \tau_2(P, T^{\text{sat}}(P))/\tau_1(P, T^{\text{sat}}(P)), \tag{II.101a}$$

$$C(P) = 1/e_1(P, T^{\text{sat}}(P)), \qquad D(P) = e_2(P, T^{\text{sat}}(P))/e_1(P, T^{\text{sat}}(P)). \tag{II.101b}$$

that we referred to as a "phase change equation" in [14].

The equilibrium pressure P is chosen as the main variable here. It is possible to use the equilibrium temperature instead as in [19].

An algorithm for computing the equilibrium

We suppose here that the evaluation of $T^{\text{sat}}(P)$ is achieved by solving (II.99b) with respect to T for a given P. For a fixed $(\tau, e) \in (0, +\infty)^2$, the resolution algorithm for the equilibrium states reads as follows.

1. If there exists $P^* > 0$ that is solution of (II.100) and if $Y^* = (\tau A(P) - 1)(B(P) - 1)^{-1} \in (0, 1)$, then one sets
$$Y^{\text{eq}}(\tau, e) = Y^*, \quad \alpha^{\text{eq}}(\tau, e) = Y^* \tau_1(P^*, T^{\text{sat}}(P^*))/\tau, \quad \psi^{\text{eq}}(\tau, e) = Y^* e_1(P^*, T^{\text{sat}}(P^*))/e, \tag{II.102a}$$
$$P^{\text{eq}}(\tau, e) = P^*, \qquad s^{\text{eq}}(\tau, e) = s(\tau, e, Y^*, \alpha^*, \psi^*). \tag{II.102b}$$
2. If (II.100) has no solution or if the corresponding $Y^* = (\tau A(P) - 1)(B(P) - 1)^{-1} \notin (0, 1)$ then the state (τ, e) is a pure fluid state defined as follows :
   (a) either $s_1(\tau, e) > s_2(\tau, e)$, then (τ, e) belongs to the phase 1 and
   $$Y^{\text{eq}}(\tau, e) = 1, \quad \alpha^{\text{eq}}(\tau, e) = 1, \quad \psi^{\text{eq}}(\tau, e) = 1, \quad P^{\text{eq}}(\tau, e) = P_1(\tau, e), \quad s^{\text{eq}}(\tau, e) = s_1(\tau, e), \tag{II.103}$$
   (b) either $s_2(\tau, e) > s_1(\tau, e)$, then (τ, e) belongs to the phase 2 and
   $$Y^{\text{eq}}(\tau, e) = 0, \quad \alpha^{\text{eq}}(\tau, e) = 0, \quad \psi^{\text{eq}}(\tau, e) = 0, \quad P^{\text{eq}}(\tau, e) = P_2(\tau, e), \quad s^{\text{eq}}(\tau, e) = s_2(\tau, e). \tag{II.104}$$

An algorithm for computing an approximate equilibrium state

For a given pair of functions $(P, T) \mapsto g_k$, $k = 1, 2$, computing $T^{\text{sat}}(P)$ can be quite cumbersome as solving (II.99b) with respect to T for a given P may not lead to an explicit formula (even in the simple case of two Stiffened Gases). We proposed to bypass this evaluation by replacing $T^{\text{sat}}(P)$ with an approximate function, so that (II.100) is replaced by the approximate phase change equation

$$\frac{\tau \widehat{A}(P) - 1}{\widehat{B}(P) - 1} = \frac{e\widehat{C}(P) - 1}{\widehat{D}(T) - 1}, \tag{II.105}$$

with

$$\widehat{A}(P) = 1/\tau_1(P, \widehat{T}^{\text{sat}}(P)), \qquad \widehat{B}(P) = \tau_2(P, \widehat{T}^{\text{sat}}(P))/\tau_1(P, \widehat{T}^{\text{sat}}(P)), \tag{II.106a}$$

$$\widehat{C}(P) = 1/e_1(P, \widehat{T}^{\text{sat}}(P)), \qquad \widehat{D}(P) = e_2(P, \widehat{T}^{\text{sat}}(P))/e_1(P, \widehat{T}^{\text{sat}}(P)). \tag{II.106b}$$

The mass fraction value resulting from the computing of the (approximate) pressure equilibrium P^* verifying (II.105) is $Y^* = (\tau\widehat{A}(P) - 1)(\widehat{B}(P) - 1)^{-1}$.

For computing the approximate function $\widehat{T}^{\text{sat}}$ we considered two different cases. In [14] we supposed that both pure phase EOSs were given using analytical formulas, so that the solution of equation (II.99b) could be expressed as the zero of a known analytical function for a given value of P using iterative methods. This allows to compute a set of $\mathcal{N}$ sample of points $(P_i, T^{\text{sat}}(P_i))_{i=1,\dots,\mathcal{N}}$ that is used for fitting a polynomial interpolation $P \mapsto \widehat{T}^{\text{sat}}(P)$. In [17], we studied the case of EOSs available through tabulated data, like the International Association for the Properties of Water and Steam (IAPWS) water tables[PS]. Such table enables a direct access to sample points $(T_i, \tau_k^{\text{sat}}(T_i))$ and $(T_i, e_k^{\text{sat}}(T_i))$. Therefore it is possible to bypass the evaluation of $T \mapsto P^{\text{sat}}$ and propose a direct alternative definition for $\widehat{A}$, $\widehat{B}$, $\widehat{C}$ and $\widehat{D}$ by seeking approximations respectively for $1/\tau_1^{\text{sat}}(T)$, $\tau_2^{\text{sat}}(T)/\tau_1^{\text{sat}}(T)$, $1/e_1^{\text{sat}}(T)$, and $e_2^{\text{sat}}(T)/e_1^{\text{sat}}(T)$. In [17], we proposed fitted polynomials for $\ln(\widehat{A})$, $\ln(\widehat{B})$, $\ln(\widehat{C})$ and $\ln(\widehat{D})$ over a set of 83 points spanning $T \in [283\,\text{K}, 524\,\text{K}]$. The resulting approximate phase change equation was tested over a set of 15 points in the range $T \in [283\,\text{K}, 524\,\text{K}]$ and provided approximate values for $T^{\text{eq}}(\tau, e)$ with a relative accuracy of 10^{-5} and $Y^{\text{eq}}(\tau, e)$ with an accuracy of 10^{-5}.

The method proposed in [17] was implemented by T. PADIOLEAU in the simulation code ARK and used for running a grand challenge simulation of water drops impacting a wall at high-velocity (see section III.3).

Chapitre III

Scientific computing practice

The present chapter may appear a bit unusual as I intend to share an overview of a part of my work that has not been tightly structured by publications although it represents a substantial portion of my activities. I chose to loosely refer to these elements as *scientific computing practice*.

The elaboration of models and discretization strategies are substantiated in computer programs and simulations. In the early years of my work, I simply considered delivering an efficient implementation of algorithms to be the sole aim of my scientific computing work. In some sense, it was an *output* of a previous captivating work. This (wrong) opinion was probably the result of both my personal inclinations (although I had always been interested in programming) and my scientific education.

Over the years, I gradually discovered many other aspects of scientific computing. I realized how I had vastly undervalued the contribution it could bring to my work. I will try to briefly illustrate this experience in the following sections. It is possible that some of these remarks may seem quite trivial for people skilled in terms of software engineering : I beg them for a tolerant reading of the following.

III.1 Software engineering matters

For a period of time spanning approximately from 2002 to 2013, I have been working for the CEA/DM2S/STMF (previously CEA/DM2S/SFME) on a simulation code called TRITON as its sole developer. This code was a three-dimensional parallel compressible flow simulation program on Cartesian grid written entirely in C. The core model of the code was the five-equation model that was elaborated during my PhD thesis [27, 26]. The parallelism was a very standard approach using MPI and domain decomposition. The emphasis was put on simplicity aiming at efficiency for High Perfomance Computing (HPC).

The development of this code was the opportunity for me to learn many things in term of scientific computing. The code was used on several supercomputers, sometimes in a very constrained context. I learned the hard way that reliability and the ability to rapidly adapt part of the code were as important as pure computing performance.

An important element that came into play was the audit of TRITON by a third-party company called Logilab [Log]. This work was achieved by Ludovic AUBRY, a highly skilled programmer, who worked for several weeks on TRITON. L. AUBRY issued a complete report, suggested relevant enhancements and took the time to discuss many aspects of the code with me. It was an enlightening experience.

I realized that my point of view concerning scientific computing was very narrow-minded and inexperienced. For example, I was convinced that the main way towards better understanding a code was to study the models and the numerical scheme it relies on. I saw that an experienced software engineer was able to "make his way" into the code very quickly and efficiently using a radically different approach.

This motivated me to totally revamp not only the software I was writing but to completely renovate my programming methodology. I have been trying since to continuously question and (if possible) improve my methods. I need to underline that the opportunity to discuss or work with people who are much more skilled than I am have been a great source of progress.

Another very enriching experience came from working with less experienced collaborators. I had the opportunity to co-supervise with C. CHALONS the Master thesis internship of L. ANGO [Ang10] who served as "guinea pig" for testing elements of methodology in terms of software development. The idea was to build and modify a workflow that finally led to a continuous mutual code review. The more "naive eye" of Laurent in term of programming allowed me to substantially question and modify on the fly my own coding habits.

Providing a clear, well articulated and exhaustive method for scientific software development is out of the scope of my work. However I would like to highlight a few elements that are important in my view. I try to teach these to the less experienced students I supervise and I try to improve these when I work with students or collaborators who are more skilled than I am.

Before going any further, I would like to emphasize that the following is mostly the result of development practice and trial and error. Software engineering methods like *Agile software development* or *Extreme programming* that have been popularized in the past years may probably include these elements.

Aim of the code : not only what, but who
A simulation code obviously requires efficient implementation of the algorithms it is intended to execute. However, if the code is meant to be used by a group of people, it is important to think about the profile of the people who will use the code and what purpose they will have. For example, a physicist, an applied mathematician may have very different interactions with the code depending on the task they need to accomplish. A naive image would be that a torx screw requires a torx head screwdriver while a slotted screw requires a flat screwdriver. In terms of programming, I believe this can be achieved by providing specific Application Programming Interface (API) that are suited for each use. This requires the developer to have a good understanding of the work methods of the "target audience" of the code. I need to emphasize that this should not necessarily impact the whole structure of the code.

While I have not found out a universal way of designing these API, I built a simple "metric". This metric boils down to the following question : how much time is required to fulfill a given task (*e.g.* run a simulation, add a new boundary condition, modify the algorithm) for a person with a given skill (*e.g.* zero, average, strong knowledge of the code) ?

Software engineering : an effort towards the end-users
The requirement of specified API suggests that the code should be built using "layers". This requires to invest time into developing a minimal set of software engineering skills. This layer design can be influenced of course by the functionalities of each part of the code, but also in term of skills profile of the people that will work in each layer. This matter echoes to the "not only what but who ?" question that was mentioned above.

Use of norms
Programming languages are evolving, even legacy languages like C, C++ or Fortran. If possible, it is important to use a clearly defined set of features of these languages that are coherent with a given norm. Of course, exceptions may happen. In this case documenting these exceptions and what motivated them and possible caveats is useful.

Software tools
Since I started my career, the world of software has been vastly transformed. It is way richer and a lot of very useful tools are available. I think it is a good practice to take advantage of these. I will only mention them by category : debuggers, profiling software, unit test environments, (modern) build process managers, version-control system softwares (and even better : forges), documentation system. I strongly encourage the students I work with to incorporate these tools in their work routine.

Modularity
I claim for a profound expertise in programming paradigms or software design. However, over the years, I must admit that I tend to favor a form of modularity (sometimes over a form of genericity). By modularity, I mean the ability to separate the code into (relatively) independent elements. The goal is to allow modifying a specific part of the code while minimizing the required knowledge of the overall code. It also eases the replacement of portion of the code. Of course, a complete modularity is not always possible and the dependence between different parts of the code should be documented.

Documenting and testing
I firmly believe that a great part of the value of a code consists in its documentation. This documentation can take many forms : a formal code documentation that is maintained and using a documentation generator software or a collection of informal notes that can be browsed and searched using keywords. Tests and snippets of code, template code are also a very useful and efficient form of documentation.

III.2 Scientific computing as a sharing tool

In the same way that programming for scientific computing is not limited to the efficient implementation of an algorithm, scientific computing is not solely about enabling simulations. Scientific computing is also a communication tool in many aspects.

A CEMRACS experiment : genuinely-many programming
In 2010, F. CAETANO, F. LAGOUTIÈRE and I had the opportunity to propose a research project for the CEMRACS 2010. The goal of the project was to improve the accuracy of an anti-diffusive interface capture method for two-phase flows. We succeeded in gathering 4 junior researchers in our project : B. BOUTIN, G. FACCANONI, L. NAVORET and M. BILLAUD-FRIESS. Testing numerical methods was a clear objective therefore organizing the coding effort very quickly became an issue. The overall team was composed of 7 people [1] with different programming skills in different programming languages !

We opted for an *a priori* odd solution : we spent days working in collective programming sessions using a video projector that was displaying the screen of a computer [2].

People were taking turn on the computer for typing and the code that was written was discussed collectively while it was entered in the machine. Very surprisingly, this method turned out to be very efficient : the burden of focusing on both entering the code without typos, avoiding syntax errors and implementation mistakes was "distributed" over the group. This enabled longer and less tiring working session. At the end of the session the knowledge of the code content was equally shared among the members of the team. Moreover, we realized that less experienced programmers were learning "on-the-fly" programming techniques or new syntax details.

Another side effect was that the collective tests or debugging sessions naturally motivated many discussions concerning the numerical method and suggested many modifications.

Scientific computing enabling theoretical loopback
A physicist friend of mine told me once that, in his opinion, performing simulation was only a way to verify what we already know. As disappointing as it seems, I would generally agree with his opinion (after all, he's a physicist… so he must be right !). Performing simulations is often a way for engineers to assess the "stability" of rough estimates that are derived thanks to simple hypotheses. This is not really surprising : our ancestors did not use computers to build boats that would carry goods and people across the oceans. Nevertheless, I believe I had the chance to witness a counter-example to my friend's statement.

I would like to share in this section an experience of a "positive loopback" that is connected to my work. I met P. TREMBLIN while we were both working at the Maison de la simulation. Pascal had been working for some years on the convection mechanisms that can take place within the atmosphere of Brown Dwarfs and extrasolar giant planets[Tre+15, Tre+16, Tre+17]. At the time, M. STAUFFERT, C. CHALONS and P. KESTENER and I were working on the extension of the acoustic/transport splitting method to the shallow water model with the goal of deriving a well-balanced method that accounts for non-conservative terms (see section II.8).

P. TREMBLIN was interested in the acoustic/transport splitting method and thought that the method could be adapted for the simulation of atmospheres he was interested in. This goal set the ground for an important part of the work achieved by T. PADIOLEAU during his Ph.D. that was co-supervised by P. TREMBLIN, E. AUDIT, P. KESTENER and me. A first version of the numerical scheme presented in section II.9 was proposed relying on the ideas presented in sections II.8 and II.5. The key feature of this numerical scheme was to combine both well-balanced properties for the gravity source terms and the all-Mach regime accuracy. These features allowed Pascal to perform simulations of instabilities that challenged the commonly accepted convective theory for the atmosphere of Brown Dwarfs and planets.

Indeed, the numerical scheme that had been developed was able to preserve equilibrium profiles, including unstable equilibria. Consequently, injecting "by hand" seeds of perturbations in the initial condition was mandatory to trigger instabilities. Armed with the confidence that they were not spuriously triggered by the numerical scheme, additional terms were added into the model like chemical reaction terms or radiative transfer terms. These additional terms showed a clear impact on the development of the instabilities in the simulations.

These numerical experiments acted as an incentive for Pascal to revisit the instability analysis underlying the Brown Dwarfs atmosphere convective models. This led to a new analytical analysis accounting for coupling effects between convection, evolution of the composition and source terms in the system pertaining to different effects like chemical reaction, radiative transfer models or latent heat pumping. It was shown that this approach can embrace others convection systems like thermohaline convection in Earth oceans and moist convection in the Earth atmosphere. This work was published in [3].

III.3 Scientific computing outcomes

As I mentioned in the introduction, an important incentive in my work is not only to contribute to the scientific literature but also to provide computational tools for physicists and engineers. Some of the models and numerical schemes I studied were implemented into research and production simulation codes. I will briefly give a list of these hereafter. I need to underline that except for the code TRITON, my role was often limited to supervision or counseling.

1. All the team members were not present at the same time during the whole project.
2. I discovered afterwards that a similar practice (involving two people) called *pair programming* was promoted among the Agile software development techniques.

TRITON
The anti-diffusive interface capture Lagrange-Remap for the case of two-phase flows (see section II.3 and [Lag02]) was implemented in the simulation code TRITON that I developed for the CEA/DM2S/STMF (previously CEA/DM2S/SFME). The code was used in 2007 to run a *Grand Challenge* computation on the supercomputer Platine of the CCRT over 1024 cores. The simulation results were exploited in a safety study for the CEA [3].

HERACLES
The anti-diffusive interface capture Lagrange-Remap algorithm for the case of N-component flows, $N \geq 2$ (see section II.3 and [10]) was implemented by M. BILLAUD-FRIESS in the code HERACLES[AG06] that is dedicated to the simulation of astrophysical fluid flows.

Europlexus
The anti-diffusive interface capture Lagrange-Remap for the case of two-phase flows (see section II.3) was adapted to fluid-structure interaction simulation algorithms in fast transient regime[12]. The implementation in the code Europlexus[Eur] that is co-owned by Joint Research Centre (JRC) of the European Union and the CEA was led by V. FAUCHER.

CANOP
CANOP is an open source code for parallel simulation on AMR grid that is issued from a CEMRACS research project [9]. It has been developed by many contributors from CEA, Maison de la simulation, CentraleSupélec, CMAP/Ecole Polytechnique and IFPEN. P. Kestener was the main contributor and architect of the code. F. Drui during her Ph.D.[Dru17] developed and implemented in CANOP several solvers based on the acoustic-transport splitting presented in section II.4 with A. Larat. Other important contributions (through research works I was not involved in) to CANOP were brought by : M. Essadki [Ess17], Q .Wargnier [War19], F. Chen [Che19].

ARK
The simulation code ARK [ARK] is a multi-architecture code that was developed by T. PADIOLEAU during his Ph.D. thesis [Pad20] on the ground of first developments achieved by P. KESTENER. T. PADIOLEAU implemented the well-balanced scheme for compressible with potential source terms described in section II.9. The code was used to perform a high-resolution *Grand Challenge* simulation of the atmosphere of an exo-planet on the KNL partition of the super computer Joliot-Curie (CEA/TGCC). This was achieved by S. Daley-Yates over a 5000^3-cell Cartesian grid. It aimed at describing convective motions in the atmosphere due radiative transfer, concentration variations and chemical reaction between CO and CO_2.

Another grand challenge simulation was performed with ARK by T. PADIOLEAU on the AMD partition of the Joliot-Curie. This simulation was a high-velocity impact of a water drop over a wall with defects. The model described in section I.5 and the acoustic-transport method of section II.4 were used. This study aimed at better understanding impacts of water droplet issued from the vapor generator onto pipes in a nuclear power plant. Two simulations were performed respectively over a 1024^3 and a 2048^3 Cartesian grid. The model showed that the presence of surface defect on the wall could lead to pressure wave interactions that trigger cavitation effects and important pressure peaks on the wall (see figure III.1).

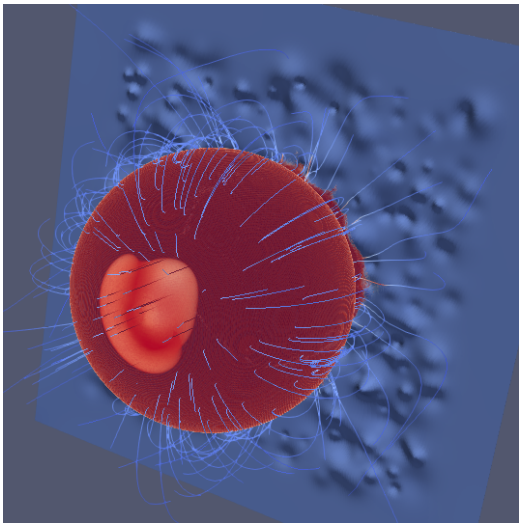

Figure III.1 – Profile of the droplet after impact on a wall with defect. A vapor region appears at the back of the droplet (white region) due to cavitation. Simulation performed by T. PADIOLEAU with the code ARK.

3. This work led to a technical report that is not available to the public.

Chapitre IV

Perspectives

Towards multi-scales interface flows
In section I.8 I presented a model for flows involving multiple components separated by interfaces. This framework is tightly limited to describe the interfaces by discontinuity surfaces. In many situations this assumption is too restrictive. I will propose two examples to illustrate this issue.

Let us consider first the destabilization of a liquid jet leading to atomization into a population of droplets. This type of flow can put at play phenomena over a genuine cascade of scales spanning from 10^{-2}m to 10^{-7}m. Describing a surface over such a wide range of scales is out of reach in terms of computing capacity.

The problems does not deals with computing but also with modeling. Indeed, a second and troubling example deals with the description of a stationary bubble attached to a wall. At first sight, it seems quite reasonable to describe the shape of this inclusion as a smooth surface far from the wall. Things are not so clear when one looks at the contact locus between the bubble and the wall. Indeed physicists may use different contact angles like the Young contact angle and the apparent contact angle (see for example [Fad+16]) for describing the shape of the bubble in the vicinity of the wall. If one additionally considers the wall to be a heating source, very thin layers of liquid beneath the bubble may play a crucial role in term of heat transfer. Apparent contact angles do not account for such layer. Somehow, one could say that contact angles give information about the shape of the bubble at a given scale.

The above observations suggest that what we usually refer to as two-phase interface may have different characteristics depending on the scale of the description. Representing this interface by a surface dooms us to only consider a "best fitted surface" at a given scale.

The above lines, suggests to depart from the idea that the interface can be unequivocally described by a surface. The main lead I intend to examine has been gradually shaped during the Ph.D. thesis of P. CORDESSE [Cor20] and also relies on the work of F. DRUI [Dru17] and M.ESSADKI /citemohamed-these. The main idea consists in characterizing the interface thanks to a probability density function. Similar approach are used in combustion theory for modeling flames [Pop88]. Joint works with R. DI BATTISTA, P. CORDESSE, A. LOISON, M. MASSOT and T. PICHARD are in progress on this topic.

A long-run goal of this effort is to propose a unified model for both separate phase and disperse phase flows.

Numerical schemes
The acoustic/transport splitting approach presented in section II.4 has provided interesting results. This encourage to improving the method and extending it to other systems.

The IMEX variant of the acoustic/transport splitting has not been thoroughly studied yet. For example : some tests have shown that the linear system that is involved with the acoustic step may not be well-conditioned. I believe it is worth investigating in order to derive simple but efficient production-ready simulation methods.

Another means of improving the method consists in developing higher-order methods. This topic was studied by T. PADIOLEAU in his Ph.D. thesis [Pad20] and the topic is also investigated by R. BOURGEOIS in the framework of his Ph.D. thesis that is supervised by P. TREMBLIN and me.

The extension of the acoustic/transport method to Magnetohydrodynamics is being investigated by S. BULTEAU, P. TREMBLIN for the ERC ATMO. This tasks implies to reconsider the operator splitting in order to account for the magnetic field. Another interesting question deals with the behavior of the system with respect to the Mach number.

Some simulation codes in both the industrial and the research community rely on a staggered grid discretization. I think it is possible to use the acoustic/transport approach into to this context. Straightforward adaptations of the algorithm will probably yield non-conservative numerical scheme. However I intend to investigate possible means of designing conservative numerical methods for staggered grids.

References

[Ang10] L. Ango. *Approximation implicite des équationd d'Euler 2D par une méthode de relaxation sur maillage non-structurés*. Mém. de mast. Sup Galilée, 2010.

[ARK] ARK.

[AG06] E. Audit et M. González. *HERACLES : a three dimensional radiation hydrodynamics code*. *EAS Publications Series* 18, p. 115-128, 2006.

[BN86] M. R. Baer et J. W. Nunziato. *A two-phase mixture theory for the Deflagration-to-Detonation Transition (DDT) in reactive granular materials*. *Int. J. Multiphase Flow* 12, p. 861-889, 1986.

[BH05] T. Barberon et P. Helluy. *Finite volume simulation of cavitating flows*. *Computers & Fluids* 34, p. 832-858, 2005.

[Bau+04] M. Baudin, C. Berthon, F. Coquel, R. Masson et Q. H. Tran. *A relaxation method for two-phase flow models with hydrodynamic closure law*. *Numerische Mathematik* 99, p. 411-440, 2004.

[Bed85] A. Bedford. *Hamilton's Principle in Continuum Mechanics*. Pitman Publishing Ltd., 1985.

[Ber09] V. Berdichevsky. *Variational Principles of Continuum Mechanics : I. Fundamentals*. Interaction of Mechanics and Mathematics. Springer Berlin Heidelberg, 2009.

[BLT10] C. Berthon, P. LeFloch et R. Turpault. *Late-time relaxation limits of nonlinear hyperbolic systems. A general framework*. *Math. of Comput.*, 2010.

[Bou04] F. Bouchut. *Nonlinear Stability of Finite Volume Methods for Hyperbolic Conservation Laws*. Birkhäuser Basel, 2004.

[BH19] D. Bresch et M. Hillairet. *A compressible multifluid system with new physical relaxation terms*. *Annales scientifiques de l'École normale supérieure* 52, p. 255-295, 2019.

[BBL20] D. Bresch, C. Burtea et F. Lagoutière. *Physical Relaxation Terms for Compressible Two-Phase Systems*, 2020.

[Cal85] H. Callen. *Thermodynamics and an introduction to thermostatistics*. John Wiley & sons, 1985.

[Car04] F. Caro. *Modélisation et simulation numérique des transitions de phase liquide vapeur*. Thèse de doct. Ecole Polytechnique, 2004.

[CG89] P. Casal et H. Gouin. *Invariance properties of inviscid fluids of grade n*. In : *PDEs and Continuum Models of Phase Transitions*. Springer-Verlag, 1989, p. 85-98.

[CC08] C. Chalons et J.-F. Coulombel. *Relaxation approximation of the Euler equations*. *Journal of Mathematical Analysis and Applications* 348, p. 872-893, 2008.

[CVV02a] G. Chanteperdrix, P. Villedieu et J. P. Vila. *A compressible model for separated two-phase flows computations*. In : *ASME Fluids Engineering Division Summer Meeting*. 31141. Montreal, 2002.

[CVV02b] G. Chanteperdrix, P. Villedieu et J. Vila. *Un modèle bifluide compressible pour la simulation numérique d'écoulements diphasiques à phases séparées*. Rapp. tech. ONERA, CNES, 2002.

[Che19] F. Chen. *Modélisation d'un jet de gaz dans le collecteur sodium des échangeurs àplaques compacts sodium gaz des réacteurs nucléaires de la filière RNR-Na*. Thèse de doct. Aix-Marseille Univ., 2019.

[CDL83] L. Y. Cheng, D. A. Drew et R. T. Lahey. *An analysis of wave dispersion, sonic velocity and critical flow in two-phase mixtures*. Rapp. tech. U.S. Nuclear Regulatory Commission, 1983.

[CDL85] L. Y. Cheng, D. A. Drew et R. T. Lahey. *An analysis of wave propagation in bubbly two-component, two-phase flow*. *Journal of Heat Transfer* 107, p. 402-408, 1985.

[Cle00] S. Clerc. *Numerical Simulation of the Homogeneous Equilibrium Model for Two-Phase Flows*. *Journal of Computational Physics* 161, p. 354-375, 2000.

[Coq+02] F. Coquel, T. Gallouët, J.-M. Hérard et N. Seguin. *Closure laws for a two-fluid two-pressure model*. *C.R. Math.* 334, p. 927-932, 2002.

[Coq+08] F. Coquel, Q. L. Nguyen, M. Postel et Q. .-. Tran. *Large Time Step Positivity-Preserving Method for Multiphase Flows*. In : *Hyperbolic Problems : Theory, Numerics, Applications*. Sous la dir. de S. Benzoni-Gavage et D. Serre. Berlin, Heidelberg : Springer Berlin Heidelberg, 2008, p. 849-856.

[Coq+10] F. Coquel, Q. L. Nguyen, M. Postel et Q. H. Tran. *Entropy-satisfying relaxation method with large time-steps for Euler IBVPs*. *Mathematics of Computation* 79, p. 1493-1533, 2010.

[Cor20] P. Cordesse. *Contribution to the study of combustion instabilities in cryotechnic rocket engines : coupling diffuse interface models with kinetic-based moment methods for primary atomization simulation*. Thèse de doct. Paris-Saclay Univ., 2020.

[CM20] P. Cordesse et M. Massot. *Entropy supplementary conservation law for non-linear systems of PDEs with non-conservative terms : application to the modelling and analysis of complex fluid flows using computer algebra*. en. *Communications in Mathematical Sciences* 18, p. 515-534, 2020.

[CG06] J.-F. Coulombel et T. Goudon. *The strong relaxation limit of the multidimensional isothermal Euler equations*. *Transactions of the American Mathematical Society* 359, p. 637-648, 2006.

[Cro+15] F. Crouzet, F. Daude, P. Galon, J.-M. Hérard, O. Hurisse et Y. Liu. *Validation of a two-fluid model on unsteady liquid–vapor water flows*. *Computers & Fluids* 119, p. 131-142, 2015.

[Dau+08] F. Dauvergne, J.-M. Ghidaglia, F. Pascal et J.-M. Rovarch. *Renormalization of the numerical diffusion for an upwind finite volume method. Application to the simulation of Kelvin-Helmholtz instability*. *Finite volumes for complex applications. V. Proceedings of the 5th International Symposium, Aussois, June 2008, R. Eymard and J.-M. Hérard editors*, pp. 321-328, 2008.

[Deg+09] P. Degond, F. Deluzet, M.-H. Vignal et A. Sangam. *An Asymptotic Preserving Scheme for the Euler equations in a strong magnetic field*. *J. Comp. Phys.* 228, p. 3540-3558, 2009.

[Del10] S. Dellacherie. *Analysis of Godunov type schemes applied to the compressible Euler system at low Mach number*. *J. Comp. Phys.* 229, pp. 978-1016, 2010.

[Del+16] S. Dellacherie, J. Jung, P. Omnes et P.-A. Raviart. *Construction of modified Godunov-type schemes accurate at any Mach number for the compressible Euler system*. *Mathematical Models and Methods in Applied Sciences* 26, p. 2525-2615, 2016.

[DOR10] S. Dellacherie, P. Omnes et F. Rieper. *The influence of cell geometry on the Godunov scheme applied to the linear wave equation*. *Journal of Computational Physics* 229, p. 5315-5338, 2010.

[Del03] S. Dellacherie. *Relaxation schemes for the multicomponent Euler system*. *ESAIM : Mathematical Modelling and Numerical Analysis* 37, p. 909-936, 2003.

[DBF12] B. Després, C. Buet et E. Frank. *Design of asymptotic preserving finite volume schemes for the hyperbolic heat equation on unstructured meshes*. *Numerisch Math.* 122, p. 227-278, 2012.

[Des97] B. Després. *Inégalité entropique pour un solveur conservatif du système de la dynamique des gaz en coordonnées de Lagrange*. *Comptes Rendus de l'Académie des Sciences - Series I - Mathematics* 324, p. 1301-1306, 1997.

[Des10] B. Després. *Lois de conservations euleriennes, lagrangiennes et methodes numeriques*. Avec la coll. de S. de mathématiques appliquées et industrielles. Mathematiques & applications v. 68. Heidelberg ; New York : Springer, 2010. 284 p.

[Des17] B. Després. *Numerical Methods for Eulerian and Lagrangian Conservation Laws*. Frontiers in Mathematics. Cham : Springer International Publishing, 2017.

[DL01] B. Després et F. Lagoutière. *Journal of Scientific Computing* 16, p. 479-524, 2001.

[Des+10] B. Després, F. Lagoutière, E. Labourasse et I. Marmajou. *An antidissipative transport scheme on unstructured meshes for multicomponent flows*. *Int. J. Finite Vol.* 7, p. 36, 2010.

[DP11] G. Dimarco et L. Pareschi. *Exponential methods for kinetic equations*. *SIAM J. Num. Anal.* 49, p. 2057-2077, 2011.

[Dru17] F. Drui. *Eulerian modeling and simulations of separated and disperse two-phase flows : development of a unified modeling approach and associated numerical methods for highly parallel computations*. PhD Thesis. Université Paris-Saclay, juill. 2017.

[Ess17] M. Essadki. *Contribution à la modélisation eulérienne unifiée de l'injection : de la zone dense au spray polydispersé.* Thèse de doct. Université Paris-Saclay - CentraleSupélec, 2017.

[Eur] Europlexus.

[Fac08] G. Faccanoni. *Étude d'un modèle fin de changement de phase liquide-vapeur. Contribution à l'étude de la crise d'ébullition*. Thèse de doct. École Polytechnique, 2008.

[Fad+16] E. Fadeeva, S. Schlie-Wolter, B. Chichkov, G. Paasche et T. Lenarz. *Structuring of biomaterial surfaces with ultrashort pulsed laser radiation*. In : *Laser Surface Modification of Biomaterials*. Elsevier, 2016, p. 145-172.

[FJ10] F. Filbet et S. Jin. *A class of asymptotic preserving schemes for kinetic equations and related problems with stiff sources*. *J. Comp. Phys.* 229, p. 7625-7648, 2010.

[Gal03] G. Gallice. *Positive and Entropy Stable Godunov-type Schemes for Gas Dynamics and MHD Equations in Lagrangian or Eulerian Coordinates*. *Numerische Mathematik* 94, p. 673-713, 2003.

[Gal02] G. Gallice. *Solveurs simples positifs et entropiques pour les systèmes hyperboliques avec terme source*. *Comptes Rendus Mathematique* 334, p. 713-716, 2002.

[Gav14] S. Gavrilyuk. *The structure of pressure relaxation terms : one-velocity case*. Internal report. H-I83-2014-00276-EN. EDF, 2014.

[GG99] S. Gavrilyuk et H. Gouin. *A new form of governing equations of fluids arising from Hamilton's principle*. *International Journal of Engineering Science* 37, p. 1495-1520, 1999.

[GG00] S. Gavrilyuk et H. Gouin. *Symmetric form of governing equations for capillary fluids, Interaction of mechanics and mathematics, in : Trends in applications of mathematics to mechanics", Monographs and Surveys in Pure and Applied Mathematics*. In : sous la dir. d'A. N. G. Iooss O. Gus. T. 106. Chapman et Hall/CRC, 2000. Chap. IX, p. 306-312.

[GS02] S. Gavrilyuk et R. Saurel. *Mathematical and Numerical Modeling of Two-Phase Compressible Flows with Micro-Inertia*. 175, p. 326-360, 2002.

[GGP97] S. Gavrilyuk, H. Gouin et Y. Perepechko. *A variational principle for two-fluid models*. *Comptes Rendus de l'Académie des Sciences - Series IIB - Mechanics-Physics-Chemistry-Astronomy* 324, p. 483-490, 1997.

[Geu86] J. Geurst. *Variational principles and two-fluid hydrodynamics of bubbly liquid/gas mixtures*. *Physica A* 135, p. 455-486, 1986.

[GSS99] J. Glimm, D. Saltz et D. H. Sharp. *Two-phase modelling of a fluid mixing layer*. *Journal of Fluid Mechanics* 378, p. 119-143, 1999.

[GSS96] J. Glimm, D. Saltz et D. H. Sharp. *Renormalization group solution of two-phase flow equations for Rayleigh-Taylor mixing*. *Physics Letters A* 222, p. 171-176, 1996.

[GR96] E. Godlewski et P.-A. Raviart. *Numerical Approximation of Hyperbolic Systems of Conservation Laws*. Springer, 1996.

[GS06] E. Godlewski et N. Seguin. *The Riemann problem for a simple model of phase transition*. *Communications in Mathematical Sciences* 4, p. 227-247, 2006.

[Gos00] L. Gosse. *A Well-Balanced FLux-Vector Splitting Scheme Designed for Hyperbolic Systems of Conservation Laws with Source Terms*. *Computers and Mathematics with Applications* 39, p. 135-159, 2000.

[GL96a] L. Gosse et A.-Y. Le Roux. *A well-balanced scheme designed for inhomogeneous scalar conservation laws*. *C. R. Math. Acad. Sci. Paris* 323, p. 543-546, 1996.

[GT04] L. Gosse et G. Toscani. *Asymptotic-preserving and well-balanced schemes for radiative transfer and the Rosseland approximation*. *Numer. Math.* 2, p. 223-250, 2004.

[Gou78] H. Gouin. *Contribution à une étude géométrique et variationnelle des milieux continus*. Thèse de doct. Université d'Aix-Marseilles I, 1978.

[Gou90] H. Gouin. *Variational Theory of Mixtures in Continuum Mechanics*. *European Journal of Mechanics - B/Fluids* 9, p. 469-491, 1990.

[GR09] H. Gouin et T. Ruggeri. *The Hamilton principle for fluid binary mixtures with two temperatures*. *Bollettino della Unione Matematica Italiana* 9, p. 403-422, 2009.

[Gou07] H. Gouin. *The second gradient theory applied to interfaces : Models of continuum mechanics for fluid interfaces*. In : *Dynamics of Multiphase Flows Across Interfaces*. Springer Berlin Heidelberg, 2007, p. 8-13.

[GL96b] J. Greenberg et A. Y. Leroux. *A Well-Balanced Scheme for the Numerical Processing of Source Terms in Hyperbolic Equations*. *SIAM J. Numer. Anal.* 33, pp. 1-16, 1996.

[GM04] H. Guillard et A. Murrone. *On the behavior of upwind schemes in the low Mach number limit : II. Godunov type schemes*. *Computers & Fluids* 33, p. 655-675, 2004.

[GV99] H. Guillard et C. Viozat. *On the behaviour of upwind schemes in the low Mach number limit*. en. *Computers & Fluids* 28, p. 63-86, 1999.

[Gui07a] V. Guillemaud. *Modélisation et simulation numérique des écoulements diphasiques par une approche bifluide à deux pressions*. Thèse de doct. Université de Provence (Aix-Marseille I), 2007.

[Gui07b] V. Guillemaud. *Modelling and Numerical Simulation of Strongly Unbalanced Two-Phase Flows*. In : *18th AIAA Computational Fluid Dynamics Conference*. American Institute of Aeronautics et Astronautics, juin 2007.

[HJM20] H. H. Ghazi, F. James et H. Mathis. *A Nonisothermal thermodynamical model of liquid-vapor interaction with metastability*. *to appear in Discrete Contin. Dyn. Syst.-B (accepted)*, 2020.

[HS06] P. Helluy et N. Seguin. *Relaxation models of phase transition flows*. *ESAIM : Mathematical Modelling and Numerical Analysis* 40, p. 331-352, 2006.

[Hel05] P. Helluy. *Quelques exemples de méthodes numériques récentes pour le calcul des écoulements multiphasiques.* Mémoire d'habilitation à diriger des recherches. 2005.

[Her55] J. W. Herivel. *The derivation of the equations of motion of an ideal fluid by Hamilton's principle*. *Mathematical Proceedings of the Cambridge Philosophical Society* 51, p. 344-349, 1955.

[HL92] L. Hsiao et T.-P. Liu. *Convergence to nonlinear diffusion waves for solutions of a system of hyperbolic conservation laws with damping*. *Communications in Mathematical Physics* 143, p. 599-605, 1992.

[JM16] F. James et H. Mathis. *A relaxation model for liquid-vapor phase change with metastability*. *Communications in Mathematical Sciences* 14, p. 2179-2214, 2016.

[JL07] S. Jaouen et F. Lagoutière. *Numerical transport of an arbitrary number of components*. *Comput. Methods Appl. Mech. Engrg.* 196, p. 3127-3140, 2007.

[Jao01] S. Jaouen. *Étude mathématique et numérique de stabilité pour des modèles hydrodynamiques avec transition de phase*. Thèse de doct. Université Paris 6, 2001.

[Jin95] S. Jin. *Runge-Kutta Methods for Hyperbolic Conservation Laws with Stiff Relaxation Terms*. *J. Comp. Phys.* 122, pp. 51-67, 1995.

[JL96] S. Jin et C. Levermore. *Numerical Schemes for Hyperbolic Conservation Laws with Stiff Relaxation Terms*. *J. Comp. Phys.* 126, pp. 449-467, 1996.

[JP00] S. Jin et L. Pareschi. *Uniformly accurate diffusive relaxation schemes for multiscale transport equations*. *SIAM J. Numer. Anal.* 38, p. 913-936, 2000.

[Kla98] A. Klar. *An asymptotic-induced scheme for nonstationary transport equations in the diffusive limit*. *SIAM J. Numer. Anal.* 35, p. 1073-1094, 1998.

[Kle74] M. Klein. *The historical origins of the Van der Waals equation*. *Physica* 73, p. 28-47, 1974.

[Lag02] F. Lagoutière. *Modélisation mathématique et résolution numérique de problèmes de fluides à plusieurs constituants*. Thèse de doct. Univ. Paris 6, 2002.

[Ler+08] V. Leroy, A. Strybulevych, J. Page et M. G. Scanlon. *Sound velocity and attenuation in bubbly gels measured by transmission experiments*. *Journal of Acoustical Society of America* 123, p. 1931-1940, 2008.

[LKY03] T. Liu, B. Khoo et K. Yeo. *Ghost fluid method for strong shock impacting on material interface*. *Journal of Computational Physics* 190, p. 651-681, 2003.

[Liu76] T.-P. Liu. *The entropy condition and the admissibility of shocks*. *Journal of Mathematical Analysis and Applications* 53, p. 78-88, 1976.

[Loc16] H. Lochon. *Modélisation et simulation d'écoulements transitoireseau-vapeur en approche bifluide*. Thèse de doct. Aix-Marseille Univ., 2016.

[Loc+16] H. Lochon, F. Daude, P. Galon et J.-M. Hérard. *Comparison of two-fluid models on steam-water transients*. *ESAIM : Mathematical Modelling and Numerical Analysis* 50, p. 1631-1657, 2016.

[Log] Logilab.

[MM90] P. Marcati et A. Milani. *The one-dimensional Darcy's law as the limit of a compressible Euler flow*. *Journal of Differential Equations* 84, p. 129-147, 1990.

[Mat20] H. Mathis. *Entropie en dynamique des fluides.* Mémoire d'habilitation à diriger des recherches. 2020.

[OF03] S. Osher et R. Fedkiw. *Level Set Methods and Dynamic Implicit Surfaces*. Springer New York, 2003.

[OS88] S. Osher et J. A. Sethian. *Fronts propagating with curvature-dependent speed : algorithms based on Hamilton-Jacobi formulations*. *Journal of Computational Physics* 79, p. 12-49, 1988.

[Pad20] T. Padioleau. *Développement de méthodesde simulation AMR "tout régime" pour la dynamique des fluides, applications en astrophysique et aux écoulements diphasiques*. Thèse de doct. Paris-Saclay Univ., 2020.

[Pai+00] H. Paillere, C. Viozat, A. Kumbaro et I. Toumi. *Comparison of low Mach number models for natural convection problems*. *Heat and Mass Transfer* 36, p. 567-573, 2000.

[Pes+18] I. Peshkov, M. Pavelka, E. Romenski et M. Grmela. *Continuum mechanics and thermodynamics in the Hamilton and the Godunov-type formulations*. *Continuum Mechanics and Thermodynamics* 30, p. 1343-1378, 2018.

[PP77] M. S. Plesset et A. Prosperetti. *Bubble Dynamics and Cavitation*. en. *Annual Review of Fluid Mechanics* 9, p. 145-185, 1977.

[Pop88] S. B. Pope. *The evolution of surfaces in turbulence*. *Int. J. Eng. Sci.* 26, p. 445-469, 1988.

[PS] I. A. for the Properties of Water et Steam. *IAPWS95 standard*.

[Pro77] A. Prosperetti. *Thermal effects and damping mechanisms in the forced radial oscillations of gas bubbles in liquids*. *The Journal of the Acoustical Society of America* 61, p. 17-27, 1977.

[QK96] J. Quirk et S. Karni. *On the dynamics of a shock-bubble interaction*. *J. Fluid Mech.* 318, pp. 129-163, 1996.

[Ray17] L. Rayleigh. *On the pressure developed in a liquid during the collapse of a spherical cavity*. *Philosophical Magazine* 6, p. 94-98, 1917.

[Rom98] E. Romensky. *Hyperbolic systems of thermodynamically compatible conservation laws in continuum mechanics*. *Mathematical and Computer Modelling* 28, p. 115-130, 1998.

[Sal88] R. Salmon. *Hamiltonian Fluid Mechanics*. *Annual Review of Fluid Mechanics* 20, p. 225-256, 1988.

[Sal83] R. Salmon. *Practical use of Hamilton's principle*. *Journal of Fluid Mechanics* 132, p. 431-444, 1983.

[SA99] R. Saurel et R. Abgrall. *A Multiphase Godunov Method for Compressible Multifluid and Multiphase Flows*. *J. Comput. Phys.* 150, p. 435-467, 1999.

[SGR03] R. Saurel, S. Gavrilyuk et F. Renaud. *A multiphase model with internal degrees of freedom : application to shock–bubble interaction*. *Journal of Fluid Mechanics* 495, p. 283-321, 2003.

[Ser59] J. Serrin. *Mathematical Principles of Classical Fluid Mechanics*. In : *Fluid Dynamics I / Strömungsmechanik I*. Sous la dir. de C. Truesdell. Berlin, Heidelberg : Springer Berlin Heidelberg, 1959, p. 125-263.

[Set99] J. A. Sethian. *Level set methods and fast marching methods. Evolving interfaces in computational geometry, fluid mechanics, computer vision, and materials science.* English. T. 3. Cambridge : Cambridge University Press, 1999, p. xx + 378.

[Shy01] K. Shyue. *A fluid-mixture type algorithm for compressible multicomponent flow with Mie-Gruneisen equation of state*. 171, pp. 678-707, 2001.

[Sil57] E. Silberman. *Sound Velocity and Attenuation in Bubbly Mixtures Measured in Standing Wave Tubes*. *Journal of Acoustical Society of America* 29, p. 925-933, 1957.

[Sul90] I. Suliciu. *On modelling phase transitions by means of rate-type constitutive equations, schock wave structure*. *International Journal of Engineering Science* 1, p. 829-841, 1990.

[SSO94] M. Sussman, P. Smereka et S. Osher. *A Level Set Approach for Computing Solutions to Incompressible Two-Phase Flow*. *Journal of Computational physics* 114, p. 146-159, 1994.

[TSS94] E. F. Toro, M. Spruce et W. Speares. *Restoration of the contact surface in the HLL-Riemann solver*. *Shock Waves* 4, p. 25-34, 1994.

[Tor09] E. F. Toro. *Riemann Solvers and Numerical Methods for Fluid Dynamics*. Springer Berlin Heidelberg, 2009.

[TKP99] I. Toumi, A. Kumbaro et H. Paillere. *Approximate Riemann solvers and flux vector splitting schemes for two-phase flow.* In : *VKI LS 1999-03, Computational Fluid Dynamics*. 1999.

[Tre+16] P. Tremblin, D. S. Amundsen, G. Chabrier, I. Baraffe, B. Drummond, S. Hinkley, P. Mourier et O. Venot. *Cloudless atmospheres for l/t dwarfs and extrasolar giant planets*. *The Astrophysical Journal* 817, p. L19, 2016.

[Tre+15] P. Tremblin, D. S. Amundsen, P. Mourier, I. Baraffe, G. Chabrier, B. Drummond, D. Homeier et O. Venot. *Fingering convection and cloudless models for cool brown dwarf atmospheres*. *The Astrophysical Journal* 804, p. L17, 2015.

[Tre+17] P. Tremblin, G. Chabrier, I. Baraffe, M. C. Liu, E. A. Magnier, P.-O. Lagage, C. Alves de Oliveira, A. J. Burgasser, D. S. Amundsen et B. Drummond. *Cloudless Atmospheres for Young Low-gravity Substellar Objects*. *The Astrophysical Journal* 850, p. 46, 2017.

[Tru91] L. Truskinovsky. *Kinks versus shocks. In ,Shock induced transitions and phase structures in general media*. Sous la dir. de R. Fosdick et al. Springer Verlag, 1991.

[Tur87] E. Turkel. *Preconditioned methods for solving the incompressible and low speed compressible equations*. *J. Comp. Phys.* 72, pp. 277-298, 1987.

[Van] J. D. Van der Waals. *The Equation of State for Gases and Liquids*. in Nobel Lectures in Physics 1901-1921.

[War19] Q. Wargnier. *Mathematical modeling and simulation of non-equilibrium plasmas :application to magnetic reconnection in the Sun atmosphere*. Thèse de doct. Centrale-Supélec, 2019.